

Reliability Updating of Sheet Pile Walls

An analysis on the parameter updating process

J.M. Büller



Reliability Updating of Sheet Pile Walls

An analysis on the parameter updating process

by

J.M. Büller

to obtain the degree of

Master of Science

in

Geotechnical Engineering

at the Delft University of Technology,

to be defended publicly on Friday December 20, 2019 at 09:00 AM.

Student number: 4609506

Project duration: December 10, 2019 – December 20, 2019

Thesis committee: Dr. P. J. Vardon, TU Delft, Geotechnical Engineering, chair
Dr. ir. R. B. J. Brinkgreve, TU Delft, Geotechnical Engineering
Dr. ir. T. Schweckendiek, TU Delft, Hydraulic Engineering
Ir. J. de Greef, Witteveen+Bos, daily supervisor

An electronic version of this thesis is available at <http://repository.tudelft.nl/>.

Preface

Throughout the last year I had the opportunity to learn about the process of reliability updating. This is an interesting technique which can be applied to re-evaluate structure's limits and usability. A collaboration between the TU Delft and Witteveen+Bos made it possible to complete this project. Therefore I would like to thank Jos, my supervisor from Witteveen+Bos, and my committee for being critical and. At last I would like to express my appreciation to my family and friends. In particular I would like to thank Florentine for listening to my non-thesis related stories.

Jeroen Büller
Delft, 14 December 2019

"I do not know what I may appear to the world, but to myself I seem to have been only like a boy playing on the sea-shore, and diverting myself in now and then finding a smoother pebble or a prettier shell than ordinary, whilst the great ocean of truth lay all undiscovered before me."

Sir Isaac Newton (1643-1727)

Summary

Throughout the years the use and requirements of sheet pile walls have changed. Because of the changing requirements, there is a need for re-evaluating the reliability of sheet pile wall structures. This applies to both the already existing structures and the ones to be built in the (near) future. Defining a structure's reliability is done by defining its ultimate limit states, which refer to the failure or collapse of the total structure or individual elements.

Updating a structure's reliability requires measurements. Because of practical and economical reasons ultimate limit state measurements are seldom available. Regularly available measurements are obtained during construction or from within the structure's service domain. A structure's service domain is defined by the uppermost service domain boundaries, also called the serviceability limit states. These serviceability limit states refer to the state of the structure that is required for it to perform its functions unhindered. This gives rise to the question if a sheet pile wall's ultimate limit states can be updated by using service domain measurement data.

The objective of this thesis is to provide insight into the process of parameter updating, using the adaptive Bayesian Updating with Structural reliability methods with Subset Sampling. This method is applied in a series of numerical analyses. In these analyses, the method is used to update the soil parameters of a finite element method model which is based on the Hochstetten sheet pile wall field test. For all the analyses, a set of artificial observations is used which are generated with the sheet pile wall model in combination with an artificial parameter set. Performing an indirect reliability update using these artificial observations is called a synthetic inverse analysis. It allows for testing the effectiveness of the adaptive Bayesian Updating with Structural reliability methods with Subset Sampling without model and measurement errors.

Different observation configurations are used for the analyses. These observation configurations are based on the available observations of the Hochstetten sheet pile wall field test. The purpose of these analyses is determining if a unique solution of the synthetic inverse analysis can be enforced with the used types of observations. From the results, it is concluded that neither of the used observation configurations is successful in enforcing a unique solution. Although the most elaborate observation configuration, with forty-one observations over five different types of observations, did return the most accurate results. This indicates that for a relatively complicated problem, like the model of a sheet pile wall with multiple variables, a large number of observations is required to be able to reliably perform a reliability update.

The use of (un)correlated variables and different constitutive soil models in the sheet pile wall model are also tested using the most elaborate observation configuration. Neither of the analyses was capable of returning all the true parameter values. From the results, it is concluded that using the Mohr-Coulomb model in the synthetic inverse analysis, instead of the advanced Hardening soil model, results in better-updated soil strength parameter values.

Nomenclature

Terms

<i>CBP</i>	Cantilever Beam Problem
<i>FEM</i>	Finite Element Method
<i>GWT</i>	groundwater table
<i>LF</i>	Likelihood Function
<i>LLF</i>	Logarithmic Likelihood Function
<i>LSF</i>	Limit State Function
<i>SLS</i>	Serviceability Limit State
<i>SSPWP</i>	Synthetic Sheet Pile Wall Problem
<i>ULS</i>	Ultimate Limit State

Methods

<i>aBUS – SuS</i>	adaptive Bayesian Updating with Structural reliability methods with Subset Sampling
<i>FORM</i>	First Order Reliability Method
<i>GA</i>	Genetic Algorithm
<i>KF</i>	Kalman Filter
<i>MCMC</i>	Markov Chain-Monte Carlo
<i>MCMC – MH</i>	Markov Chain-Monte Carlo method based on the Metropolis Hastings algorithm
<i>MCS</i>	Monte Carlo Simulation
<i>ML</i>	Maximum Likelihood method
<i>RPF</i>	Regularized Particle Filter
<i>SuS</i>	Subset Sampling

Models

<i>HS</i>	Hardening Soil soil model
<i>MC</i>	Mohr-Coulomb soil model

Variables

γ	Soil volumetric weight
ϕ'	internal friction angle
ψ	dilation angle
c'	effective cohesion
E_{50}^{ref}	reference Young's modulus
EI	Flexural rigidity of the cantilever beam
F	Force at the free tip of the cantilever beam
G_{50}^{ref}	reference Shear modulus
L	Length of the cantilever beam

List of Figures

2.1	Flowchart of the method of approach	5
3.1	Subdivision of the analysis method selection chapter	6
3.2	Level I reliability analysis load and resistance example	7
3.3	FORM reliability example	8
3.4	MCS reliability example	9
3.5	Direct and indirect reliability updating	9
3.6	Flowchart of the aBUS-SuS method	17
3.7	aBUS-SuS convergence process	19
3.8	Flowchart of the synthetic analysis	20
4.1	Subdivision of the Cases Set-Up chapter	22
4.2	Cantilever Beam Problem geometry	23
4.3	CBP deflection parameter sensitivity	24
4.4	Hochstetten floor plan	26
4.5	Hochstetten cross section	27
4.6	Hochstetten SPT profiles	28
4.7	Hochstetten boreholes	29
4.8	Hochstetten sensor plan	29
4.9	Linear elastic perfectly plastic behaviour	32
4.10	Hardening soil model behaviour	32
4.11	Hochstetten Plaxis 2D model	34
4.12	MC plastic points phase 7	35
4.13	HS plastic points phase 7	36
5.1	Subdivision of the Cantilever Beam Problem analysis plan	38
5.2	Data point distribution along cantilever beam span	39
5.3	CBP deflection updating results aBUS-SuS analysis with 1 variable and 1 observation	41
5.4	CBP parameter updating results aBUS-SuS analysis with 1 variable and 1 observation	41
5.5	CBP deflection updating results aBUS-SuS analysis with 2 variables and 1 observation	42
5.6	CBP parameter updating results aBUS-SuS analysis with 2 variables and 1 observation	43
5.7	CBP observation updating results aBUS-SuS analysis with 2 variables and 2 observations	44
5.8	CBP parameter updating results aBUS-SuS analysis with 2 variables and 2 observations	44
5.9	CBP observation updating results aBUS-SuS analysis with likelihood function domain	45
5.10	Correlated observation errors	46

5.11 CBP deflection updating results aBUS-SuS analysis with correlated observations	49
5.12 CBP moment force updating results aBUS-SuS analysis with correlated observations	49
5.13 CBP observations updating results aBUS-SuS analysis with uncorrelated observations	50
5.14 CBP observations updating results aBUS-SuS analysis with strongly correlated observations	50
5.15 CBP correlated variables results of the variables	53
5.16 CBP correlated variables deflection results	54
5.17 Average method parameter influence on posterior beam tip deflection of 50 iterations per N/p_0 combination	56
5.18 Average method parameter influence on posterior maximum moment of force of 50 iterations per N/p_0 combination	56
5.19 aBUS-SuS likelihood function calls method parameter analysis	57
5.20 CBP correlated observations discussion	58
6.1 Subdivision of the Synthetic Sheet Pile Wall Problem analysis plan	60
6.2 Synthetic Sheet Pile Wall Problem Observation locations	61
6.3 SSPWP aBUS-SuS results single observations number 1.1	64
6.4 SSPWP aBUS-SuS results multiple observations number 1.10	65
6.5 SSPWP aBUS-SuS results single observations numbers 1.1 – 1.5	66
6.6 SSPWP aBUS-SuS results multiple observations numbers 1.10 – 1.41	67
6.7 SSPWP aBUS-SuS results large difference prior and true parameter values uncorrelated variables	71
6.8 SSPWP aBUS-SuS variable results large difference prior and true parameter values uncorrelated variables	72
6.9 SSPWP aBUS-SuS results large difference prior and true parameter values correlated variables	74
6.10 SSPWP aBUS-SuS variable results large difference prior and true parameter values correlated variables	75
6.11 SSPWP aBUS-SuS results large difference prior and true parameter values correlated variables MC model	78
6.12 SSPWP aBUS-SuS variable results large difference prior and true parameter values correlated variables MC model	80

List of Tables

3.1	Selection of inverse analysis methods	10
3.2	Inverse analysis method comparison	15
4.1	CBP prior parameter values	24
4.2	Hochstetten field test phases	27
4.3	Hochstetten structural elements parameter values	31
4.4	Prior MC parameter values	33
4.5	Prior HS parameter values	33
4.6	Plaxis Sensitivity analyses of the MC and HS prior parameter sets	36
4.7	Soil variables for the aBUS-SuS analysis	37
5.1	CBP uniqueness analysis plan	40
5.2	CBP Solution uniqueness problem parameters	40
5.3	CBP updating results aBUS-SuS analysis with 1 variable and 1 observation	40
5.4	CBP updating results aBUS-SuS analysis with 2 variables and 1 observation	42
5.5	CBP updating results aBUS-SuS analysis with 2 variables and 2 observations	43
5.6	CBP observation correlation analysis plan	47
5.7	CBP Correlated observations problem parameters	47
5.8	CBP updating results aBUS-SuS analysis with correlated observations	48
5.9	CBP correlated variables analysis plan	51
5.10	CBP correlation matrices of the variables	51
5.11	CBP Correlated variables problem parameters	51
5.12	CBP updating results aBUS-SuS analysis with correlated variables	52
5.13	CBP method parameter values	54
5.14	CBP settings method parameter analysis	55
5.15	CBP Method parameters problem parameters	55
6.1	SSPWP observation combinations	62
6.2	SSPWP Observation plan observation standard deviations	63
6.3	SSPWP Observation plan true parameter values	63
6.4	SSPWP Increased prior variable standard deviations	70
6.5	SSPWP Increased observation standard deviations	70
6.6	SSPWP Increased true parameter values	70
6.7	SSPWP correlation matrix correlated variables	73
6.8	SSPWP Increased true parameter values MC	77
6.9	SSPWP Increased prior variable standard deviations MC model	77
6.10	SSPWP correlation matrix correlated variables MC model	77

Contents

Nomenclature	vii
List of Figures	viii
List of Tables	x
1 Introduction	1
1.1 Problem definition	1
1.2 Research questions	2
1.3 Report structure	2
2 Methodology	4
2.1 Introduction	4
2.2 Method of approach	4
2.3 Used software packages	5
3 Analysis Method Selection	6
3.1 Introduction	6
3.2 Inverse analysis	6
3.2.1 Reliability updating	6
3.2.2 Available methods	10
3.2.3 Method selection	13
3.2.4 Detailed method description	15
3.3 Synthetic analysis	20
3.3.1 Principle of the synthetic analysis	20
3.3.2 Synthetic analysis application	21
4 Cases Set-Up	22
4.1 Introduction	22
4.2 Cantilever Beam Problem	22
4.2.1 Properties of a simple problem	22
4.2.2 Cantilever beam	22
4.3 Sheet pile wall case	24
4.3.1 Properties of medium complicated and complicated problems	24
4.3.2 Sheet pile wall case	25
4.3.3 Simplification of Hochstetten field test for the medium complicated problem	30
5 Cantilever Beam Problem Analyses	38
5.1 Introduction	38
5.2 Solution uniqueness	39
5.2.1 One variable one observation	40
5.2.2 Two variables one observation	41

5.2.3	Two variables two observations	43
5.3	Multiple observations and observation correlations	45
5.3.1	Correlated observations results	47
5.4	Correlated variables	50
5.4.1	Correlated variables results	52
5.5	Method parameters	54
5.5.1	Method parameters results	55
5.6	Conclusions	57
6	Synthetic Inverse analysis of a Sheet Pile Wall	60
6.1	Introduction	60
6.2	SSPWP Observation plan analysis	62
6.2.1	Observation plan analysis results	64
6.3	Large difference between prior and true parameter values analysis	69
6.4	Correlated variables analysis	73
6.5	Different constitutive soil models analysis	76
6.6	Conclusions	79
7	Conclusions and Discussion	82
8	Recommendations	85
	Bibliography	86

Chapter 1 Introduction

1.1 Problem definition

Throughout the years the use and requirements of quay walls have changed. Also, a lot of different types of measurements of existing structures have become or will come available. The combination of the changed use of quay walls and the available measurement data raises the question; is it possible to quantify the reliability of the structure based on the available information?

Regularly available measurements are obtained during construction or from structures being loaded within their service domain. A structure's service domain is defined by the uppermost service domain boundaries, also called the Serviceability Limit States (SLS's). SLS's refer to the state of the structure that is required for it to perform its functions unhindered. For sheet pile walls this is regularly defined by maximum allowable deformations of the structure. In the case of failure, one can speak of a reached Ultimate Limit State (ULS). The ULS refers to failure or collapse of the total structure or of individual elements. Based on these definitions it can be reasoned that ULS's are mostly controlled by plastic behaviour and SLS's are controlled by a combination of elastic and plastic behaviour. This leads to the reasoning that the ULS's are largely influenced by the soil strength parameters while the SLS's are influenced by both the soil stiffness and strength parameters.

Limit states of a structure are initially defined during the design process using so-called prior information. This is information that is gathered through the process of desk studies and site investigations before the design and construction of the structure. Using this prior information the design is made with which the involved engineers attempt to estimate the structure's response under certain loading conditions. With response is, in this case, referred to every measurable response that a loaded structure experiences. Based on the estimated structural behaviour the structure's SLS's and ULS's can be estimated as well.

Upon construction, the behaviour of the structure can be observed. A structure's deformations can be constantly monitored showing how far the structure is from previously defined SLS's. This is not the case for every structure's ULS's. For example, the ULS definition of geotechnical failure is collapse- or exceptional deformation of the subsoil, where the strength of the soil (or the rock) makes a significant contribution to the resistance ([14] GEO limit state). When structures are designed they are designed according to design standards that demand certain reliability concerning geotechnical failure. This means that the chance of total structure failure is small and there is a high probability that an SLS prohibits the structure from reaching loading conditions that would provide additional information on a structure's ULS's.

To update a structure ULS's one needs additional information. This information can be provided in the form of direct observations as is mentioned above, but for practical and economic reasons a construction is not often tested until failure. The second option is obtaining additional information on the parameters used to design the structure. With updated parameters, the limit states of a structure can also be updated.

Performing additional site investigation on the soil conditions and additional laboratory tests provide extra information. But they are expensive and data interpretation errors and sample disturbance errors are not eliminated. This leads to the results having similar levels of uncertainty. Another possibility is to perform measurements on the structure and try to estimate or find the (most likely) parameter set that results in these measurements. This approach is called 'inverse analysis parameter updating'.

As mentioned earlier it is not likely for a structure to be tested until its ULS's. Therefore the most usual observations available of structures are measurements within the structure's service domain. This gives rise to the question if the ULS's can be updated by using service domain measurement data. To attempt on answering this question three sub research questions are set up below.

1.2 Research questions

The research question is:

Which types and what amounts of service domain measurement data are most effective in updating the calculated reliability (ULS's) of sheet pile walls?

With most effective is referred to as a minimum number of required measurements which result in accurate updating results in the least amount of time.

Sub-questions

1. Which reliability updating method is the most suitable for updating the calculated reliability of sheet pile walls?
2. Do advanced constitutive soil models have a parameter updating advantage over the linear elastic perfectly plastic Mohr-Coulomb soil model when applied in an inverse analysis method
3. Given the available service domain measurement data, can the soil strength parameters be updated effectively in order to update a sheet pile wall's ULS's?

1.3 Report structure

This report presents the entire process of attempting to answer the research questions. The process is divided into several chapters of which it is shortly described below what information every chapter contains:

- Chapter 2 *Methodology*; in this chapter an overview of the method of approach is given. In this method of approach, the performed research process is explained together with the materials needed for it.
- Chapter 3 *Analysis Method Selection*; this chapter provides background information on what reliability updating is after which the different available methods are explained. A suitable method is selected to be used for this research.
- Chapter 4 *Cases Set-Up*; for the research two different cases are used. In this chapter, the background information on these cases is provided together with a description of how they are applied.

- Chapter 5 *Cantilever Beam Problem Analyses*; the Cantilever Beam Problem is used as an introductory problem for applying the in chapter 3 selected reliability updating method.
- Chapter 6 *Synthetic Inverse analysis of a Sheet Pile Wall*; knowledge obtained about the application and the results of the used reliability updating method in the previous chapter is applied on a more complicated problem. This problem is a theoretical problem based on a real sheet pile wall field test.
- Chapter 7 *Conclusions and Discussion*; the conclusions of the different analyses are summed up in this chapter and used to answer the research questions. The discussion on the conclusions is also given in this chapter.
- Chapter 8 *Recommendations*; the recommendations contain possible follow up steps concerning this research.

Chapter 2 Methodology

2.1 Introduction

This chapter contains a description of the method of approach that is applied during this research. Together with this description, the reasoning behind every step in the method of approach is explained as well. Finally, the used software material and their sources are listed in the final section of this chapter.

2.2 Method of approach

The objective of this report is composing answers to the research questions that are stated in the previous chapter (chapter 1 Introduction). To accomplish this objective a method of approach is set up and visualized in (figure 2.1).

The first step is providing the background information that is necessary for understanding the successive steps. Belonging to the background information is a range of different subjects which is divided into two chapters (chapter 3 Analysis Method Selection, chapter 4 Cases Set-Up). The first chapter (chapter 3 Analysis Method Selection) contains information on the process of inverse analyses and the literature study on which the most suitable reliability updating method is selected. Additional to the reliability updating method an explanation is given on the principle of synthetic analysis. The second chapter (chapter 4 Cases Set-Up) describes the expected properties of the simple, medium complicated and complicated problems together with the selected cases for these problems.

Step two in the research is performing a series of different problem analyses. This series starts with the simple problem in (chapter 5 Cantilever Beam Problem Analyses) which has the purpose of understanding the mechanics and settings of the in (section 3.2 Inverse analysis) selected reliability updating method. Although successful analyses of the simple problem do not guarantee success with more complicated problems. Therefore the reliability updating method is applied to a geotechnical relevant case which is described in (section 4.3 Sheet pile wall case). First, this case is simplified in (chapter 6 Synthetic Inverse analysis of a Sheet Pile Wall) where the reliability updating method's parameter updating performance is tested. If the reliability updating method performs accordingly it is applied to the case with the real field test measurements to update the sheet pile wall's reliability and compare it with the field test measurements themselves.

Method obstacles

Upon performing the different analyses the complicated problem in step two couldn't be performed. The results of the medium complicated problem do not live up to the requirements to continue with the field test measurements. All the results and considerations made in this matter are described in (chapter 6 Synthetic Inverse analysis of a Sheet Pile Wall).

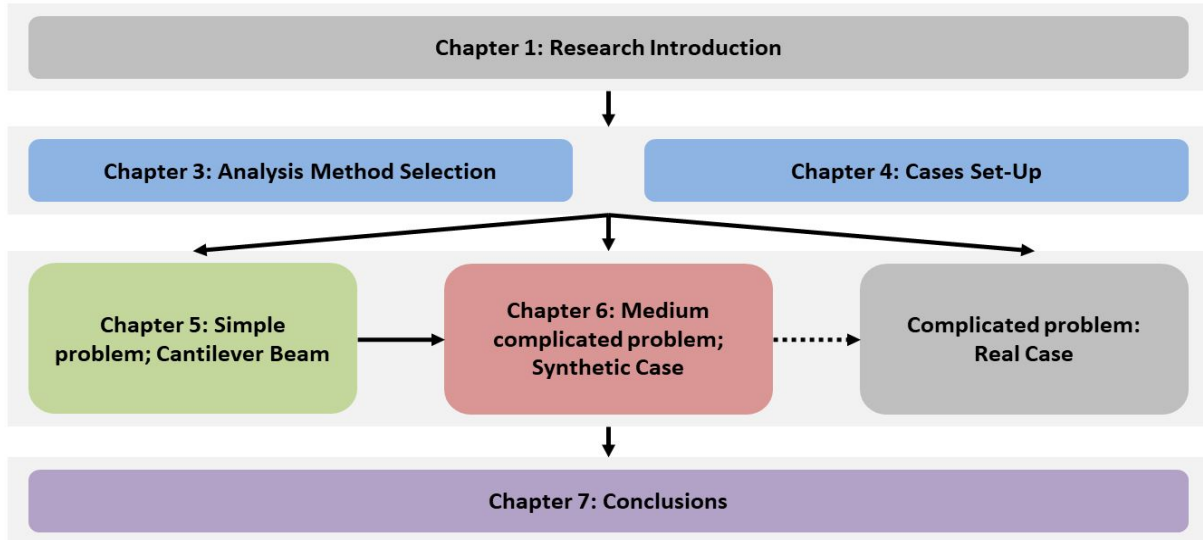


Figure 2.1: Flowchart of the method of approach

2.3 Used software packages

Two software packages that are used for this research are the open-source programming language Python (version 3.4.5) and the geotechnical Finite Element Method software Plaxis 2D (Plaxis 2D 2019.00, VIP license provided by Witteveen+Bos). Why the different software packages are used is described below.

Plaxis 2D

The main reason for applying Plaxis 2D is because it is a FEM software package specialized in geotechnical applications. Therefore it allows for relatively easy implementation and calculation of complicated geotechnical structures and its different construction phases. This is mentioned by R. Brinkgreve and W. Broere in [9]: "*PLAXIS is intended to provide a tool for practical analysis to be used by geotechnical engineers who are not necessarily numerical specialists*".

Using the Plaxis 2D program is split up in two main components being the input and the calculations. Both these aspects are explained in (section 4.3 Sheet pile wall case).

Python

Python is an open-source and versatile programming language. There are two reasons for working with this language during this research. The main reason is that the remote scripting tool of Plaxis2D is Python wrapped. The second reason is that the used aBUS-SuS method (method selection process is described in (Subsection 3.2.3 Method selection)) is provided in the Python language as well. Combining the Plaxis remote scripting tool with the Python version of the aBUS-SuS method allows for complete automation of the analysis process.

aBUS-SuS script

The aBUS-SuS method used in this thesis is developed by the Engineering Risk Analysis Group from the Technische Universitat Munchen. The python and MATLAB scripts are available on their website [16].

Chapter 3 Analysis Method Selection

3.1 Introduction

This chapter describes the analysis method selection and the necessary background information that is required to understand the in this research performed analyses and their results. The chapter is divided into two main sections which are given in (figure (3.1)).

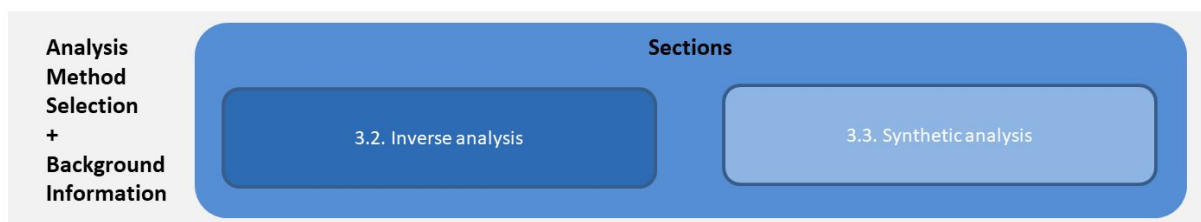


Figure 3.1: Subdivision of the analysis method selection chapter into two main sections. The numbers in the boxes correspond with the numbers of the sections in this chapter.

3.2 Inverse analysis

At the end of this section, the reliability updating method is selected which is used during the research. Although before this method is selected it needs to be understood how a structure's reliability is defined, what reliability updating is and which different reliability updating methods are available. Taking these aspects into account leads to the subdividing of this section into four subsections. First, the process of determining a structures reliability and the process of reliability updating is explained in (subsection 3.2.1 Reliability updating). Second is the subsection where different available reliability updating methods are listed (subsection 3.2.2 Available methods). The reliability updating method selection is described in the third subsection (subsection 3.2.3 Method selection). Finally, the selected reliability updating method is described in detail in the fourth subsection (subsection 3.2.4 Detailed method description).

3.2.1 Reliability updating

The reliability of a structure is a mathematical estimation of the structure's failure probability. This allows for the existence of different methods of different complexities for estimating the reliability of a structure. In this section, three different levels of reliability analyses are described after which the possible approaches of reliability updating are explained.

Level I

Determining a structure's reliability with a level I method is achieved with the use of partial factors during the design of the structure. This means that the reliability is not explicitly calculated but that it is based on the designing engineer's experience and current empirical

design codes. The partial factor values depend on the used parameter uncertainties and target reliability of the structure.

In this way of designing a set of design parameter values are defined by multiplying or dividing a characteristic parameter value by its corresponding partial factor as is shown in equations (3.1) and (3.2). Characteristic parameter values have a prescribed probability of exceedance. Characteristic values for load parameters generally have a low probability of exceedance of 5%, while resistance parameters have a high probability of exceedance of 95%.

$$X_{R,d} = \frac{X_{R,k}}{\gamma_{R,d}} \quad (3.1)$$

$$X_{S,d} = X_{S,k} \cdot \gamma_{S,d} \quad (3.2)$$

with:

- R = Resistance
- S = Load
- X_d = design parameter value
- X_k = characteristic parameter value
- γ_d = partial factor

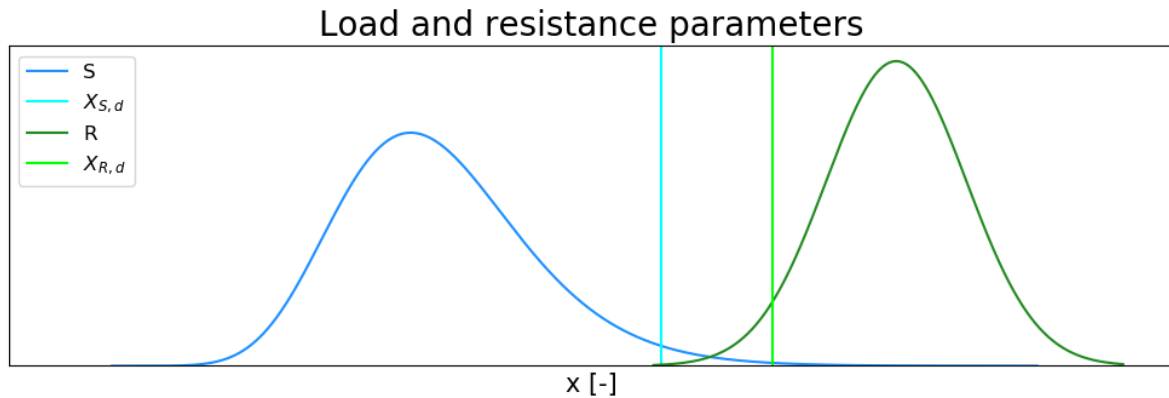


Figure 3.2: Example of the load (S) and resistance (R) design parameter values ($X_{S,d}$ and $X_{R,d}$) in a level I reliability analysis.

The reliability of the structure is defined by the probability that the load is larger than the resistance (figure 3.2). When for the case's design values holds that the resistance parameter(s) is/are larger than the load parameter(s) it means that the structure is assumed to be safe.

Level II

Oppositely to a level I analysis, in a level II analysis, the probability of failure is calculated explicitly. Although the problem is simplified by using approximated variables and limit state functions. Because of these simplifications, a level II method is not very accurate when used for complicated (non-linear) limit state functions and non-normal distributed variables. Level II methods calculate the failure probability separately for every failure mode. Therefore the failure mode's influences on each other are not taken into account during the reliability analysis.

The most widely used level II methods are the *First Order Reliability Methods* (FORM). As the name suggests no terms of the limit state function higher than the first order are included in the analysis, linearizing the problem [4]. By calculating the shortest distance from the origin in normalised parameter space to the failure space (limit state function) the reliability of the structure is assessed. A simple visualisation of this definition of a structure's reliability is given in (figure 3.3) where β represents the reliability index.

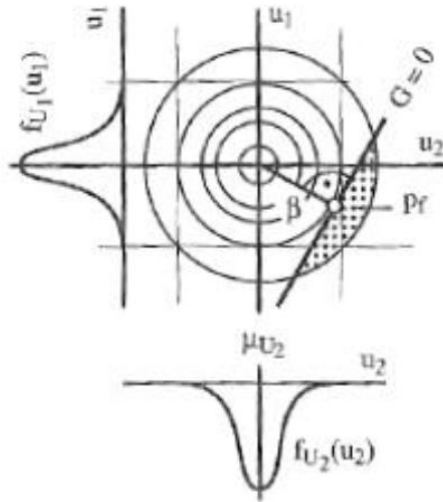


Figure 3.3: Reliability index determination of a FORM called the *Hasofer-Lind approach* (Source: [2])

Level III

Level III analyses calculate, just like level II analyses, the probability of failure explicitly. The level III probability of failure calculation is a mathematical formulation of the probability of failure. There are two ways of performing a level III analysis which depends on if the joint probability density function of the resistance and load is known. If it is known the probability of failure can be calculated by integration of the known joint probability density function. If this function is not known the probability of failure can be determined by integration.

The most common level III analysis is a Monte Carlo Simulation (MCS). The MCS generates a given number of random samples with which it is capable of approaching the limit state function if enough samples fall within the failure zone (figure 3.4). Although the MCS is known to be a straining method considering computation time when the probability of failure is very small. This is caused by the inherent small chance of the MCS of generating enough samples within the failure zone to be able to analytically describe it. More advanced methods are available which reduce the number of required samples drastically. A couple of these methods are described in (subsection 3.2.2 Available methods).

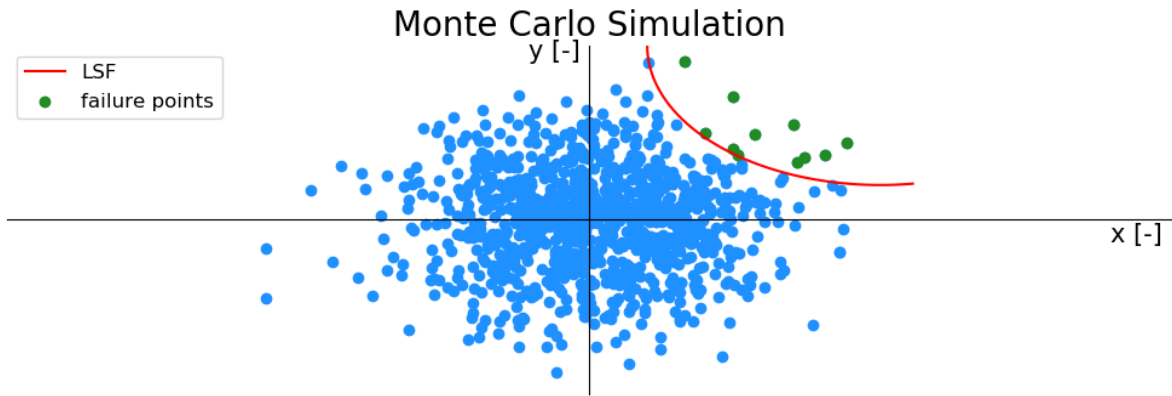


Figure 3.4: Example of a Monte Carlo simulation and an arbitrary limit state function (LSF). The LSF can be described using the blue points which fall within the failure zone. Although with a small probability of failure the MCS requires a large number of samples to generate enough failure points, making the MCS a demanding reliability analysis method.

Reliability updating approaches and inverse analysis

The process of reliability updating utilises obtained measurements from a structure to update the structure’s reliability. There are two different approaches to reliability updating. Both approaches, direct and indirect reliability updating, are visualised in the flowchart below (figure 3.5). In the process of indirect updating, the structure’s model parameters are updated allowing for the use of the calculation model to reassess the structure’s reliability. In direct updating, the updating of the model parameters is omitted and the structure’s reliability is, as the name implies, updated directly.

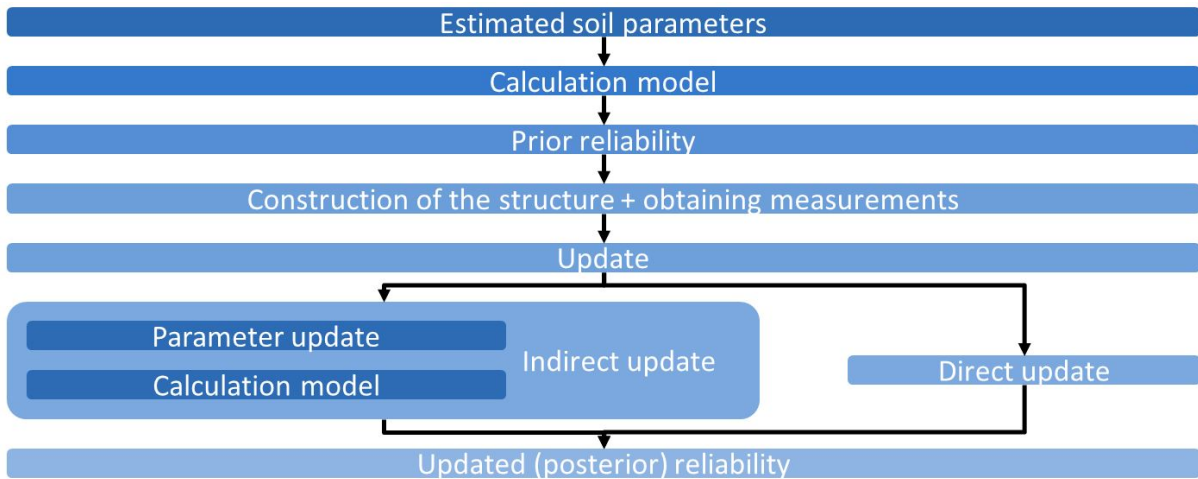


Figure 3.5: Flowchart of the reliability updating process. Starting with the prior model parameters with which the design is made and the prior probability of failure/ reliability is estimated and finishing with the updated reliability. Two different reliability updating processes are implemented in this flowchart, namely direct and indirect updating. With indirect updating, the model parameters are updated first while with direct updating the reliability is directly updated using the measurements.

As mentioned in the research questions in (section 1.2 Research questions) the interests of

this research involve updating of the parameters. Therefore the method that is selected in (subsection 3.2.3 Method selection) is expected to operate according to the indirect reliability updating. Since the final validation step of the case with the real field test measurements is not performed in this research (section 2.2 Method of approach) the main goal of the selected method is updating the model parameters (figure 3.5). Using measurements to update the model parameters is also called an inverse analysis, as it is attempted to back analyse which parameter set is the most likely parameter set to produce the used measurements. Therefore from this point on the selected method is referred to as an inverse analysis method.

3.2.2 Available methods

A wide range of different reliability updating or inverse analysis methods is available. Below a selection is presented of six different methods ([21], [29]) that are shortly described in this section. After presenting the different methods in (subsection 3.2.3 Method selection) the method considered most suitable is selected using a multi-criteria analysis.

Before the theory behind the different methods is described a short introduction is given to the Bayesian approach. With basic knowledge of this approach, the processes that are performed in the inverse analyses are expected to be more comprehensible.

Inverse analysis method selection	
Method	Abbreviations
Markov Chain Monte Carlo method with Metropolis Hastings algorithm	MCMC-MH
Maximum Likelihood method	ML
Genetic Algorithm	GA
Kalman Filter	KF
Regularized Particle Filter	RPF
adaptive Bayesian Updating with Structural reliability methods with Subset Sampling	aBUS-SuS

Table 3.1: Selection of possible inverse analysis methods and their abbreviations

Bayesian approach

Bayesian updating is based on the conditional statistics theory as proposed by Bayes in 1763 (equation (3.3)). Bayes's theorem states that the probability of an event is proportional to prior knowledge of the random variables affecting it and their likelihood of happening. Compared to traditional frequentist thinking, Bayesian analysis interprets probability as a degree of belief on a statement about unknown quantities [33].

$$p(x|y) = \frac{p(y|x)p(x)}{p(y)} \quad (3.3)$$

With:

$p(x)$	The probability that event x occurs
$p(y)$	The probability that event y occurs
$p(x y)$	The conditional probability that event x occurs when event y is true
$p(y x)$	The conditional probability that event y occurs when event x is true

The components of Bayes' theorem can be described in a different, more geotechnical relevant sense;

$p(x)$	Prior distribution, describing the knowledge of the parameter state a priori.
$p(y)$	Marginal distribution. It is often not possible to describe this term analytically, in those cases it is treated as a normalizing constant.
$p(x y)$	Posterior distribution, which is the updated estimation of the random variable distributions in case of certain measurements or observations.
$p(y x)$	Likelihood function, describing the connection between the measurements or observations and the random model variables.

MCMC-MH

The Monte Carlo Simulation method is a stochastic method relying on the random sampling of input parameters to optimize a function. To achieve this the Monte Carlo Simulation method generates large numbers of realizations (simulations) that produce parameter values out of a given prior probability distribution [15]. Because of the randomness in this method, it is an efficient method for dealing with problems where parameter uncertainty is dominant and optimization is required [21].

The Markov Chain method is a process where the next step depends solely on the current state, and not the path followed until reaching it [15]. A distribution centred around the current parameter values is used to generate and pick the next step. This way the Markov Chain method creates a 'random walk' that tries to approach the target distribution. Ensuring path convergence of the chain is achieved with an error minimization algorithm that judges which values are accepted or rejected. For this research, the Markov Chain method that is based on the Modified Metropolis-Hastings algorithm is used [10].

Combining the two methods results in the Markov Chain Monte Carlo method based on the Metropolis-Hastings algorithm (MCMC-MH). This is a method that is effective in simulating complex probabilistic processes while preserving the parameter statistics.

ML

The Maximum Likelihood method is an inverse analysis method that uses a series of iterations aiming to maximize the likelihood of producing the measurements. The likelihood is analogous to the conditional probability of generating the observations. This is achieved by including the error between the observed measurements and the produced measurements as the main term in the method's objective function. Minimizing this function equals minimizing the error and thus convergence which is expected to be to a single point.

GA

The Genetic Algorithm is an optimization algorithm that exploits the theory of genetic evolution. To achieve this the algorithm is organized in generations. Every generation exists out of sample sets which are used as input for the examined function. The result of each parameter set is judged by a fitness function that is defined by the user, assessing every individual set's efficiency. New generations are produced as long as no adequate solution is achieved. This generation production is based on three main routines ([11], [23]).

- *Selection:* All the sets are ranked based on their fitness score. 'Parent' sets are randomly

selected for 'breeding' but with the highest ranks having the highest probability of being selected.

- *Crossover*: The selected parent sets are used to generate new parameter sets. This process is performed according to a user-defined function. Although its main purpose is to exploit the best properties of the parent sets.
- *Mutation*: This is the process that adds a factor of randomness to the optimization procedure. New generation sets are generated by randomly altering the parent sets. By including this random component the algorithm is better equipped to explore variable domains.

KF

The Kalman Filter is a recursive Bayesian algorithm that works on reading measurements at multiple time stages and then tries estimating the parameter values that produce these measurements. A special feature of the Kalman Filter is that the measurements are expected to contain noise. This originates from one of the main assumptions on which the Kalman Filter is based, namely that the variables and measurement noise of a Gaussian distribution is processed through a linear function. Therefore the final product will also be distributed in a Gaussian manner [8]. For the Kalman Filter to work it heavily relies on successively handling the parameter-variable and measurement error (noise) covariance matrices. With the contribution of these matrices, the method determines the measure of change that each variable needs to undergo.

Different variations of the Kalman Filter exist but for this thesis, two versions are of interest. These are the Extended Kalman Filter and the Ensemble Kalman Filter. With slight modifications of the original method, the Extended Kalman filter is able of approximating non-linear functions with its Jacobian [31]. The Ensemble Kalman Filter is a combination of the original method and the Monte Carlo method. The Ensemble Kalman Filter reduces the computational requirements by removing the need to maintain the covariance matrix. It does so by employing an ensemble of variable values which are used to calculate the covariance in each assimilation step [13].

RPF

The Particle Filter is a similar method to the Ensemble Kalman Filter. It uses an ensemble of individuals that represent the variable states (particles) as the core of the procedure. This ensemble is initially sampled using the Monte Carlo method, making the Particle Filter a genetic type Monte Carlo scheme. The particles are weighted based on how close they approach a target distribution with the final solution being the weighted average of the ensemble [24].

A version of the Particle Filter method is the Regularized Particle Filter which deals with an inherent problem of reduced variance after weighting in the Particle Filter method. By applying a distribution kernel the influence of the particles with the largest weights is smoothed out by converting discrete cumulative distributions into continuous ones. This way it is prevented that the method collapses on a single particle after a few assimilation steps.

aBUS-SuS

The adaptive Bayesian Updating with Structural reliability methods with Subset Sampling is an inverse analysis method that uses conditional sampling in combination with the Monte Carlo method and the process of Subset Sampling ([30], [29]). Because of the use of the Subset

Sampling method the aBUS-SuS method is a very efficient method to compute small failure probabilities ([28], [5]). With this combination of properties, the aBUS-SuS method is capable of dealing with non-linear target functions.

Using the Monte Carlo approach an initial subset is generated in the normalised parameter space. With the conditional sampling method, based on a user-defined likelihood function (LF) and settings, the following subsets are generated until the method is converged. The method returns updated parameter distributions that are considered the most likely parameter combination to produce the observed measurements.

3.2.3 Method selection

No results are available where this list of methods is applied to the same problem, allowing for direct performance comparison. Therefore the methods are compared based on the following criteria. First, the methods are compared on whether they are capable of dealing with non-linear target functions. Secondly, the methods are compared to each other on the type of results that they produce, if they are stochastic or deterministic. Thirdly, the ease of use is estimated by comparing the required observations for the methods to work properly. Finally and maybe one of the most important criteria is the availability of the analysis scripts. Short descriptions of why these criteria are selected and how they are applied are given below.

Method comparison criteria:

- *Non-linear target functions:* for relatively complex cases, like FEM model calculations of sheet pile walls, the target functions (limit state functions) are usually non-linear functions. This raises the requirement of the method being able to approach these non-linear target functions.
- *Stochastic or deterministic results:* The inverse analysis methods are used to update the model parameters after which it is the intention to reassess a structure's reliability. To be able to perform a reliability analysis the parameter uncertainties are required (subsection 3.2.1 Reliability updating). This means that stochastic results are preferred over deterministic parameter results.
- *Required amount of observations:* Some methods require a relatively large period of measurements to be able to effectively perform an inverse analysis. This can significantly influence the effectiveness (section 1.2 Research questions) of the method.
- *Availability of method scripts:* Finally the availability of the analysis script is considered to be important since this influences the ease of use of the method. For this thesis the analysis script should be available for, or easy to implement in the programming language Python.

The method selection results are also given in (table 3.2). The full explanation of the method selection process is given below.

Non linear target functions

Based on the literature study performed on the different methods it is concluded that the MCMC-MH, GA, RPF and aBUS-SuS are properly equipped to approach non-linear target functions. The original KF method is fitted for linear problems. Adaptations can be made to the KF, resulting in, for example, the Extended KF (ExKF). Although it does increase the model complexity, making it not the most favourable method to apply to non-linear problems.

According to literature, the ML method is not capable of approaching non-linear target functions, making it an unfavourable method for this research.

Stochastic or deterministic results

The MCMC-MH, RPF, aBUS-SuS and KF return stochastic updated parameter results but there is doubt about the GA method. As mentioned in the description in (subsection 3.2.2 Available methods) the GA method uses generations with multiple samples which is the reason why for example the aBUS-SuS method is considered to return stochastic results. Although in [21] it is mentioned that the GA tends to converge towards a deterministic solution nevertheless. In [21] a possible adaption to the GA is proposed to counteract this tendency of the GA by artificially increasing the generation's variance after every analysis step. But this approach is not favoured in this research since the mathematical adaptations are not properly validated yet. Finally, the ML method, which returns a single (deterministic) set, is an unfavourable method for this research.

Required amount of observations

The analyses in [21] show that the methods MCMC-MH, KF, GA and ML do not require a lot of observations to be able to perform an analysis. Based on the literature research on how the aBUS-SuS method works it is concluded that the aBUS-SuS method doesn't require a lot of observations either. In theory, the MCMC-MH, aBUS-SuS, KF, GA and ML methods are capable of performing a model parameter update based on little measurements. On the opposite is the RPF method which requires a long timeline of observations for the method to be able to condition the parameter values [21]. Therefore the RPF method is not a favourable method for this research.

Method script availability

Based on the previous comparison criteria the two methods that are considered the most favourable are the MCMC-MH and aBUS-SuS. Therefore the research on the script availability is only performed for these two methods. As mentioned in (section 2.3 Used software packages) the method scripts need to be available in the programming language Python to be able to control the Plaxis software via remote scripting. From both the aBUS-SuS and MCMC-MH methods it is known that they are available in the python language. The finished script of the aBUS-SuS method is found on [16] while from the MCMC-MH it is known that there are python tools available to perform the method.

At this point in the method selection, the aBUS-SuS and MCMC-MH are both considered suitable methods. The final point of comparison, method script availability, is not decisive. Therefore the two methods are compared on additional method properties which are described below in (subsection 3.2.3 MCMC-MH aBUS-SuS comparison).

MCMC-MH aBUS-SuS comparison

According to [30], the aBUS-SuS method is an improvement on the MCMC-MH methods. Where the MCMC techniques aim to construct a chain of samples from which every drawn sample is a more likely realization of the target distribution. A disadvantage of the MCMC-MH method is the dependency on the starting values (burn-in) and the fact that the steps of the chain are dependent by definition (autocorrelation) [21]. The aBUS-SuS method is based on SuS, which is in its turn also based on the Markov Chain method. Although the adapted Markov

Chain method used in the SuS does not suffer from the burn-in problem because the seeds of the Markov Chains always follow the target distribution [30]. Nevertheless, no exclusion of the autocorrelation problem in the aBUS-SuS is given.

Both methods are expected to be able to calculate small failure probabilities. Where the MCMC-MH does it with a chain of samples the aBUS-SuS does it with a chain of subsets. In literature, the SuS implementation is considered an improvement on the MCMC method and especially for calculating small failure probabilities ([5]) which is in favour of the aBUS-SuS method.

Inverse analysis method comparison					
Method	Non-linear target functions	Deterministic results	Required observations	Availability	Additional properties
MCMC-MH	+	+	+	+	-
ML	-	-	+	<i>na</i>	<i>na</i>
GA	+	+/-	+	<i>na</i>	<i>na</i>
KF	+/-	+	+	<i>na</i>	<i>na</i>
RPF	+	+	-	<i>na</i>	<i>na</i>
aBUS-SuS	+	+	+	+	+

Table 3.2: Results of the inverse analysis method multi-criteria analysis

Method selection conclusion

Based on the method comparison above it is concluded that the aBUS-SuS is the most favourable method for the inverse analyses that are performed in this research. The margin is relatively small but with the cumulative influence of the method script availability, dependency on the starting value and the performance on calculating small failure probabilities the preference moves towards the aBUS-SuS method.

With this decision, it is important to properly understand the mechanics of the aBUS-SuS method. A detailed description of the method is given below in (subsection 3.2.4 Detailed method description).

3.2.4 Detailed method description

The process of running an inverse analysis using the aBUS-SuS method goes through four main phases. A flowchart of the entire process is given in (figure 3.6) and descriptions of the four phases and the main processes that are being performed in every phase are given below.

The four main phases of the aBUS-SuS analysis:

- **1. Problem initialization:** Almost all the actions in this phase are specific to the analysed problem and are therefore up to the user to define. Falling under these actions are defining the prior parameter distributions, defining the observations, defining a solution to or construct a (FEM) model of the problem and finally define the likelihood function (LF). Before starting the aBUS-SuS analysis the method parameter values need to be defined, these parameters are N (number of samples per subset) and $p0$ (conditional probability of each subset).

- **2. Start of the aBUS-SuS method with Monte-Carlo simulation (MCS) step:** Before the aBUS-SuS analysis can start the N , p_0 values need to be checked. The aBUS-SuS method can only handle values that meet the following conditions: $N \cdot p_0$ and $1/p_0$ have to be positive integers. When these conditions are met the initial sampling generation is initiated. The N samples are randomly generated with an MCS after which for every sample the likelihood function is evaluated.
- **3. Conditional sampling loop until the aBUS-SuS analysis is finished:** The conditional sampling loop is a process inside the aBUS-SuS analysis and the start of the SuS. This process is described in detail in (subsection 3.2.4 aBUS-SuS convergence).
- **4. Post aBUS-SuS data processing:** At this final phase the aBUS-SuS analysis results are processed which depends on the user's intentions.

Typical aBUS-SuS results, SuS behaviour and how this SuS behaviour depends on the used observations are explained and illustrated in the next chapter (chapter 5 Cantilever Beam Problem Analyses) using the cantilever beam problem as a reference model.

aBUS-SuS Likelihood Function

The function of the LF is determining the probability of every generated sample resulting in the measurements. This is a way of quantifying the distance between the observation(s) and the results of all the different parameter set calculations. How the LF quantifies this distance depends on the type of distribution that it is based on. Below an example is given for an LF that is based on a Gaussian/normal distribution.

Depending on the number of observations a mono-variate or a multi-variate Gaussian distribution is used. The mono-variate distribution (equation (3.4) is used (as the name implies) when one observation is used for the analysis and the multi-variate distribution (equation (3.5) is used in the case of multiple observations [30].

A visualization of the mono-variate Gaussian LF is given below in (section 3.2.4 aBUS-SuS convergence).

$$L(x) = \frac{1}{\sqrt{2\pi\sigma^2}} \exp\left[-\frac{(x - \mu)^2}{2\sigma^2}\right] \quad (3.4)$$

With:

- x = parameter set result(s)
- μ = observation mean
- σ = observation standard deviation

$$L(x) = \frac{1}{(2\pi)^{\frac{n}{2}} \sqrt{\det(\Sigma)}} \exp\left[-\frac{1}{2}[x_1 - \mu_1, \dots, x_n - \mu_n] \sum_{i=1}^{-1} [x_1 - \mu_1, \dots, x_n - \mu_n]^T\right] \quad (3.5)$$

With:

- x_i = parameter set result(s) at point i
- μ_i = observation mean at point i
- n = number of used observations
- Σ = observation covariance matrix

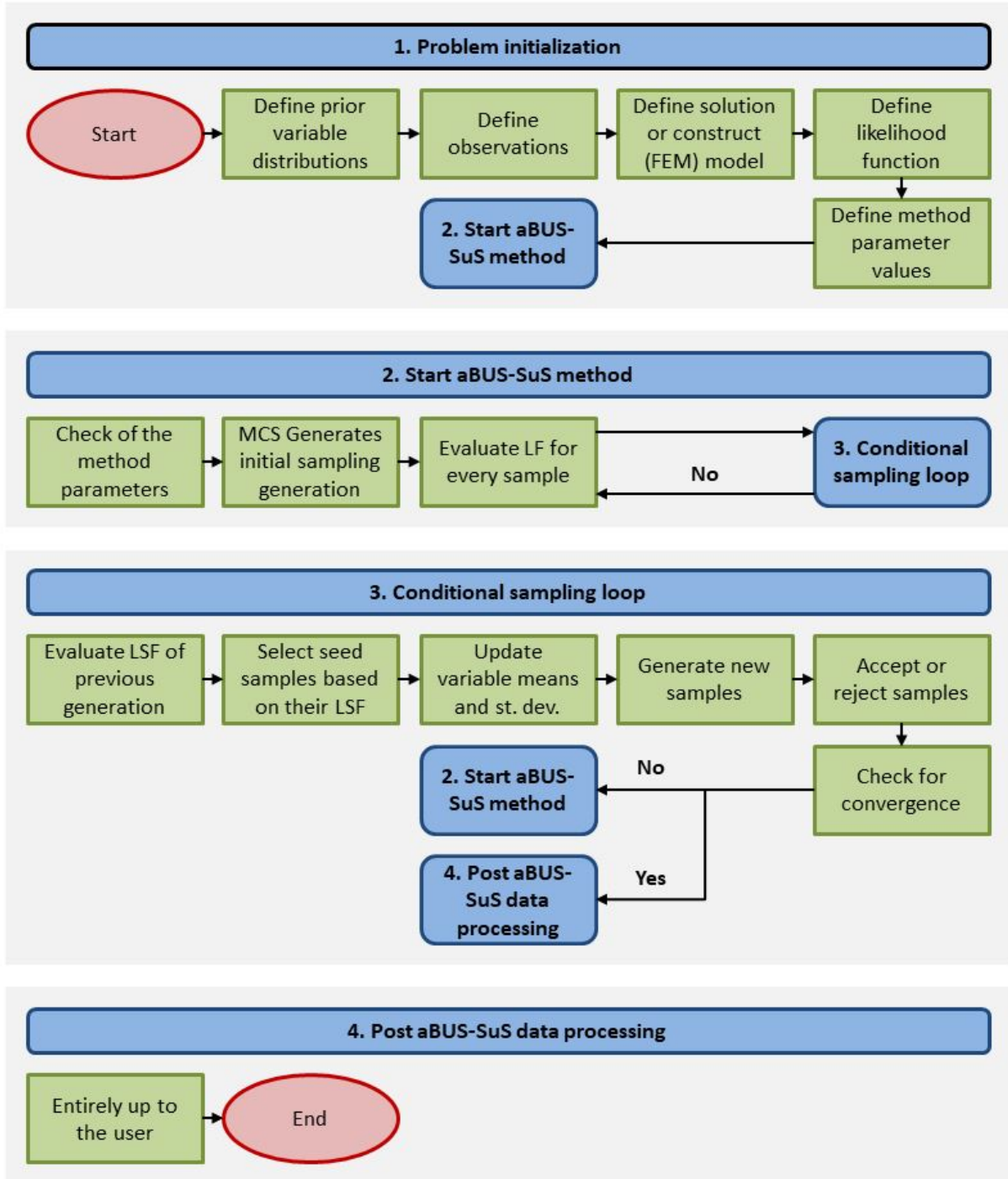


Figure 3.6: Flowchart of the aBUS-SuS method showing the four main phases in the aBUS-SuS inverse analysis method

aBUS-SuS convergence

To explain how the convergence of an aBUS-SuS analysis works an arbitrary problem is used as an example. For this exemplary problem, a series of plots are used which are given in (figure 3.7).

The aBUS-SuS method starts with the generation of the first subset of variable samples with the

initial MCS step. This initial MCS set of samples is visualised in (figure 3.7 1. aBUS-SuS subset 1var) which represents the initial MCS set of a problem with one variable and one observation. Other information that is obtained from looking at this figure is that the prior mean variable value and the true variable value are known. The true value is generally unknown but this is a property of this example being a synthetic analysis, which is explained in (section 3.3 Synthetic analysis). It can also be seen that in this case the variable is normally distributed. The samples are generated in normalised space where the normalised prior mean value is equal to zero and the normalised prior mean value plus one prior standard deviation is equal to one. Along with the sample generation, there are N normal random values between -1 and 1 generated for a variable called 'p'. This is in the method called 'the uniform variable of BUS'. These p values are used in the next step.

The second step of the aBUS-SuS method is calculating the model response for every generated variable (set). In this case, it is an arbitrary response which is visualized in (figure 3.7 2. aBUS-SuS subset 1 obs). This is the first step where the user-defined LF comes into play. This LF is visible in the figure as a normal distribution around the observation that is the result of the true variable value in (figure 3.7 1. aBUS-SuS subset 1var). After the calculation of all the model responses, the LF is used to quantify the distance of the individual model responses to the observation. The closer the model response is to the observation(s), the higher its value. With the natural logarithm of these LF values (LLF) a limit state function (LSF) is evaluated for every model response. This LSF is based on the p values of the previous step, the maximum LLF value and all the individual LLF values. The LSF is given in (equation 3.6).

$$LSF = \ln(\text{norm.cdf}(p[:]) + LLF_i - \max(LLF)) \quad (3.6)$$

The lowest $p0*100$ per cent value of all the LSF values is determined, which is used as the prior subset h value. In this case $p0$ is equal to 0.1 and h is bigger than zero which means that the $p0*100$ percentile value corresponds with the best performing $p0*100$ per cent LF values. These best performing samples are indicated in (figure 3.7 2. aBUS-SuS subset 1 obs) with the pink line. If h is smaller than zero the percentage of the N samples that returned a LSF value smaller than zero is taken for this percentile limit.

The third step in the aBUS-SuS analysis is selecting the, in this case, best performing ten per cent of the samples in the initial MCS sample set. These samples are called seed samples as they are used as 'seeds' for the generation of the next subset. The variables are updated according to the seed samples and a number of $N - \text{number of seed samples}$ new samples are generated as the seed samples are also being a part of the next subset. The new samples that are generated are roughly indicated with the purple curve in (figure 3.7 3. aBUS-SuS subset 2 var). At this point, the sample rejection criterium rejects the samples that perform worse than the pink line and a random seed sample is duplicated in the subset.

After this point the second sample set is tested for its model response and the parameter h is updated. The updated parameter is called *modified h* and is calculated using (equation 3.7). The purpose of this equation is to test if the new subset performs better than the previous one. It does so by comparing both subset's best performing samples, which can be considered as a measure for the progression of the entire subset. If the new subset moved closer to the observation *modified h* is larger than h .

$$h_{mod} = h - LLF_{max,seeds} + LLF_{max,new} \quad (3.7)$$

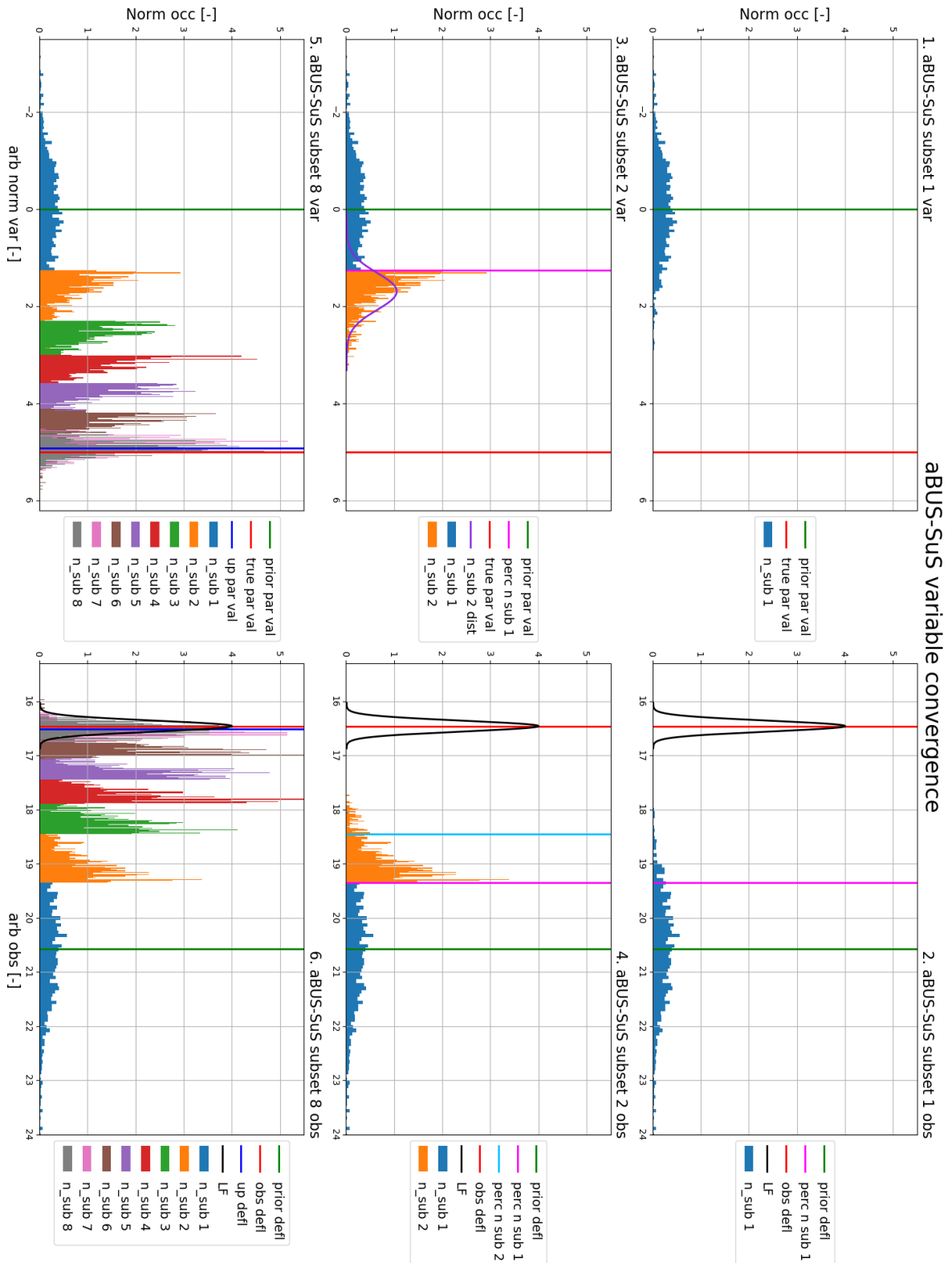


Figure 3.7: Visualization of the variable value and observation convergence process in an aBUS-SuS analysis. The process is visualised for an arbitrary case with normalised values on the x and y axes. The left column shows the convergence of the model variable and the right column shows the convergence of the model observation.

$$LLF_{max,new} = \max(LLF_{max,seeds}, \max(LLF_{new})) \quad (3.8)$$

It is also this equation (equation 3.7) through which the analysis concludes if it is converged. As long as the new subsets improve on approaching the observation the value of *modified h* returns positive, but when *modified h* returns being equal to zero the analysis is considered converged (figure 3.7 6. aBUS-SuS subset 8 obs).

The observation standard deviation influences this convergence process. It does so by widening the LF. As the LF widens the chance of a new subset diverging from the observation mean compared to the previous subset increases over distance. It is the inherent property of the analysis method to converge towards higher LF values, but as more seed samples are selected when the subsets move closer to the observation(s) the progress of each new subset automatically becomes smaller. This is also observed in the final two plots of (figure 3.7) where the final subsets almost completely overlap.

3.3 Synthetic analysis

3.3.1 Principle of the synthetic analysis

In a synthetic aBUS-SuS analysis the observations are generated with a known set of parameters, the 'true' parameter values. This way, after an analysis is performed, the updated parameter values can be compared with the true parameter values and thus allow for exact testing of the aBUS-SuS method's updating effectiveness and accuracy. The process described above is visualised with the flowchart in (figure 3.8).

The main reason for applying synthetic analyses is because it eliminates model uncertainties that are involved when real observations are used. Real observations represent real-world behaviour and therefore are accompanied by a lot of model uncertainties when they are used as observations in an aBUS-SuS analysis. This combined with the fact that the true parameter values are unknown makes it nearly impossible to validate the updated parameter values. Therefore the synthetic analysis is used to test the aBUS-SuS method's performance on relatively complicated problems like in (chapter 6 Synthetic Inverse analysis of a Sheet Pile Wall).

In this report, the updated parameter values are compared with the true values by normalising the updated parameter values on the true values. This way the normalised updated values should approach the value of one. If a normalised updated parameter value is, for example, equal to 0.8 it means that the updated value has an underestimation error of twenty per cent.



Figure 3.8: A flowchart describing the process of a synthetic analysis. The true parameter values are generally unknown as the purpose of performing an inverse analysis is to estimate these true parameter values.

3.3.2 Synthetic analysis application

In this thesis the synthetic analysis is applied in both the chapters (chapter 5 Cantilever Beam Problem Analyses, chapter 6 Synthetic Inverse analysis of a Sheet Pile Wall). In addition to the synthetic analysis, it is also possible to add noise to the synthetically generated observations. Although with the purpose of these analyses being the initial test of the parameter updating performance of the aBUS-SuS method, adding noise to the observations is at this point considered to be defeating the point of performing the synthetic analysis.

Chapter 4 Cases Set-Up

4.1 Introduction

This chapter describes the used cases and the background information that is required to understand the in this research performed analyses and their results. Two different cases are used in this thesis, therefore the chapter is divided into two main sections. Each contains the background information that led to using the described case and how it is set up for the analyses in the following chapters (chapter 5 Cantilever Beam Problem Analyses, chapter 6 Synthetic Inverse analysis of a Sheet Pile Wall). The subdivisions of this chapter are given in (figure (4.1)).



Figure 4.1: Subdivision of the Cases Set-Up chapter into two main sections. Every section contains background information that is required to understand the in this report used cases

4.2 Cantilever Beam Problem

4.2.1 Properties of a simple problem

The main property that is expected from a simple problem is the availability of an analytical solution. Performing an inverse analysis using an analytical solution is beneficial because of the low complexity of the individual calculations which results in short computation times. Short computation times allow the user to quickly perform multiple analyses. Therefore a simple problem is suitable for getting to know how to apply the inverse analysis method and test the mechanics and limits of the same method.

In the subsection below (subsection 4.2.2 Cantilever Beam) the selected simple problem is explained after which the performed analyses and their results are explained in (chapter 5 Cantilever Beam Problem Analyses).

4.2.2 Cantilever beam

Cantilever beams are widely applied in the civil engineering field, for example as support beams in balconies and other overhanging structures. Different cantilever beam cases are available, but for this chapter, the cantilever beam problem (CBP) with a fixed end and a point load on the opposite end is used. The geometry of the problem is visualized in (figure 4.2) and its analytical solution to calculate the beam's deflection is given by (equation 4.1). Another measurement

that can be performed on the cantilever beam is the moment of force which is for an end-loaded beam described by the analytical solution (equation 4.2).

Three parameters are indicated in (figure 4.2). The length of the beam (L), force at the tip of the beam (F) and the flexural rigidity of the beam (EI). With these three parameters, all the necessary information is available to solve the CBP's analytical solutions.

$$w = \frac{Fx^2}{6EI}(3L - x) \quad (4.1)$$

$$M = F(L - x) \quad (4.2)$$

With:

x	= Distance away from the base of the beam	$[m]$
F	= Force at the end of the beam	$[kN]$
L	= Length of concrete beam	$[m]$
EI	= Flexural rigidity of the concrete beam	$[kNm^2]$

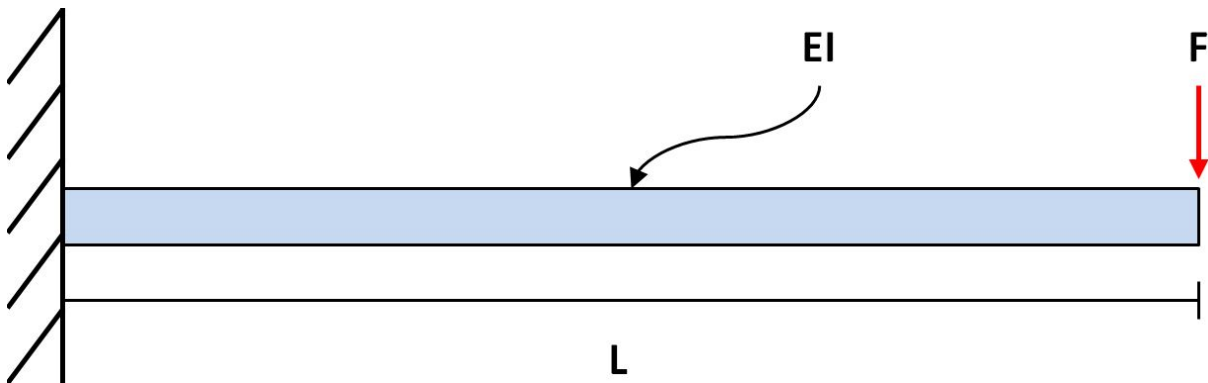


Figure 4.2: Cantilever Beam Problem geometry of a cantilever beam with a fixed base and a point load on the free end.

Cantilever beam parameter sensitivity

From the analytical solutions (equations 4.1 and 4.2) it can be deduced what influence each parameter has on the predicted response of the beam. The individual variable influences on the beam deflection at the tip of the beam are visualised in (figure 4.3) and are linear, cubic, and inverse for the parameters F , L , EI respectively. The influences of F and L on the moment of force are not visualised as they are both linear.

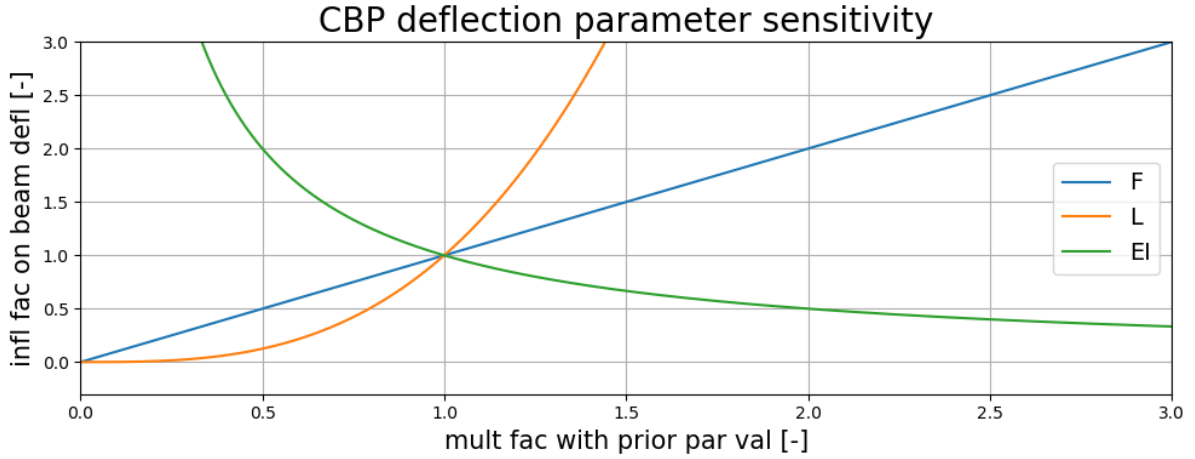


Figure 4.3: Influence of the individual parameters on the deflection of a cantilever beam. The x-axis represents the multiplication of the variable and the y-axis represents the influence on the cantilever beam deflection.

CBP prior parameters

For the CBP example the used parameter values are based on the CBP in [32]. These parameter values are given in (table 4.1). The CBP as it is described above is in (chapter 5 Cantilever Beam Problem Analysis) implemented in the aBUS-SuS analysis. For this reason, the parameter set in (table 4.1) is defined as the prior parameter set which is used to create the prior parameter distributions mentioned in (subsection 3.2.2 Bayesian approach). For simplicity reasons the defined prior parameter values are used to describe the prior parameter distributions as Gaussian/normal distributions.

Cantilever beam problem prior parameter values					
Parameter	Symbol		Mean value	Standard deviation	Distribution
Force	F	[kN]	10.0000	0.5000	normal
Length	L	[m]	5.0000	0.1000	normal
Flexural rigidity	EI	[kNm ²]	2.0250 · 10 ⁴	1.0125 · 10 ⁺³	normal

Table 4.1: Prior parameter values of the cantilever beam problem. Based on the cantilever beam problem described in [32]

4.3 Sheet pile wall case

4.3.1 Properties of medium complicated and complicated problems

Compared to the properties expected from a simple problem as described in (subsection 4.2.1 Properties of a simple problem), for the medium complicated and complicated problems no analytical solution is expected. The simple problem is used for understanding the inverse analysis method mechanics and processes after which the method is applied to the medium complicated and complicated problems.

The medium complicated problem is used to test the aBUS-SuS's (section 3.2 Inverse analysis) capability of updating model parameters of a sheet pile wall case. Instead of an analytical

solution, it should be possible to perform model computations of the selected geometry and it is assumed that the true parameter values are known, which is called a synthetic analysis explained in (section 3.3 Synthetic analysis).

If the results of the medium complicated problem are conclusive enough it is decided if it is worth it to perform complicated problem analyses. Compared to the medium complicated problem the complicated problem is also a sheet pile wall case, although in this problem the true parameter values are not known and real field measurements are used. To be able to update the soil parameters and subsequently the structure's ULS, field test measurements of a structure tested till failure are required. These measurements are then used to compare the updated expected behaviour with the structure's real behaviour.

A sheet pile wall case is required which is tested till failure and is elaborately monitored in the process. This case can be used for both the medium complicated and complicated problems with only minor adaptations. Two potential cases are shortly described and compared below, after which the most suitable one is described in detail in the rest of this section.

Two sheet pile wall failure field tests are found in literature, the Hochstetten field test performed in Hochstetten Germany in the year 1993 [34] and the Rotterdam field test performed in Rotterdam the Netherlands in the year 2000 [18], [17]. Both tests have the purpose of observing the sheet pile wall failure and are therefore both extensively monitored. The main difference between the tests is the soil conditions. The Hochstetten case is performed in medium dense sands with sections of silty sands and gravely sands while the Rotterdam case is performed in soft soils with alternating clay, peat and sandy layers. The relative homogeneous sandy soil conditions of the Hochstetten case are preferred over the strongly heterogeneous soft soil conditions of the Rotterdam case for the parameter updating process. Therefore the Hochstetten case is selected as a reference case for the medium complicated and complicated problems.

4.3.2 Sheet pile wall case

Hochstetten field test background information

The Hochstetten field test is performed in the year 1993 in Hochstetten, Germany. The test is mentioned in many papers and articles. A couple of examples are [7], [6], [19], [20], [12] and [34] with the last one being the most extensive as this is a full report of the test describing the preparations, executions and analysis of the field test measurements in full detail. The downside of this report is that it is written in German and no English translation is found. Two sketches of the field test geometry are given in (figure 4.4) and (figure 4.5).

For the field test, a pit is constructed of five meters deep, nine meters long and four meters wide. The length of the test wall section is seven meters. Two different types of sheet pile elements are used, heavy and stiff *ARBED PU 8* elements are used for the pit itself and weaker *KRUPP KD VI* elements are used for the test wall. The *ARBED* and *KRUPP* elements reach to a depth of eight and six meters respectively. For support of the test wall, three *KRUPP Gi-SV-380* struts are installed which are connected to *HEB 240* waling beams on both the support (Spundwand) and test walls. A four-meter wide and seven-meter long, one-meter deep water basin is positioned between one and five meters behind the test wall to act as a surface load. One of the major intentions of the Hochstetten field test was that it could be used to update the design norms of that time. With this in mind and the fact that sheet pile walls are usually linear structures, the field test was designed in such a fashion that the cross-sectional profile would experience as little influence from the out of plane directions as possible. This was achieved by installing two seven-meter long, five-centimetre thick bentonite walls (*Schmalwand*)

to act as gliding surfaces (figure (4.4)). This allows the central cross-section (figure 4.5) to be simulated using two-dimensional approaches.

To reduce the deformations of the support and side walls these sections are fixed together which results in a very stiff configuration of the test pit. Combined with the high stiffness of the *ARBED* elements it is assumed that the deformations of the support wall are negligible.

Two additional waling beams of the type *HEB 140* are indicated to on the test wall in (figure 4.5). These beams don't have any stiffening or load distributing function. Instead, they function as measuring points for the horizontal displacements of the test wall. More information on the performed measurements is given below in (subsection 4.3.2 Hochstetten measurements).

Hochstetten construction phases

Construction of the test pit and execution of the field test took place in nine phases. These phases are listed below in (table 4.2) together with a short description of the performed actions in every phase.

In the initial phase, all the sheet piles are installed after which the test pit is excavated in several steps to the final depth of five meters. In the third phase, the struts were installed and pre-loaded with a normal force of 4.29 kN/m, representing the average normal force on the three struts induced by the test wall. Construction of the test pit was completed with the positioning of the water basin as the surface load behind the wall.

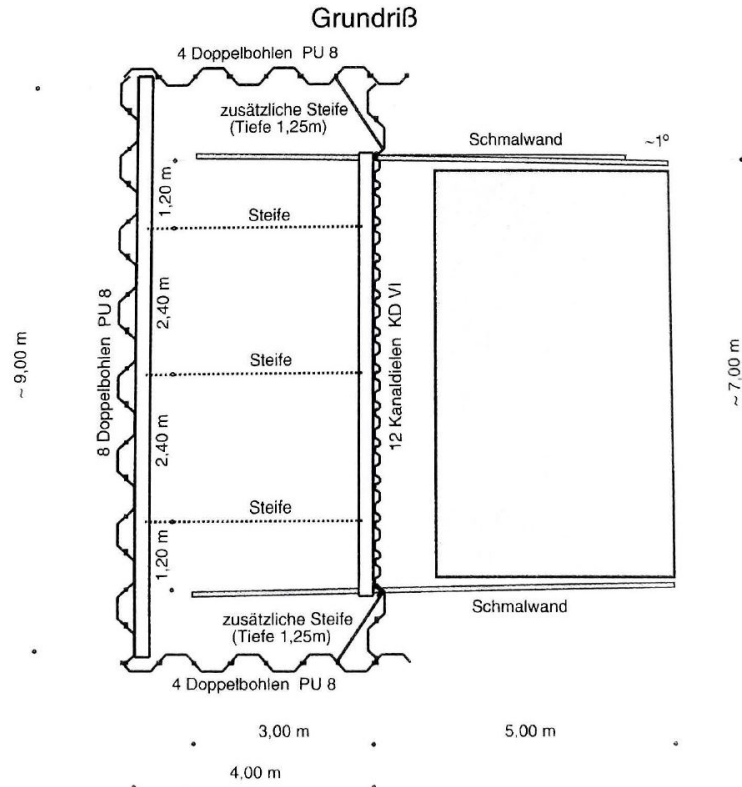


Figure 4.4: Sketch of the Hochstetten field test floor plan. Source: [34] figure 3.10 *Versuchsstand im Schnitt nach Süden und im Grundriß*

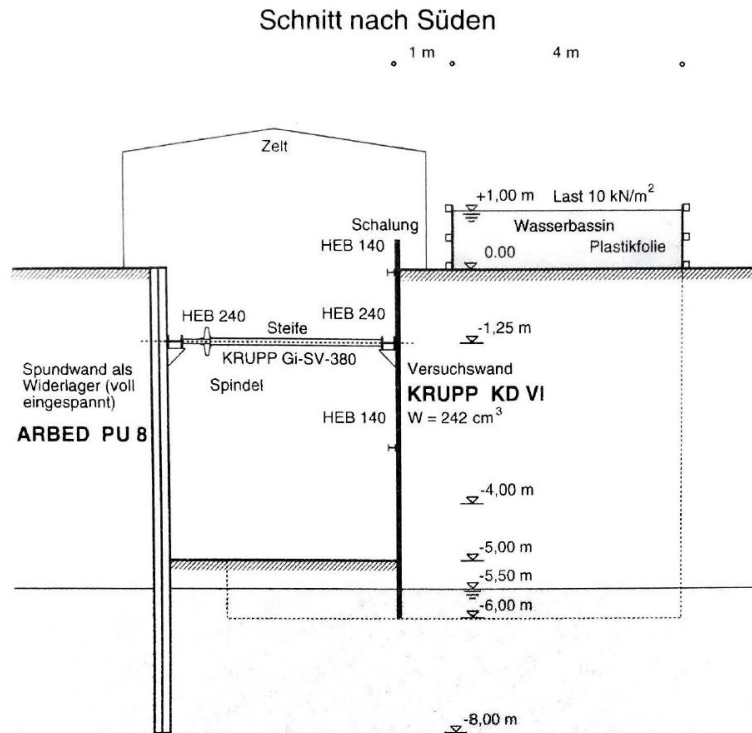


Figure 4.5: Sketch of the Hochstetten field test cross section to the South. Source: [34] figure 3.10 *Versuchsstand im Schnitt nach Süden und im Grundriß*

The final phase of the field test was the failure phase. Failure of the test wall was induced by progressive shortening of the struts until the normal force on the struts reached a constant value. A constant normal force is considered to correspond to the limit state of the ground behind the wall.

Hochstetten field test phases	
Phase	Description
Initial phase	Installation of the sheet piles
phase 1	Excavation of the pit to a depth of 1 meter
phase 2	Excavation down to 1.75 meters
phase 3	Strut installation at 1.25 meters depth pre-loaded at 4.29 kN/m
phase 4	Excavation down to 3 meters
phase 5	Excavation down to 4 meters
phase 6	Excavation down to 5 meters
phase 7	Application of a 10 kPa surface load between 1 and 5 meters behind the wall
phase 8	Progressive shortening of the struts until a constant normal force is reached

Table 4.2: List of the Hochstetten field test construction and test phases together with a short description of the actions performed in every phase.

Hochstetten soil stratigraphy

The stratigraphy of the Hochstetten test site is composed of mainly medium dense silty sands, sands and gravely sands [34]. Below in (figure 4.7) and (figure 4.6) three soil penetration test (SPT) logs and three borehole profiles are given. These profiles and test logs originate from the test site investigation performed in the year 1990 right around the perimeter of the Hochstetten test site.

A complete site investigation plan is performed on-site containing boreholes, SPT's, cone penetration tests (CPT), piézometers and pressure plate tests. Plots of most of the site investigation tests are provided in [34] but no digital files are found. By looking at (figure 4.6) it is evident that based on solely the SPT logs several soil layers can be defined and that the groundwater table (GWT) is at 5.3 to 5.4 meters depth at the time of the site investigation. In [6] the GWT is placed at 5.5 meters depth at the time that the field test was performed.

Hochstetten measurements

The Hochstetten field test has been extensively monitored according to an elaborate sensor plan. This sensor plan is shown in (figure 4.8). As a result of this sensor plan, the following types of measurements are available for every field test phase mentioned in (table 4.2).

Available types of measurements of the Hochstetten field test:

1. Horizontal displacements of the sheet pile wall
2. Surface and sheet pile wall settlements
3. Strut force
4. Bending moments of the sheet pile wall
5. Lateral earth pressures on the sheet pile wall

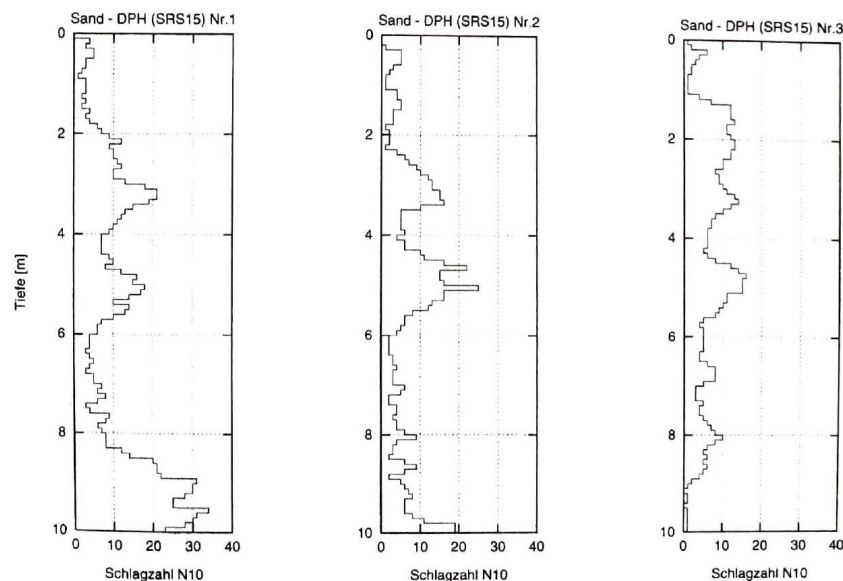


Figure 4.6: Hochstetten SPT profiles from around the Hochstetten test site in the year 1990. Source: [34] figure 3.3 *Bohrprofile Bk 1 bis Bk 3 und Ergebnisse der Schweren Rammsondierungen*

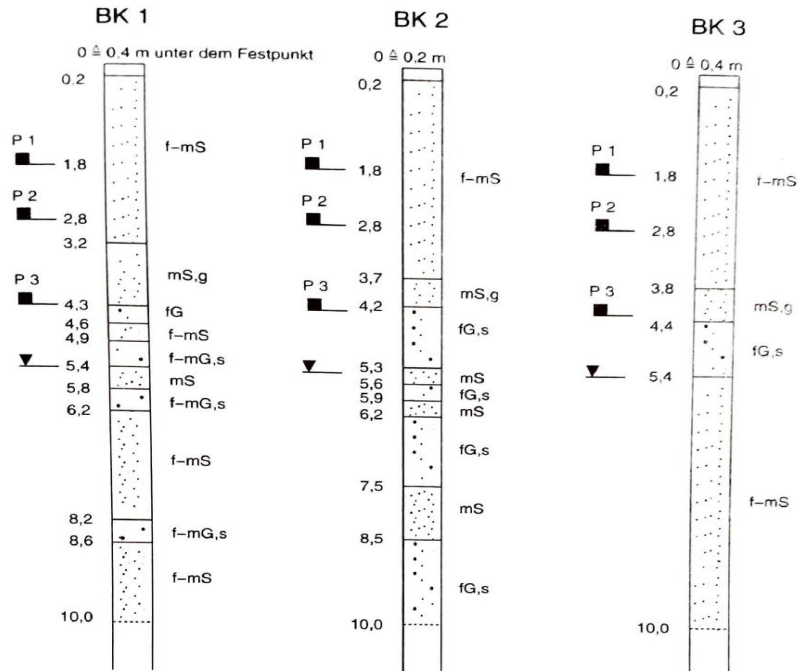


Figure 4.7: Hochstetten borehole data from around the Hochstetten test site in the year 1990. Source: [34] figure 3.3 *Bohrprofile Bk 1 bis Bk 3 und Ergebnisse der Schweren Rammsondierungen*

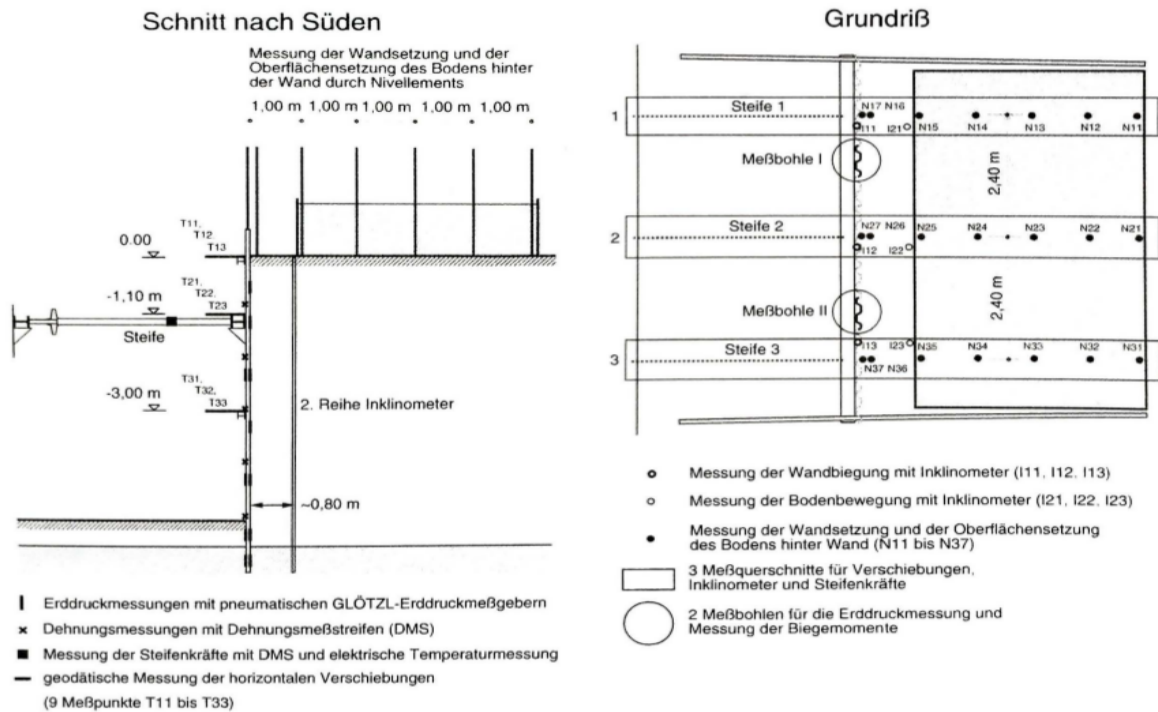


Figure 4.8: Sketch of the sensor plan for the Hochstetten field test. Both a cross section and the top view of the field test with the sensors and measurement points are shown. Source: [34] figure 3.11 *Anordnung der Meßsysteme im Schnitt nach Süden un im Grundriß*

4.3.3 Simplification of Hochstetten field test for the medium complicated problem

As described in (subsection 4.3.1 Properties of medium complicated and complicated problems) the Hochstetten case is used as an inspiration for the medium complicated problem. To perform an inverse analysis on a sheet pile wall case some sort of model needs to be used with which the structure's behaviour can be estimated. As mentioned in (subsubsection 4.3.2 Hochstetten field test background information) a two dimensional model of the cross-section in (figure 4.5) can be used. For this research the model is made in the FEM software Plaxis 2D as mentioned in (section 2.3 Used software packages) of which the set-up is explained in detail below

Hochstetten Plaxis 2D model domain

As mentioned above a Plaxis 2D cross-sectional model of the Hochstetten field test is made based on the cross-section through the middle strut (figure 4.5). The exact test pit dimensions given in the cross-section are used in the Plaxis model. But the outer dimensions of the Plaxis model are based on a combination of the principles of minimal boundary influence and calculation time reduction. To reduce the boundary influences to practically zero the boundaries can be positioned infinitely far away from the excavation, which is of course not realistic. Using a large model domain also has the downside that it increases the computation time of the FEM analysis. Based on multiple iterations of trial and error a stable model with a relatively short computation time is achieved with the model domain having the following dimensions.

Plaxis 2D model domain:

x_{min}	-6 meters	6 meters behind the support wall
x_{max}	+26 meters	22 meters behind the test wall
y_{min}	-16 meters	8 meters below the bottom tip of the support wall elements
y_{max}	0.5 meters	top of the test wall

Hochstetten Plaxis 2D model structural elements

Belonging to the structural elements are the sheet pile walls, the strut and the surface load. All three elements require to be implemented as a different type of element.

The support and test walls are implemented as plate elements with each their own parameter set. As the support wall is assumed to be fixed in space and its deformations are negligible (subsubsection 4.3.2 Hochstetten field test background information) the plate element representing it has zero degrees of freedom and unrealistic high parameter values. The strut is implemented as a fixed end anchor with a length of four meters. The used parameter values of the sheet piles and the strut are given in (table 4.3).

Finally, a line load of 10 kPa is used to simulate the surface load between one and five meters behind the test wall.

Hochstetten structural elements parameter values				
Structural element	Bending stiffness (EI) [kNm^2]	Axial stiffness (EA) [kN]	Strut stiffness (EA/L) [kN/m]	Pretension force [kN/m]
KRUPP DK VI	2033	2200000		
ARBED PU 8	$1 \cdot 10^7$	$1 \cdot 10^9$		
HEB 240			20938	4.29

Table 4.3: Hochstetten structural element parameter values of the used plate elements and fixed end anchor

Hochstetten Plaxis 2D model soil layers

Selecting the number of soil layers is where the largest model simplification is made. This Plaxis model serves as the computation model for the medium complicated problem which is analysed using a synthetic inverse analysis (section 3.3 Synthetic analysis). More soil layers in the Plaxis model equals more soil parameters that influence the structure. To keep the model as simple as possible the number of soil layers in the model is chosen to be equal to two. This simplification is based on the approach in the paper [22] where the stratigraphy is divided into two layers as well, one unsaturated layer above the GWT and one saturated layer below the GWT.

Hochstetten Plaxis 2D model soil parameters and soil models

The used soil parameters for the two soil layers depend on the used constitutive soil model. As the second sub-question states; *"do advanced constitutive soil models have a parameter updating advantage over the linear elastic perfectly plastic Mohr-Coulomb soil model when applied in an inverse analysis"* (section 1.2 Research questions), it is decided to use two different constitutive soil models to generate two different parameter sets.

There is a wide variety of available soil models but for the relatively simple sandy stratigraphy of the Hochstetten field test (section 4.3.2 Hochstetten soil stratigraphy) the two following soil models are considered relevant. One, the Mohr-Coulomb model (MC) and two, the Hardening Soil model (HS) [35].

The MC model describes soil-strain relations as linear elastic- perfectly plastic at the element level (figure 4.9). In this soil-strain relation, the soil stiffness parameters control the elastic behaviour and the soil strength parameters control the plastic limit. This way the stiffness and strength parameters are not interacting at the element level. The more advanced constitutive HS model describes soil-strain relations as a non-linear relation where upon being subjected to primary deviatoric loading the soil stiffness decreases and plastic strains develop at the same time (figure 4.10) [25], [26]. Therefore in the HS model, the soil stiffness and strength parameters do interact at the element level.

When looking at the large scale response of a geotechnical structure, the MC model is capable of showing a non-linear response of the structure as a whole. This is the result of a fraction of the nodes behaving plastically as others are still in the elastic range. Because of this large scale response both the MC and the HS models can provide a platform that allows for updating the soil strength and soil stiffness parameters.

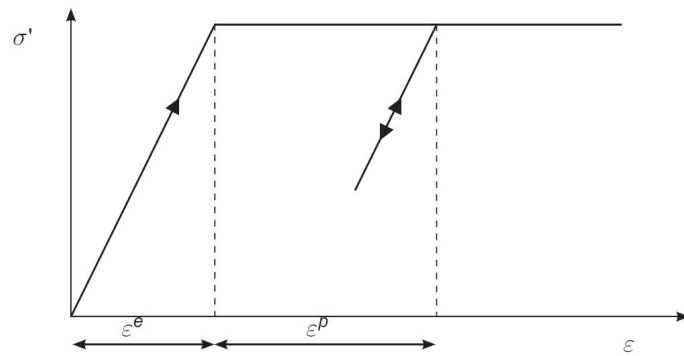


Figure 4.9: Linear elastic- perfectly plastic behaviour of the Mohr-Coulomb constitutive soil model. Source: [25] figure 3.1 *Basic idea of an elastic perfectly plastic model*

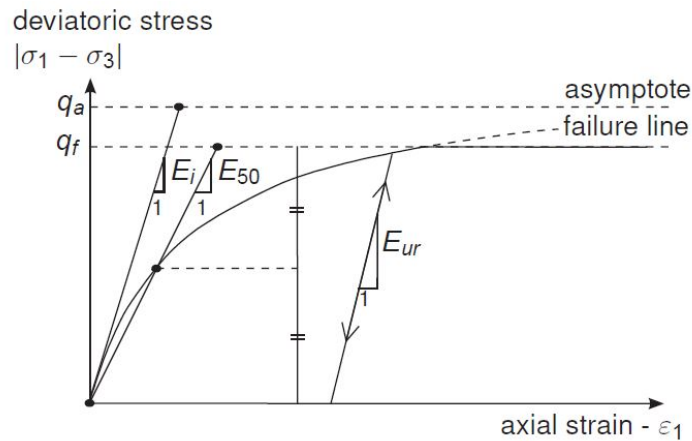


Figure 4.10: non-linear soil behaviour of the Hardening Soil constitutive soil model. Source: [25] figure 6.1 *Hyperbolic stress-strain relation in primary loading for a standard drained triaxial test*

In [7] an advanced MC parameter set is described for the Hochstetten field test prediction of Rijkswaterstaat. The advanced MC model uses a stress-dependent stiffness, but with minor adaptations both an MC and HS parameter set could be composed (table 4.4) and (table 4.5). Both the MC and HS soil parameter sets represent the prior parameter values (section 3.2.2 Bayesian approach).

For the MC model, the shear stiffness (G) values for the two sand layers are determined at the middle of the dry and wet sand layers based on the stress-dependent G . For the advanced MC parameter set a ' m ' parameter value of 0.8 is used, while a value of 0.5 is preferred for the HS parameter set. This value of 0.5 is advised for sand by literature [7]. The coefficients of variation (COV) for the MC and HS parameters are based on values of table 2b of [14].

Adaptations of this kind, using mean parameter values for a layer instead of stress-dependent ones, have a large influence on the model's behaviour. Although for a synthetic inverse analysis case study the used parameter sets don't matter. What matters is the aBUS-SuS method's parameter updating performance which can be tested with any realistic prior parameter set. For this specific case, the parameter set has to represent a similar geotechnical problem as the Hochstetten field test.

Mohr Coulomb prior parameter values					
Parameter	Unit	Sand layer 1 (un-saturated)	Sand layer 2 (sat-urated)	COV [%]	Distribution
γ_{dry}	$[kN/m^3]$	16.5	16.5	5	normal
γ_{wet}	$[kN/m^3]$	19.0	19.0	5	normal
$G_{1,50}$	$[kN/m^2]$	7075	18660	10	normal
ν	$[-]$	0.3	0.3	5	normal
c	$[kN/m^2]$	3	3	20	normal
ϕ'	$[^\circ]$	38	38	10	normal
ψ	$[^\circ]$	8	8	10	normal

Table 4.4: MC prior parameter values for the medium complicated problem based on the Hochstetten field test. The values in this table are based on the advanced MC parameter set described in [7]

Hardening Soil prior parameter set					
Parameter	Unit	Sand layer 1 (un-saturated)	Sand layer 2 (sat-urated)	COV [%]	Distribution
γ_{dry}	$[kN/m^3]$	16.5	16.5	5	normal
γ_{wet}	$[kN/m^3]$	19.0	19.0	5	normal
E_{50}^{ref}	$[kN/m^2]$	34616	34616	10	normal
E_{ur}^{ref}	$[kN/m^2]$	138464	138464	10	normal
m	$[-]$	0.5	0.5	-	normal
ν	$[-]$	0.3	0.3	5	normal
c	$[kN/m^2]$	3	3	20	normal
ϕ'	$[^\circ]$	38	38	10	normal
ψ	$[^\circ]$	8	8	10	normal

Table 4.5: HS prior parameter values for the medium complicated problem based on the Hochstetten field test. The values in this table are based on the advanced MC parameter set described in [7]

Hochstetten Plaxis 2D model calculation settings

The meshing coefficient of the model is set equal to 0.1, which is considered high resulting in a relatively coarse mesh. A coarse mesh is unfavourable for the model's accuracy but it reduces the computation time significantly. With this model being implemented in the selected aBUS-SuS method (subsection 3.2.3 Method selection) a short computation time is a favourable property of the model since many Plaxis computations are required for a single analysis.

The construction phases of the Plaxis model correspond with the construction phases of the Hochstetten field test (table 4.2). There is only one difference, namely that in the Plaxis model the Initial phase is a K0-consolidation phase. After this phase, the displacements and stresses are reset to zero before continuing with the successive phase, sheet pile wall installation. For the inverse analysis process, the final failure phase of the field test is not used since the objective of this research is to use measurement data from within the structure's SLS domain for the parameter updating (chapter 1 Introduction).

An exemplary cross-section of the Plaxis2D model is shown below in (figure 4.11).

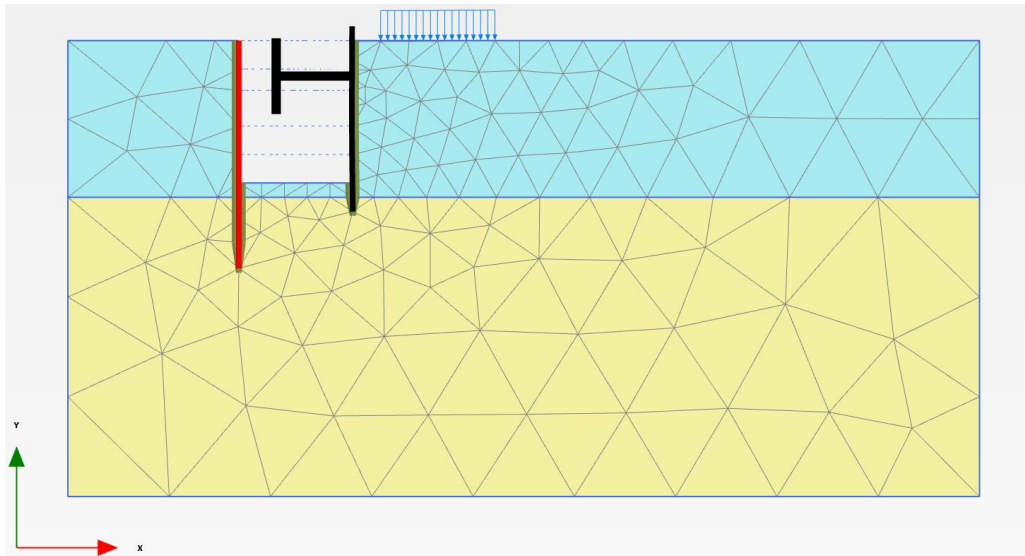


Figure 4.11: Plaxis 2D model of the Hochstetten field test. This figure shows the model in the final construction phase of the field test right after the surface load is applied behind the wall. The domain of the model is $x=[-6;26]$, $y=[-16;0.5]$

Hochstetten selection of variables

The prior parameter values for both the constitutive soil models and the structural elements are determined in (subsection 4.3.3 Hochstetten Plaxis 2D model soil parameters and soil models, subsection 4.3.3 Hochstetten Plaxis 2D model structural elements). But Using all these parameters as variables in the aBUS-SuS analysis is considered to straining and unnecessary.

It is assumed that the parameters of the structural elements are constants. This assumption is based on the assumption that man-made materials are homogeneous with known material parameters, compared to soils being natural materials and heterogeneous. To reduce the number of variables in the aBUS-SuS analysis further a series of sensitivity analyses is performed to determine which soil parameters have to most influence on the FEM model of the sheet pile wall.

The build-in Plaxis 2D 'Sensitivity Analysis and Parameter Variation' tool is used to perform the sensitivity analysis. The Plaxis tool analyses the influence of every parameter on the by the user-defined criteria. It does so by running two model calculations for every parameter, once with a minimum parameter value and once with a maximum value. These minima and maxima are also user-defined, which are for these sensitivity analyses defined as the prior mean values plus and minus one standard deviation (table: 4.4, table: 4.5).

The sensitivity analysis criteria can be any stress-strain, displacement or other output result in any phase that the user sees fit. With the research question in mind ("*Which types and what amounts of service domain measurement data are most effective in updating the calculated reliability (ULS's) of sheet pile walls?*", chapter 1 Introduction) the criteria is chosen to be of the displacement type in *phase 7* (table 4.2). *Phase 7* is expected to provide measurement data from within the SLS domain and the two criteria that are used for the sensitivity analyses are mentioned below.

Sensitivity analysis criteria:

1. total horizontal displacements of the sheet pile wall at $y = -3 \text{ meters}$
2. total vertical displacements of the surface 2 meters behind the sheet pile wall at $x = 6 \text{ meters}$

Parameter sensitivity results

All the sensitivity analyses results are presented in (table 4.6). The soil parameters of the unsaturated sand layer have the most influence on the surface settlements and horizontal displacements of the sheet pile wall model. This is an expected result as the sheet pile wall penetrates the saturated sand layer by only half a meter. For both constitutive soil models, the sheet pile wall model displacements are strongly controlled by the soil strength parameters.

The influences of the soil strength parameters on the sheet pile wall model displacements are confirmed by the figures below (figure 4.12, figure 4.13) which show the plastic point plots, generated by Plaxis 2D Output.

As usually the SLS conditions are expected to be largely influenced by the soil stiffness behaviour and not so much plastic behaviour. The sensitivity analyses results are supported by (figure 4.12), where almost a complete shear band is developed in *phase 7*. A large amount of plastic points in *phase 7* substantiates the large influence of the ϕ and c parameters.

As the HS model is an advanced non-linear constitutive soil model it is difficult to quantify the direct influence of the strength and stiffness parameters. But the vast amount of cap and hardening points behind the test wall in (figure 4.13) show the interference of the soil strength parameters in *phase 7*.

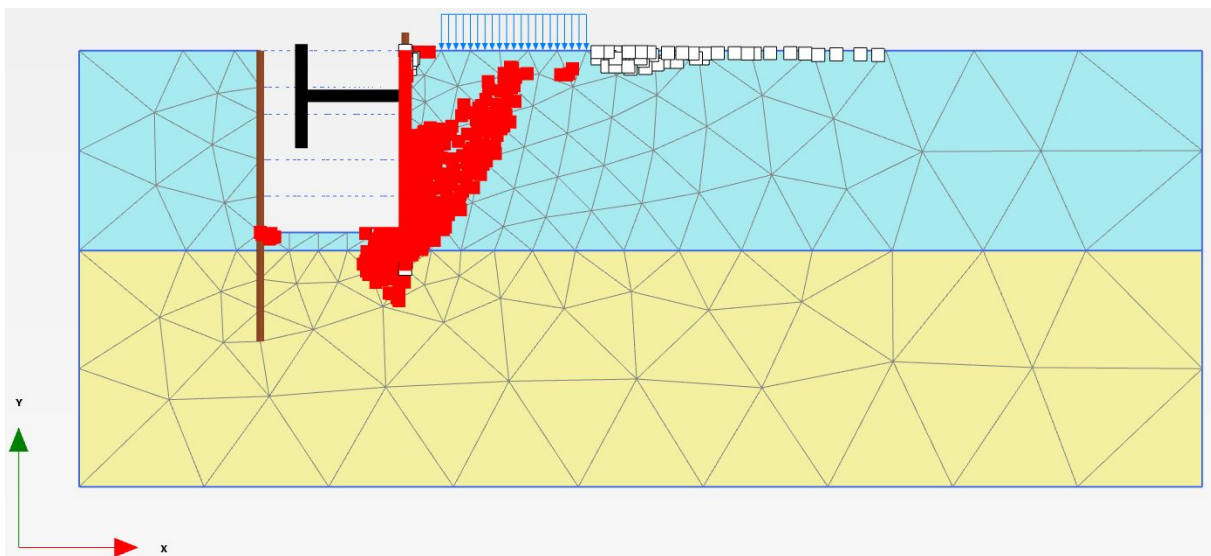


Figure 4.12: Plastic points in *phase 7* of the sheet pile wall Plaxis model with the MC constitutive model

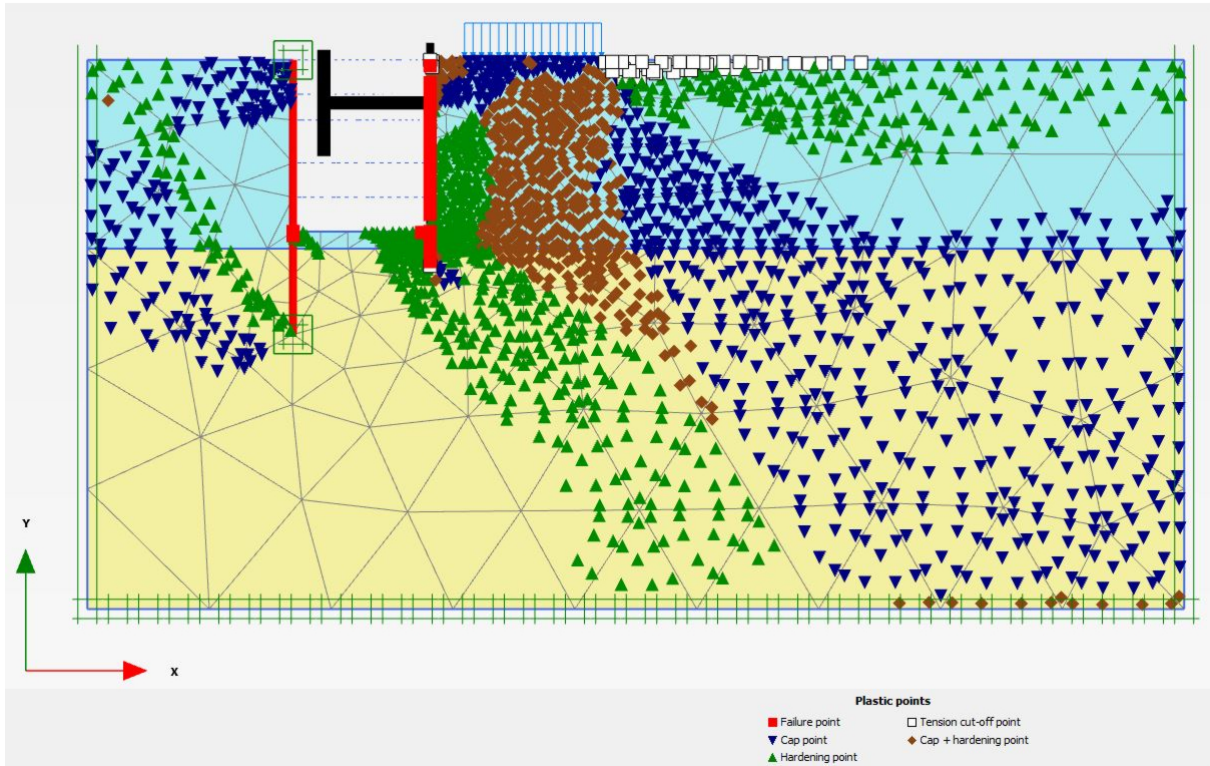


Figure 4.13: Plastic points in *phase 7* of the sheet pile wall Plaxis model with the HS constitutive model

Sensitivity analyses results						
Soil	MC	Criteria 1	Criteria 2	HS	Criteria 1	Criteria 2
<i>Sand</i> _{1,unsat}	$\gamma_{1,unsat}$	13	9	$\gamma_{1,unsat}$	13	11
<i>Sand</i> _{1,unsat}	$E_{1,50}^{ref}$	4	3	$E_{1,50}^{ref}$	8	8
<i>Sand</i> _{1,unsat}	ν_1	1	1	$\nu'_{1,ur}$	2	2
<i>Sand</i> _{1,unsat}	$c'_{1,ref}$	23	25	$c'_{1,ref}$	17	21
<i>Sand</i> _{1,unsat}	ϕ'_1	52	51	ϕ'_1	53	45
<i>Sand</i> _{1,unsat}	ψ_1	2	6	ψ_1	2	5
<i>Sand</i> _{2,sat}	$\gamma_{2,sat}$	1	1	$\gamma_{2,sat}$	0	1
<i>Sand</i> _{2,sat}	$E_{2,50}^{ref}$	1	0	$E_{2,50}^{ref}$	2	2
<i>Sand</i> _{2,sat}	ν_2	0	0	$\nu'_{2,ur}$	0	0
<i>Sand</i> _{2,sat}	$c'_{2,ref}$	0	1	$c'_{2,ref}$	1	2
<i>Sand</i> _{2,sat}	ϕ'_2	2	1	ϕ'_2	3	3
<i>Sand</i> _{2,sat}	ψ_2	1	1	ψ_2	0	0
	Total	100	99	Total	101	100

Table 4.6: Plaxis Sensitivity analyses of the MC and HS prior parameter sets

Selection of variables for the aBUS-SuS analyses

Based on the sensitivity analysis of the MC and HS soil models the following soil parameters are selected as input variables for the aBUS-SuS analysis (table 4.7).

Input variables aBUS-SuS analysis						
Variables	$\gamma_{1,dry}$	$E_{1,50}^{ref}$	c'_1	ϕ'_1	ψ_1	ϕ'_2

Table 4.7: The selected variables that have the most influence on the service domain behaviour of the FEM model of the sheet pile wall.

Chapter 5 Cantilever Beam Problem Analyses

5.1 Introduction

As described in (section 4.2 Cantilever Beam Problem) the CBP is selected to test and understand the in (subsection 3.2.3 Method selection) selected aBUS-SuS method. In the process of understanding the method mechanics and the influences that the different method and problem settings have on the aBUS-SuS updating results this chapter is subdivided into four main sections (figure 5.1).

In every section, different processes and influences are tested. In order to perform these analyses to their fullest potential slightly different settings of the CBP are used. Therefore the method and problem settings are shortly described in every section together with the analyses that are performed with it.

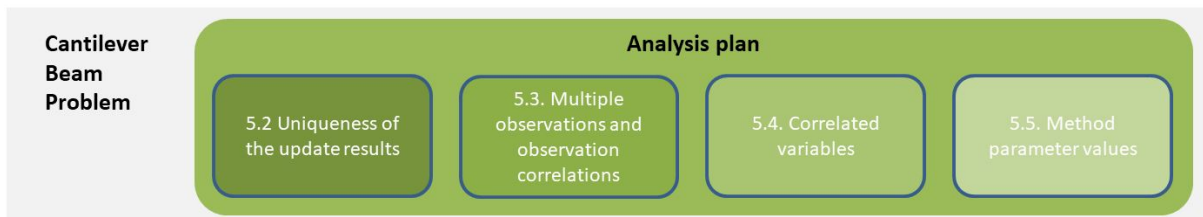


Figure 5.1: Subdivision of the Cantilever Beam Problem analysis plan into four main sections.

Data point positioning

A process that is the same throughout this chapter is the positioning of the measurement points, also called data points. At a data point, any kind of measurement can be performed. In this research only the beam deflection (equation 4.1) and moment of force (equation 4.2) are used. In all the analyses the length of the beam is considered to be constant to allow for consistent data point comparison. The data point positioning is visualized in (figure 5.2) where the moment of force is only measured at the fixed end of the beam ($x = 0$) while the deflection of the beam is measured at the free tip of the beam ($x = L$) (figure 5.2.a). With the outermost data point fixed on the horizontal axis, additional data points can be positioned by equally dividing the distance between the beam's origin and the outermost data point (figure 5.2.b). For comparing the beam displacement results of the different analyses only the outermost deflection data point is used since this is the only one that is fixed in space ($x = L$).

CBP likelihood function

Another aspect that is constant throughout this chapter is the used LF during the CBP analyses. As described in (subsection 3.2.4 aBUS-SuS Likelihood Function) the LF can be based on

the Gaussian distribution, whether it is a mono-variate or multi-variate Gaussian distribution. For the CBP the mono-variate and multi-variate Gaussian LF's are used because their symmetry allows for consistent performance no matter from which side the analysis approaches the measurement(s).

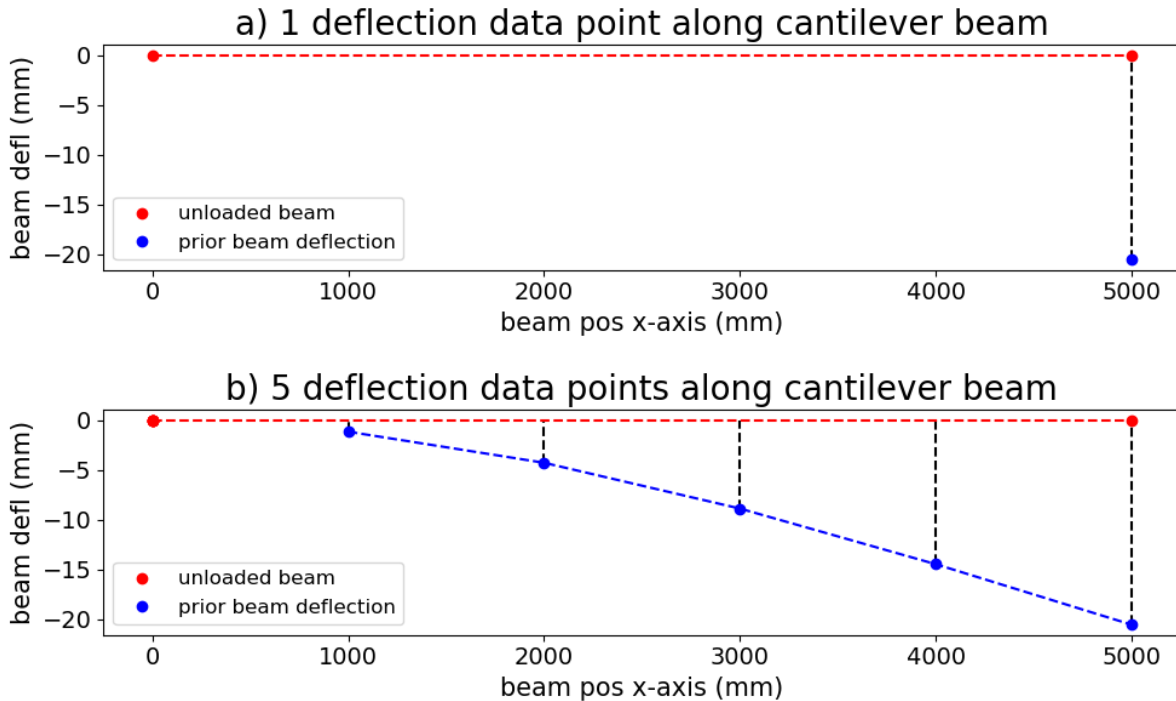


Figure 5.2: Two plots of the prior cantilever beam deflection and the data point distribution along the beam span. a) 1 data point along the cantilever beam span with parameter L considered a constant. b) 5 data points along the cantilever beam span with parameter L considered a constant. The distance between the fixed end of the beam and the outermost data point is equally divided based on the used number of data points.

aBUS-SuS method parameter values

The for the CBP used method parameter values (p_0 and N) are equal to $p_0 = 0.1$ and $N = 1000$. The value for p_0 is mentioned in literature as an efficient and reliable value [30]. The value of N is arbitrary. Other possible values for the method parameters and their influences on the aBUS-SuS analysis are tested in (section 5.5 Method parameters).

5.2 Solution uniqueness

Solution uniqueness analysis plan

In this section, it is tested how the method reacts to different numbers of variables and observations together with how the method performs under conditions that do not guarantee unique solutions. To test this the following three synthetic inverse analyses are performed (table 5.1).

Cantilever Beam Problem uniqueness analysis plan							
Analysis	Variables			Observations			
	nr.	var.	cor./uncor.	nr.	type	pos $[x]$	cor/uncor
1.1	1	EI	uncor.	1	Defl.	L	uncor.
1.2	2	F, EI	uncor.	1	Defl.	L	uncor.
1.3	2	F, EI	uncor.	2	Defl., Mom.	L, θ	uncor.

Table 5.1: Cantilever Beam Problem analysis plan to test the method's performance when the solution is not unique

Solution uniqueness true parameter values

The used true parameter values are based on the prior parameter values mentioned in (subsection 4.2.2 CBP prior parameters). For EI the true parameter value is 20% larger than its prior parameter value. The prior standard deviation of EI is set equal to five per cent of its prior mean value. The true value of F is taken to be 15% larger than its prior parameter value. If a parameter is considered a constant it means that its value is equal to the prior parameter value (table 4.1).

Solution uniqueness problem parameters					
Parameter	Unit	Prior mean	Prior stdev.	True mean	Distribution
F	$[kN]$	10.0000	0.5000	11.5000	normal
L	$[m]$	5.0000	-	-	-
EI	$[kNm^2]$	$2.0250 \cdot 10^4$	$1.0125 \cdot 10^3$	$2.4300 \cdot 10^4$	normal

Table 5.2: The problem parameter values used in the Cantilever Beam Problem Solution uniqueness analysis step.

5.2.1 One variable one observation

With the use of one variable (EI) and one observation (Deflection) there is in theory only one possible solution to the analytical solution of the CBP deflection (equation (4.1)). Since the beam deflection is used as an observation for the aBUS-SuS analysis it is the cantilever beam deflection that is updated, together with the only variable (EI). The aBUS-SuS updating results of analysis 1.1 (table 5.1) are presented in (table 5.3). These same results are visualised in (figure 5.3) and (figure 5.4).

CBP aBUS-SuS results for 1 variable and 1 observation				
	Norm. par. $[-]$	Par cov. $[%]$	Defl. mean $[mm]$	Defl. std. $[mm]$
	EI	EI		
Prior	[0.8333]	[5.0000]	20,5761	1.0141
Obs.	[1.0000]	$[-]$	17.1468	0.1000
Up.	[0.9969]	[0.5715]	17.1997	0.0983

Table 5.3: CBP updating results aBUS-SuS analysis with 1 variable and 1 observation

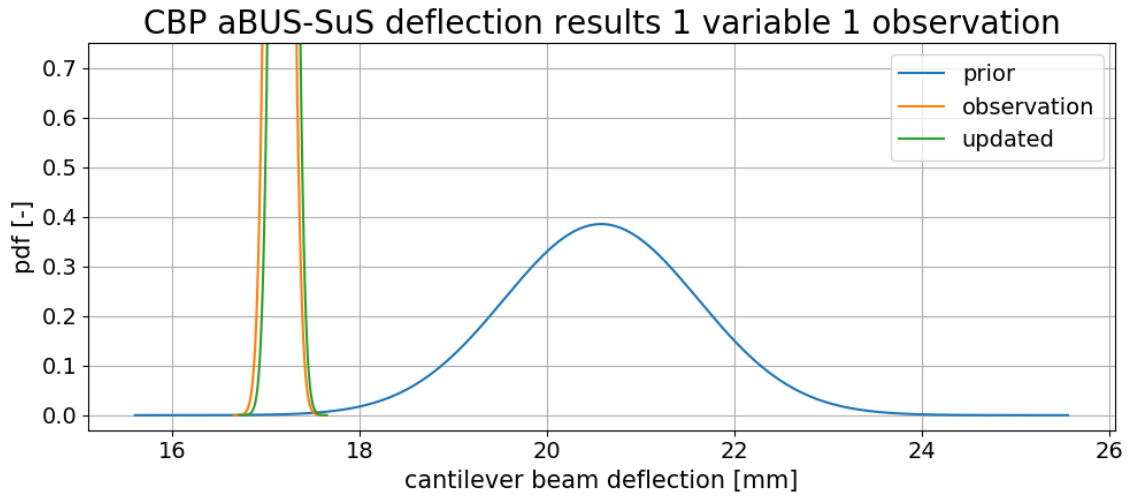


Figure 5.3: CBP deflection updating results of the aBUS-SuS analysis with 1 variable and 1 observation.

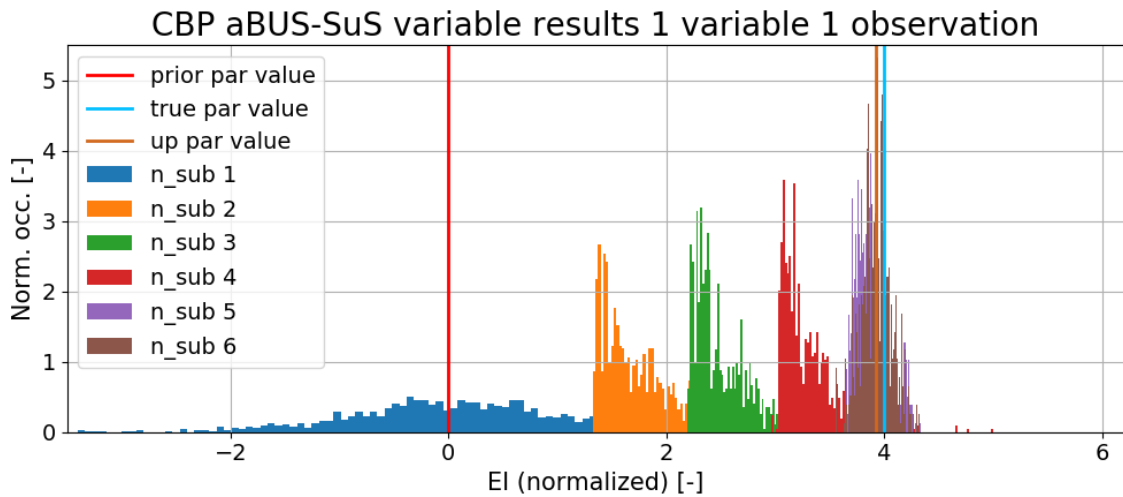


Figure 5.4: CBP parameter updating results of the aBUS-SuS analysis with 1 variable and 1 observation. The convergence process behaves according to the in (subsection 3.2.4 aBUS-SuS convergence)

Both in (table 5.3) and (figure 5.3) do the results show that the aBUS-SuS method is successful in approaching the observed beam deflection. Concerning the updated EI value the results (table 5.3) and (figure 5.4) show that like the updated deflection the updated EI value corresponds with the in (table 5.2) true value of EI .

5.2.2 Two variables one observation

For this test, it is expected that because of the use of two variables and only one observation the solution to this problem is not unique. For this series of tests (table 5.1) the true value of F promotes an increase in beam deflection while the true value of EI promotes a decrease in beam deflection compared to the prior parameter values. Consulting the analytical solution for the

beam deflection (equation 4.1) and (subsection 4.2.2 Cantilever beam parameter sensitivity) show that the influences of the variables F (linear) and EI (inverse) level each other out. Therefore it is also expected that the method will converge towards a more likely parameter combination than the used true parameter values.

Results of analysis 1.2 (table 5.1) are given in table (5.4) and figures (5.5, figure 5.6). The results prove that the aBUS-SuS successfully performed the inverse analysis as the updated beam deflection corresponds with the observed beam deflection. Although the variable updating results confirm the expectations described earlier. From (figure 5.6) it is concluded that the aBUS-SuS method converges towards the most likely parameter combination of resulting in the observations. The black line shows the possible parameter combinations that result in the same beam displacement as the true parameter combination (the pink dot). The aBUS-SuS method converged to the point on this line which tends to be the closest point on the solution line to the prior parameter combination. Although because of the inherent randomness of the aBUS-SuS method this updated point is not the exact closest point to the prior parameter combination.

CBP aBUS-SuS results for 2 variables and 1 observation						
	Norm. par. [-]		Par cov. [%]		Defl. mean [mm]	Defl. std. [mm]
	F, EI		F, EI			
Prior	[0.8696]	[0.8333]	[5.0000]	[5.0000]	20.5761	1.4253
Obs.	[1.0000]	[1.0000]	[-]	[-]	19.7188	0.1000
Up.	[0.8511]	[0.8510]	[3.5549]	[3.5749]	19.7204	0.1025

Table 5.4: CBP updating results aBUS-SuS analysis with 2 variables and 1 observation.

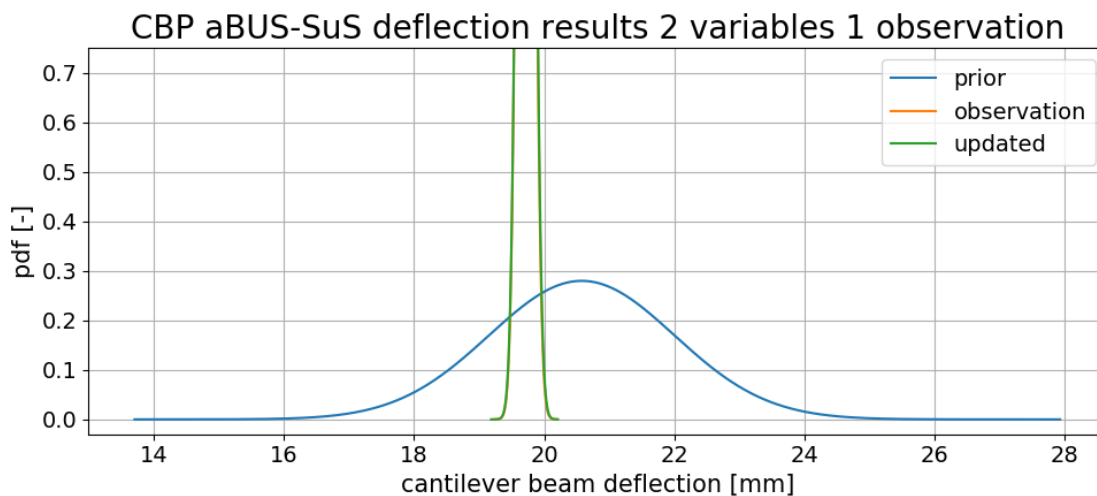


Figure 5.5: CBP deflection updating results of the aBUS-SuS analysis with 2 variables and 1 observation.

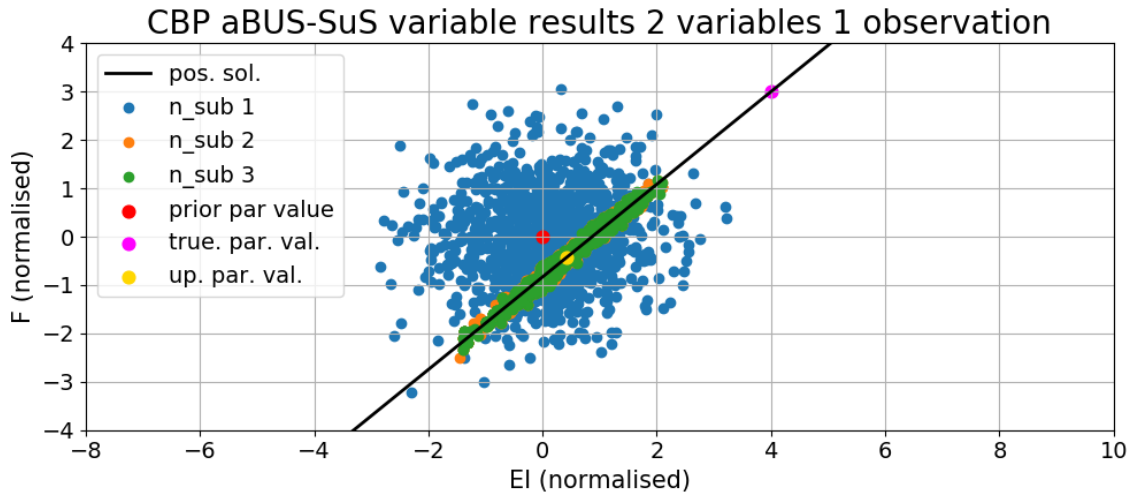


Figure 5.6: CBP parameter updating results of the aBUS-SuS analysis with 2 variables and 1 observation.

5.2.3 Two variables two observations

Other than the CBP test with two variables and one observation this third analysis 1.3 (table 5.1) with two variables and two types of observations is again expected to have a unique solution. With the use of the additional moment of force measurement which is only influenced by F , F has only one solution which automatically leads to a unique solution for EI .

The results of the third test are given in (table 5.5) and (figure (5.7), figure 5.8). For this third test, the method again performs as expected. The aBUS-SuS method approached the used measurements very closely with the updated beam deflection and moment force (figure 5.7). Compared to test 1.2 described above (subsection 5.2.2 Two variables one observation) this time the aBUS-SuS method does converge towards the true parameter values as opposed in (table 5.2).

CBP aBUS-SuS results for 2 variables and 2 observations				
	Norm. par. [-]	Par cov. [%]	Defl. mean [mm]	Defl. std. [mm]
	F, EI	F, EI		
Prior	[0.8696] [0.8333]	[5.0000] [5.0000]	20.5761	1.4253
Obs.	[1.0000] [1.0000]	[-] [-]	19.7188	0.1000
Up.	[0.9995] [0.9967]	[0.1777] [0.5219]	19.7744	0.0958
			Mom. mean [kNm]	Mom. std. [kNm]
Prior			50.0000	2.4975
Obs.			57.5000	0.1000
Up.			57.4730	0.1021

Table 5.5: CBP updating results aBUS-SuS analysis with 2 variables and 2 observations.

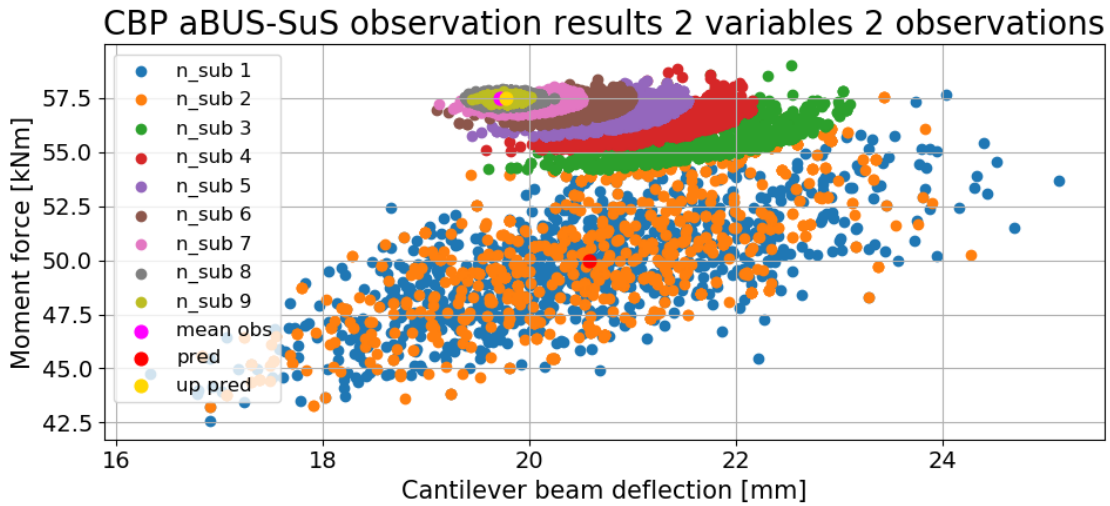


Figure 5.7: CBP observation updating results of the aBUS-SuS analysis with 2 variables and 2 observations.

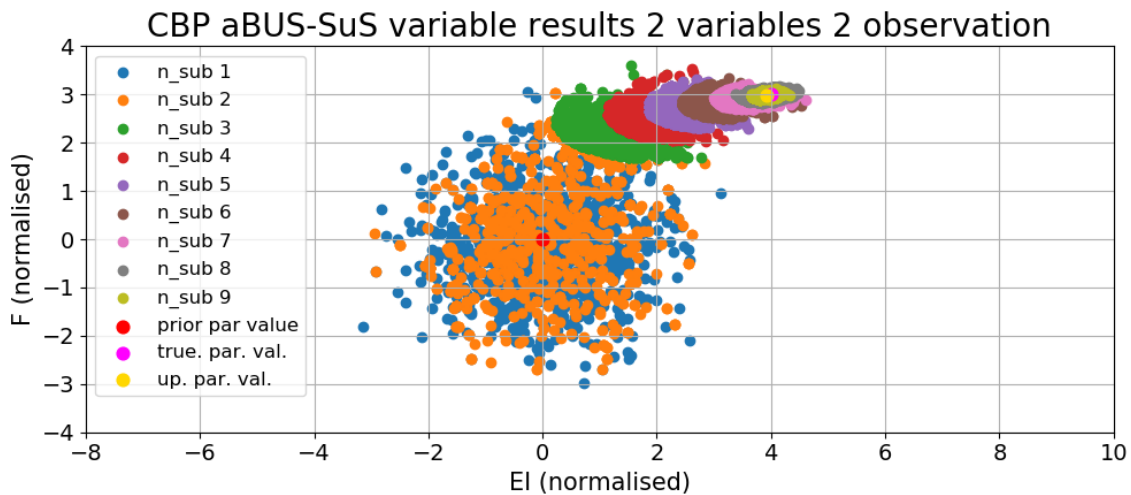


Figure 5.8: CBP parameter updating results of the aBUS-SuS analysis with 2 variables and 2 observations.

Three additional interesting processes are observed in the results of this third test.

As a first, there seems to be an observation correlation in the first subset. This is caused by the influence that the parameters have on the beam's moment of force and deflection. The moment of force depends linearly on F (equation 4.2) while the deflection depends on both F and EI . With a larger F value the deflection increases and vice versa. This results in an inherent positive correlation between the beam deflection and moment of force.

Secondly, when the figures of the subsets with the values of the variables and the subsets with the measurement convergence of the third test 1.3 (figure 5.7, figure 5.8) are compared to the variable convergence of the second test 1.2 (figure 5.6) it is noticed that in 1.3 the second subset has a remarkable, seemingly random, overlap with the first MC subset. This is thought to be a conditional sampling issue (subsection 3.2.4 Detailed method description) at the point when

the minimum number of seed samples is to be selected. If the distance between the observations and the prior predictions is too large the LF returns a value of zero, this boundary of the LF is visualized in (figure 5.9) in the shape of a red ellipse. This ellipse shape also comes back in the shapes of the subsets as a consequence of the in (subsection 3.2.4 aBUS-SuS convergence) described process of sample rejection. In this case, it is thought that less than the minimum number of seed samples have been assigned a value not equal to zero. Therefore when the seed samples are selected, a lot of seed samples are randomly selected from throughout the initial MCS step. It doesn't seem to influence the analysis final results in any other way than that it possibly increased the convergence time.

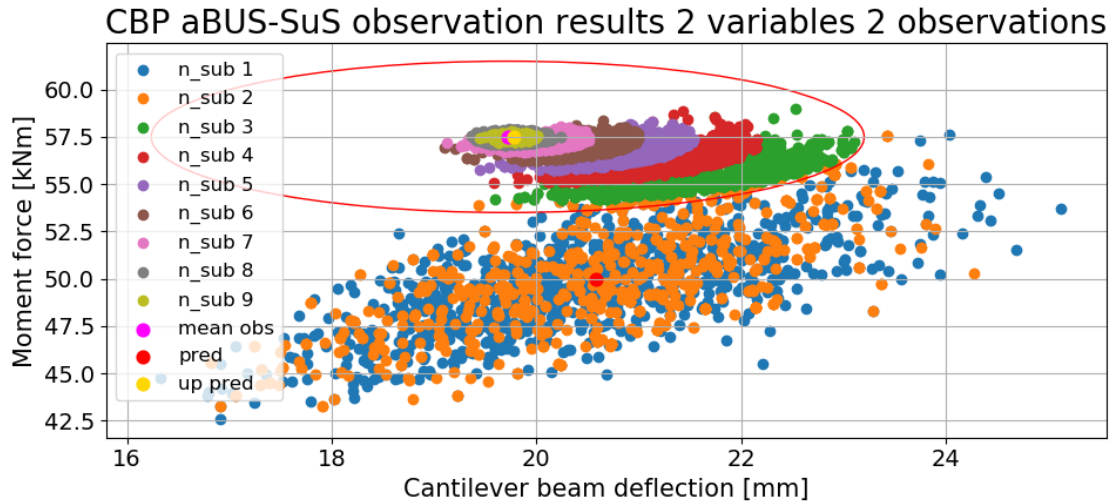


Figure 5.9: CBP observation updating results of the aBUS-SuS analysis with 2 variables and 2 observations and the domain of the multi-variate likelihood function plotted over it. This ellipse represents the boundary of where the likelihood function is able to assign a positive value to the samples. Outside this domain the likelihood function returns a value of zero.

Thirdly when one observes the convergence path of the cantilever beam behaviour towards the observations one can ask the question why the convergence path doesn't progress towards the observations along the shortest path? The second and third subsets originate from the top part of the deflection and moment force scatter of the first subset (MC step) in (figure 5.7) after which the subset trail moves sideways to the observed deflection and moment force. This is also caused by the influence range of the used multivariate likelihood function and the uncorrelated observations. In this specific case, the deflection and moment of force combinations on the upper right corner had the highest likelihood function score. This is confirmed by the problem described above about the overlap of the first and second subsets. It can be concluded that the sample sets of the first subset that are positioned on the straight line between the prior model predictions to the observations got assigned a value of zero by the multivariate likelihood function. Therefore convergence along the shortest path to the observations is prohibited.

5.3 Multiple observations and observation correlations

In theory, the use of multiple data points along the span of the beam should improve the inverse analysis results as it increases available knowledge on the curvature of the beam, narrowing down the range of possible solutions. In this section, it is tested how the method reacts to multiple

numbers of observations and how the method performs when correlated observations are used. Before these analyses are performed one needs to know what correlated observations are, which is therefore explained in (subsection 5.3 Correlated observations).

Correlated observations

The aBUS-SuS method has the option of defining the used observations as correlated or uncorrelated by using a correlation coefficient with a value between -1.0 and 1.0 . This correlation coefficient is used to indicate correlations in the observation measurement errors which is visualized in (figure 5.10).

If the observations are strongly correlated ($\rho \approx 1$ or $\rho \approx -1$) it means that the errors in both measurements have the same significance on the observation. Thus a positive error of for example one standard deviation from the mean observation on one observation means that the error is also a positive error of one standard deviation from the observation mean. If the observation errors are considered uncorrelated it means that the observation errors do not influence each other as is visualised in the right plot of (figure 5.10).

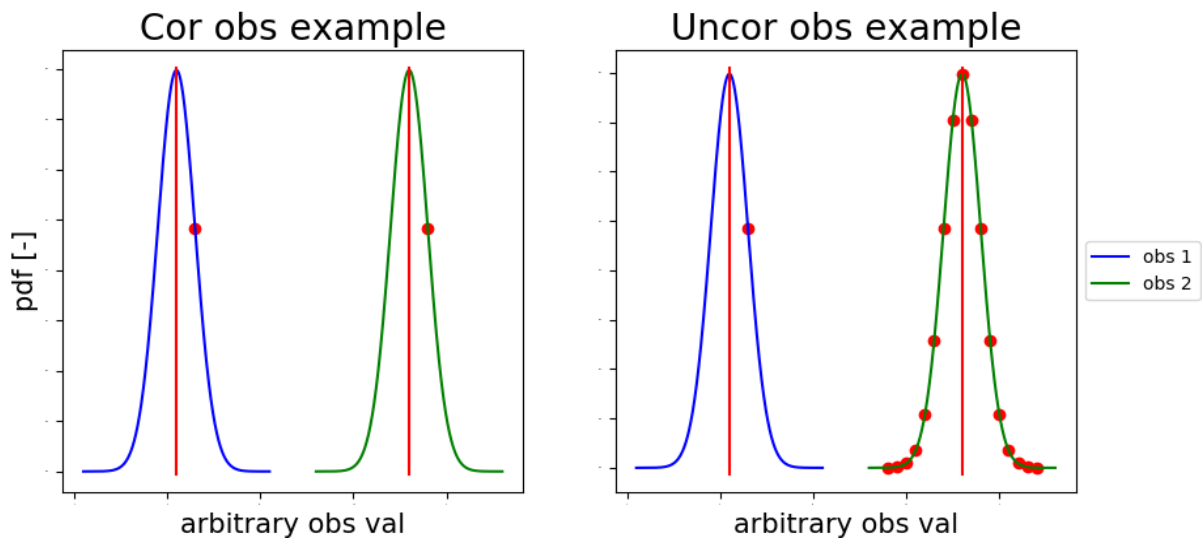


Figure 5.10: Example of correlated observation errors. The left plot shows two strong correlated observation errors ($\rho \approx 1$) and the right plot shows uncorrelated observation errors ($\rho \approx 0$)

In practice, the observation error is used in these analyses since the user doesn't know what the exact measurement deviations are. It is even more complicated to quantify the errors respective to different measurements. Therefore the observations are usually interpreted as uncorrelated. But in order to test how the method responds to correlated observations the following series of analyses is performed on the CBP (table 5.6).

Cantilever Beam Problem observation correlation analysis plan							
Analysis	Variables			Observations			
	nr.	var.	cor./uncor.	nr.	type	pos $[x]$	cor./uncor
2.1	2	F, EI	uncor.	6	Defl. [5], Mom. [1]	$0:L, 0$	uncor.
2.2	2	F, EI	uncor.	6	Defl. [5], Mom. [1]	$0:L, 0$	cor. ($\rho = 0.5$)
2.3	2	F, EI	uncor.	6	Defl. [5], Mom. [1]	$0:L, 0$	cor. ($\rho = 0.95$)

Table 5.6: Cantilever Beam Problem analysis plan to test the method's performance when multiple correlated observations are used

Correlated observations true parameter values

The used true parameter values are based on the prior parameter values mentioned in (subsection 4.2.2 CBP prior parameters). For EI the true parameter value is 25% larger than its prior parameter value. The prior standard deviation of EI is set equal to five per cent of its prior mean value. The true value of F is taken to be 20% smaller than its prior parameter value. If a parameter is considered a constant it means that its value is equal to the prior parameter value (table 4.1).

Correlated observations problem parameters					
Parameter	Unit	Prior mean	Prior stdev.	True mean	Distribution
F	$[kN]$	10.0000	0.5000	8.0000	normal
L	$[m]$	5.0000	-	-	-
EI	$[kNm^2]$	$2.0250 \cdot 10^{+4}$	$1.0125 \cdot 10^{+3}$	$2.5313 \cdot 10^{+4}$	normal

Table 5.7: The problem parameter values used in the Cantilever Beam Problem Correlated observations analysis step.

5.3.1 Correlated observations results

All the results of the in (table 5.6) performed analyses are collectively presented in (table 5.8) and (figure 5.11, figure 5.12) along with a base analysis where one deformation and one moment of force observation are used.

The results show that the aBUS-SuS results approach the observations closer and with higher reliability when multiple deflection observations and a single moment of force observation are used. As expected the use of more observation points increases the aBUS-SuS updating performance in approaching the observed mean deflection. This effect is stronger for strongly correlated observations ($\rho = 0.95$) while for medium correlated observations ($\rho = 0.5$) no significant influence is observed compared to the updating results of the uncorrelated observations test.

For these tests the observation standard deviations are increased for both the deflection and moment of force (table 5.8) compared to the observation standard deviations in the previous section (section 5.2 Solution uniqueness). Therefore it is interesting to observe that most of the updating error is in updating the beam deflection since the updated moment of force results are very similar to the observed moment of force for the three different tests.

CBP aBUS-SuS results for correlated observations						
	Norm. par. [–] <i>F, EI</i>		Par cov. [%] <i>F, EI</i>		Defl. mean [mm]	Defl. std. [mm]
Prior	[1.2500]	[0.8000]	[5.0000]	[5.0000]	20.5761	1.4740
Obs.	[1.0000]	[1.0000]	[–]	[–]	13.1687	0.5000
Single	[1.0004]	[0.9185]	[1.2417]	[2.8104]	14.3432	0.4118
Uncor.	[0.9970]	[0.9417]	[1.2441]	[2.4846]	13.9420	0.3323
Medium	[0.9979]	[0.9349]	[1.0893]	[2.2301]	14.0568	0.3009
Strong	[0.9906]	[0.9774]	[1.1044]	[1.4140]	13.3472	0.1465
					Mom. mean [kNm]	Mom. std. [kNm]
Prior					50.0000	2.4735
Obs.					40.0000	0.5000
Single					40.0152	0.4969
Uncor.					39.8814	0.4962
Medium					39.9172	0.4348
Strong					39.6248	0.4376

Table 5.8: CBP updating results aBUS-SuS analysis with correlated observations. The single results represent a comparison analysis performed with one deflection and one moment of force observation while in the other analysis (uncor, medium and strong) five deflection observations are used.

Plotting the beam behaviour predictions for the different subsets reveals the cause of this discrepancy. The deflection and moment of force of the uncorrelated observations (test 2.1) and the strongly correlated observations (test 2.3) are plotted in (figure 5.13, figure 5.14). Both figures show similar convergence paths where the subsets first reach the observed moment of force before reaching the observed deflection. This is thought to be caused by the fact that the prior predicted behaviour is positioned closer to the observed moment of force than the observed deflection. This leads to the moment of force having a larger influence on the likelihood function resulting in the faster moment of force convergence compared to the beam deflection.

Another noticeable effect is the reduced domain of the LF in the case of strongly correlated observations. This is a direct result of the strong observation correlation that directly influences the LF in the variance matrix (equation 3.5). With a large correlation coefficient, the LF domain becomes narrower. This has a couple of consequences which are discussed in the computation time section below.

Computation time

From the results in (figure 5.13, figure 5.14) it is observed that with the strongly correlated observations the convergence process of the aBUS-SuS method requires more subsets than for uncorrelated observations, eleven versus ten. This is not a significant difference but upon observing the analyses results there are two different aspects that might be consistently contributing to an increase in computation time when correlated observations are used.

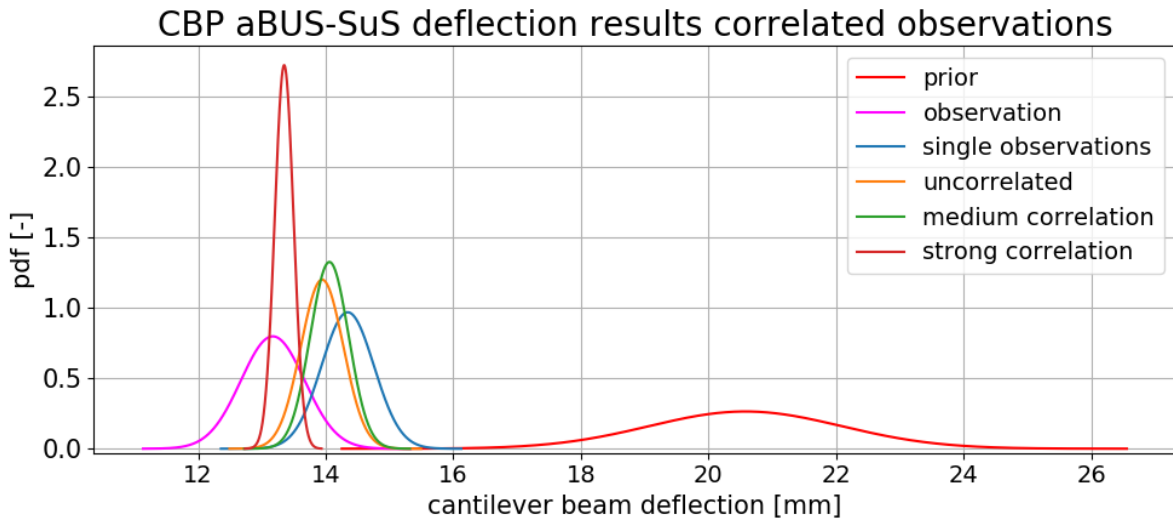


Figure 5.11: CBP deflection updating results of the aBUS-SuS analysis with correlated observations.

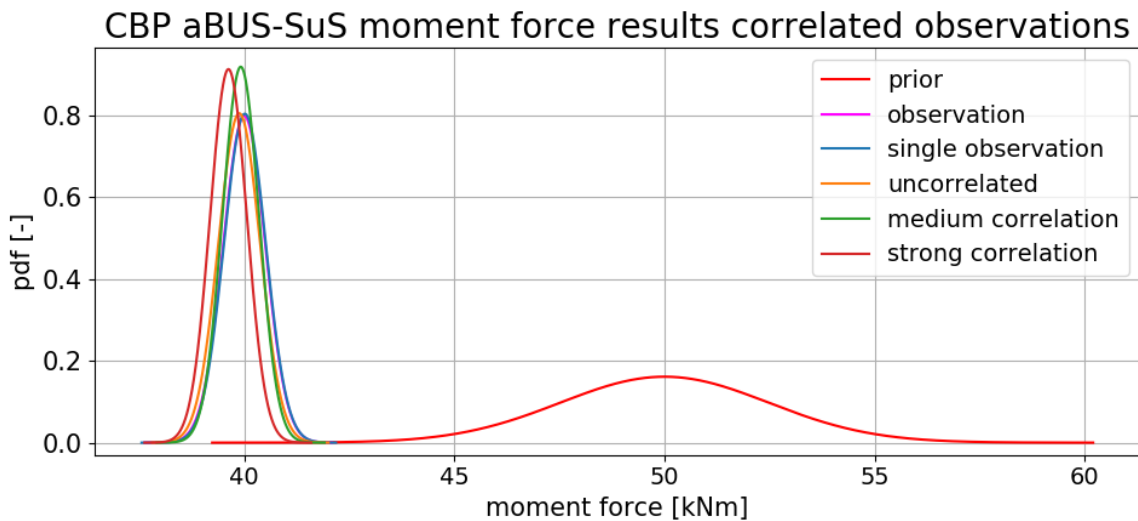


Figure 5.12: CBP moment force updating results of the aBUS-SuS analysis with correlated observations.

First, it is observed that the second subset has a large random overlap with the first MCS subset. This issue is described in the previous section (section 5.2.3 Two variables two observations). Here the cause of this issue is assigned to the distance between the prior behaviour prediction and the observations combined with the reduced range of influence of the LF as mentioned earlier. This issue might influence the progression of the third subset as the second subset seed samples overlapping with the first subset have an influence on the updated parameter values that are used to generate the samples of the third subset.

The second aspect is that because of the strong correlation between the observations the aBUS-SuS method has stricter convergence criteria, requiring the analysis to converge closer to the observations. This is especially noticeable in the beam deflection in (figure 5.11, figure 5.13,

figure 5.14) where the width of the beam deflection curve and the final subset cloud are much smaller for the strongly correlated observations compared to the uncorrelated observations. This is also a direct consequence of the large correlation coefficient which decreases the influence domain of the LF.

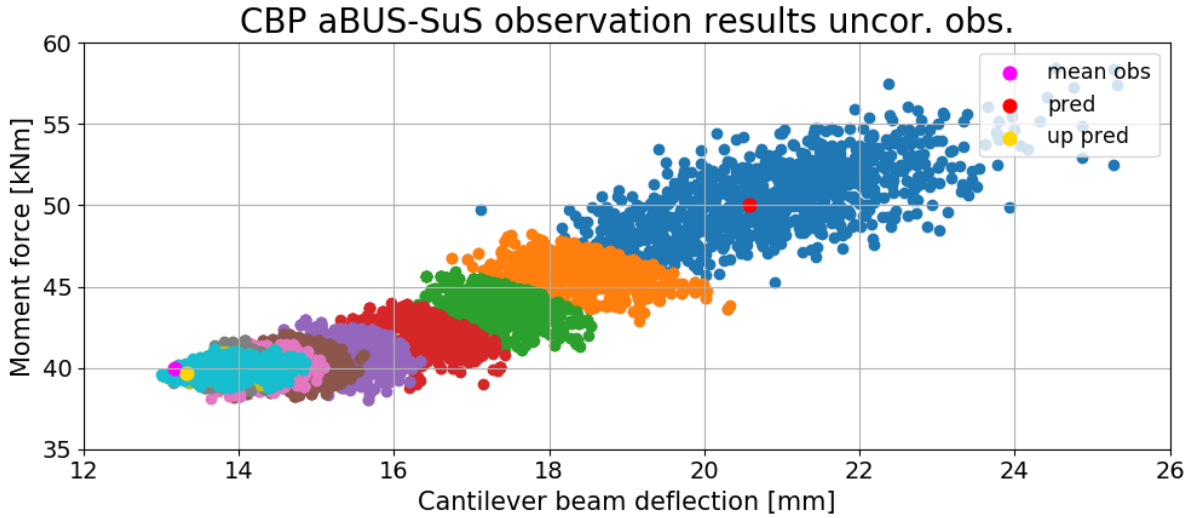


Figure 5.13: CBP observations updating results of the aBUS-SuS analysis with uncorrelated observations.

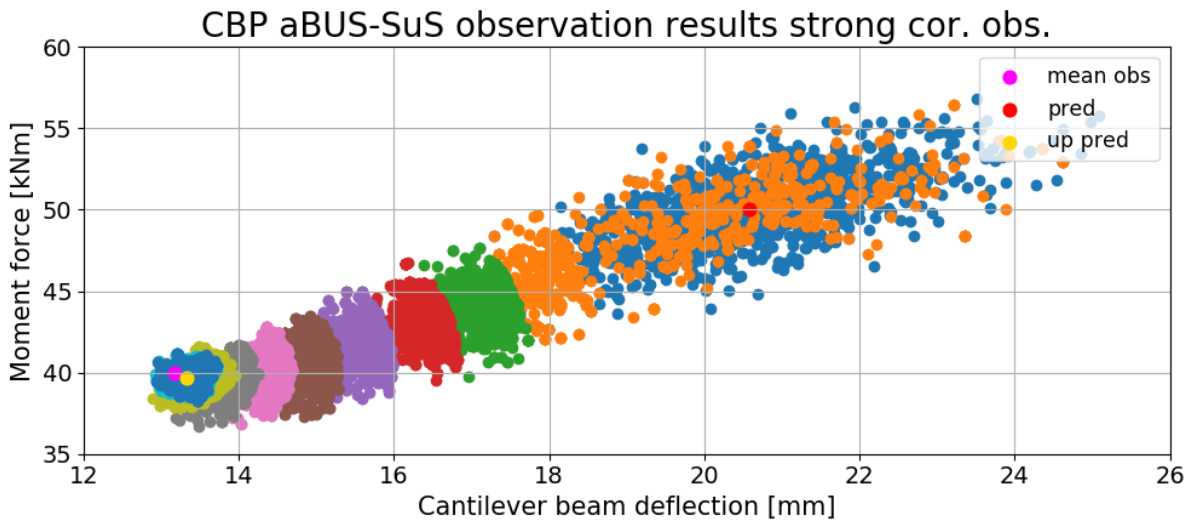


Figure 5.14: CBP observations updating results of the aBUS-SuS analysis with strongly correlated observations.

5.4 Correlated variables

Implementing the variables as uncorrelated can be considered a conservative inverse analysis approach. In theory, the aBUS-SuS analysis method will analyse all possible parameter combinations depending on the coverage of the first subset which in its turn depends on the value of N . Implementing correlated variables might reduce the physical space of the initial param-

ter sets, reducing the number of possible parameter combinations, leading to the possibility of reducing N and possibly even a reduced number of subsets. As a reduction in the number of subsets significantly reduces the computation time it is worth it to test if the use of correlated parameters has the potential to increase the practical applicability of the aBUS-SuS method. Therefore in this section, it is tested how the aBUS-SuS method reacts to correlated variables. To test this the following three synthetic inverse analyses are performed (table 5.9).

Cantilever Beam Problem correlated variables analysis plan							
Analysis	Variables			Observations			
	nr.	var.	cor./uncor.	nr.	type	pos $[x]$	cor/uncor
3.1	2	F, EI	uncor.	2	Defl., Mom.	$L, 0$	uncor.
3.2	2	F, EI	cor. (set 1)	2	Defl., Mom.	$L, 0$	uncor.
3.3	2	F, EI	cor. (set 2)	2	Defl., Mom.	$L, 0$	uncor.

Table 5.9: Cantilever Beam Problem analysis plan to test the method's performance when correlated variables are used. The variable correlation matrices (set 1 and set 2) are given in (table 5.10).

Additional to this table another table is given which contains the correlation matrices of the variables used in the analyses (table 5.10). Why these two different correlation matrices are used is explained in (subsection 5.4.1 Correlated variables results).

Cantilever beam problem correlated variables	
correlation set 1	correlation set 2
$R_1 = \begin{bmatrix} & F & EI \\ F & 1.0 & -0.5 \\ EI & -0.5 & 1.0 \end{bmatrix}$	$R_2 = \begin{bmatrix} & F & EI \\ F & 1.0 & 0.5 \\ EI & 0.5 & 1.0 \end{bmatrix}$

Table 5.10: Cantilever beam problem correlation matrices of the variables

Correlated variables problem parameters					
Parameter	Unit	Prior mean	Prior stdev.	True mean	Distribution
F	$[kN]$	10.0000	0.5000	8.0000	normal
L	$[m]$	5.0000	-	-	-
EI	$[kNm^2]$	$2.0250 \cdot 10^4$	$1.0125 \cdot 10^3$	$2.5313 \cdot 10^4$	normal

Table 5.11: The problem parameter values used in the Cantilever Beam Problem Correlated variables analysis step.

Correlated variables true parameter values

The used true parameter values are based on the prior parameter values mentioned in (subsection 4.2.2 CBP prior parameters). For EI the true parameter value is 25% larger than its prior parameter value. The prior standard deviation of EI is set equal to five per cent of its prior mean value. The true value of F is taken to be 20% smaller than its prior parameter value. If a

parameter is considered a constant it means that its value is equal to the prior parameter value (table 4.1).

CBP aBUS-SuS results for correlated variables						
	Norm. par. [-]		Par cov. [%]		Defl. mean [mm]	Defl. std. [mm]
	F, EI		F, EI			
Prior	[1.2500]	[0.8000]	[5.0000]	[5.0000]	20.5761	1.4554
Obs.	[1.0000]	[1.0000]	[-]	[-]	13.1687	0.5000
Uncor.	[0.9970]	[0.9417]	[1.2441]	[2.4846]	14.3553	0.3148
Set 1	[0.9979]	[0.9349]	[1.0893]	[2.2301]	13.9944	0.3465
Set 2	[0.9906]	[0.9774]	[1.1044]	[1.4140]	15.1215	0.3388
					Mom. mean [kNm]	Mom. std. [kNm]
Prior					50.0000	2.4701
Obs.					40.0000	0.5000
Uncor.					40.0217	0.4629
Set 1					39.9947	0.4317
Set 2					39.8273	0.4648

Table 5.12: CBP updating results aBUS-SuS analysis with correlated variables.

5.4.1 Correlated variables results

All the results of the analyses in (table 5.9) are collectively presented in (table 5.12) and (figure 5.16). The moment of force results are not plotted since just like in the correlated observation results there is no significant variation in the results. Although there are significant differences between the results of the updated model deflections. The correlated variables set 1 (table 5.10) shows the closest approach of the observed deflection of the two correlation sets.

How the correlated variables influence the aBUS-SuS analysis becomes clear from (figure 5.15) which shows the development of the subsets with the values of the variables for three different correlations of the sets of variables. The top plot shows the subsets of the analysis with uncorrelated variables which can also be deduced from the first subset, the MCS subset, not being skewed. The plots showing the subsets of the analyses with the correlated variables have a skewed first subset. In this particular case, the MCS subset skewness caused by correlation set 1 is favourable for the aBUS-SuS analysis as it results in subset 1 being oriented towards the true parameter values. The opposite occurs in the analysis with correlation set 2. The results of the analysis with the uncorrelated variables fall in between the results of the analyses with the correlated variables.

Computation time

From the three plots in (figure 5.15), it is evident that the use of correlated variables can have either a positive or negative influence on the analysis computation time. This influence can be significant, in these analyses the analysis with correlation set 2 took almost twice as long to converge as the analysis with correlation set 1. The computation time of the analysis with the uncorrelated variables is again in between the computation times of the analyses with the correlated variables.

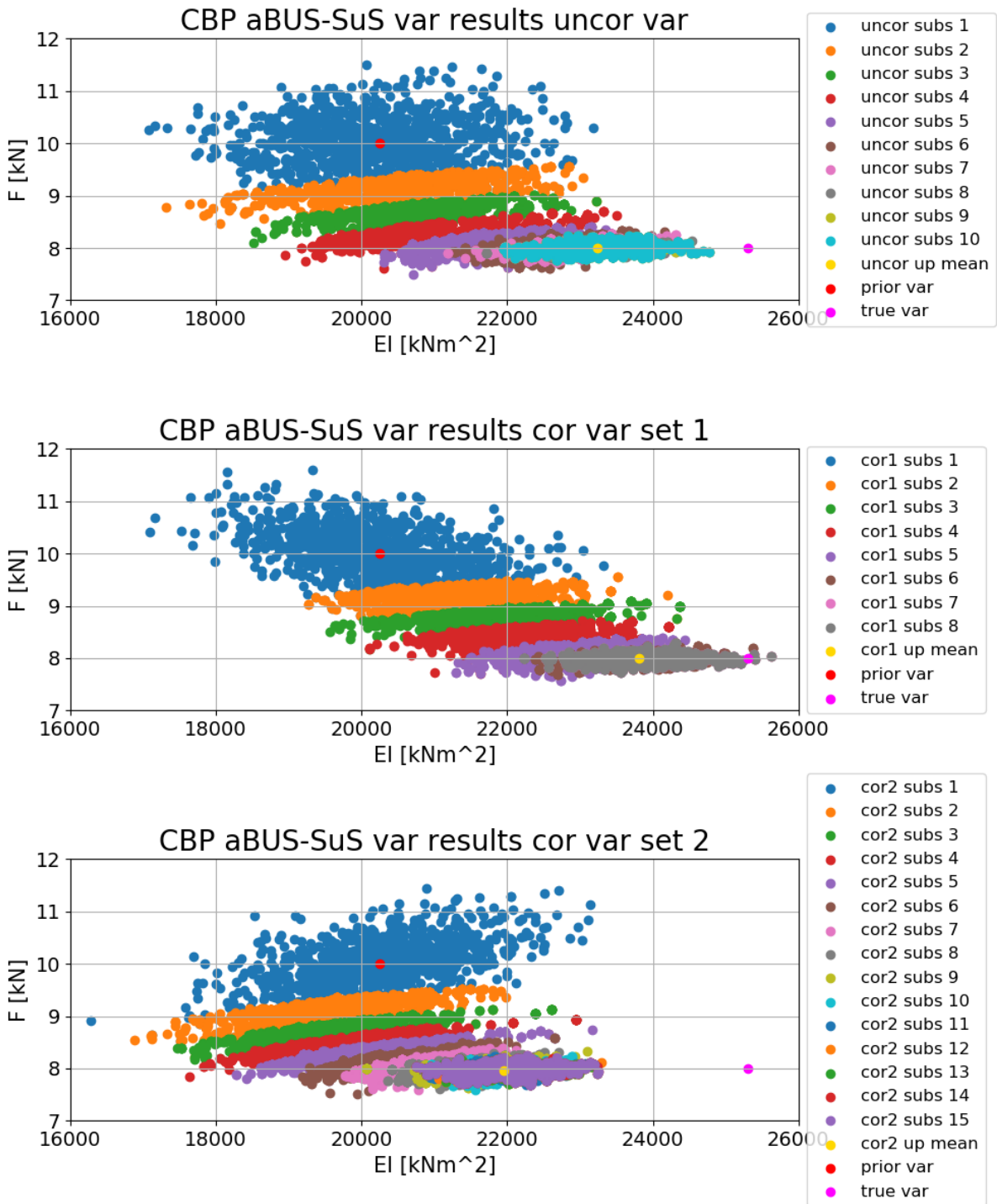


Figure 5.15: CBP updating results of the variables from the aBUS-SuS analysis with correlated variables

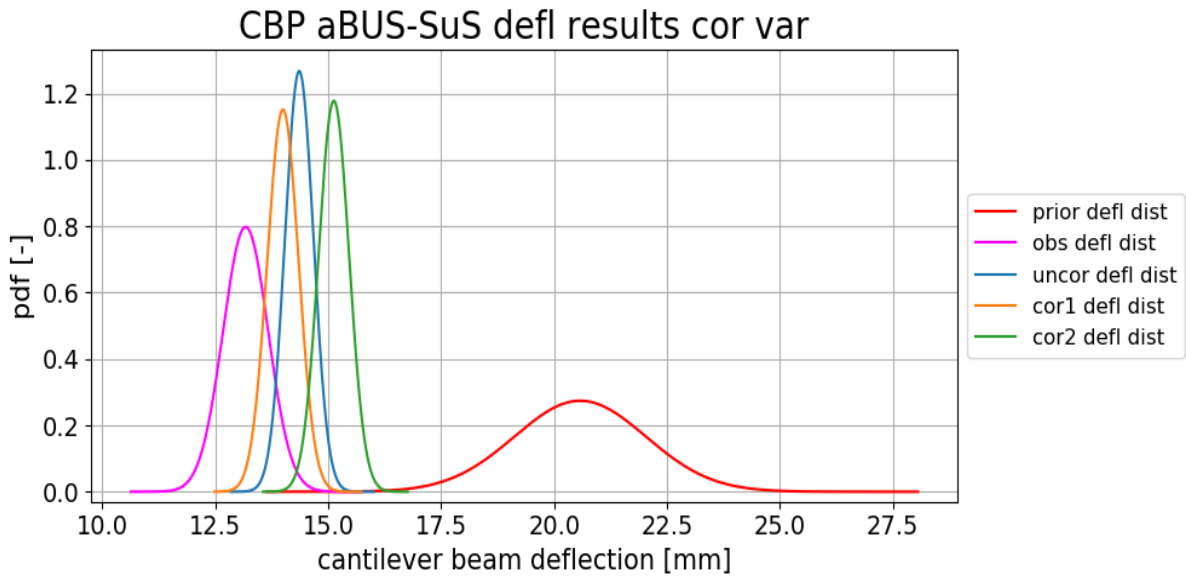


Figure 5.16: CBP deflection updating results of the aBUS-SuS analysis with correlated variables

5.5 Method parameters

Up to this point the N and $p0$ method parameter values have been set equal to the default values mentioned in (subsection 5.1 aBUS-SuS method parameter valued). As the parameters play a large role in the aBUS-SuS method it is important to understand their influences. Therefore in this section, it is tested how the aBUS-SuS method reacts to different method parameter values. To test this a series of analyses with the $p0$ and N values in (table 5.13) are performed. These values for the method parameters meet the conditions that are set in (subsection 3.2.4 Detailed method description).

To level out the influence of the random component in the aBUS-SuS method, every $p0$ and N combination is calculated 50 times to generate the average results. For every analysis, the same CBP settings are used of which the used parameters, observations and correlations are listed in (table 5.14).

Method parameter values					
N	100	400	700	1000	1500
$p0$	0.02	0.05	0.1	0.2	0.5

Table 5.13: Method parameter values used to test their influences on the aBUS-SuS analysis results.

Cantilever Beam Problem values method parameter analysis							
Analysis	Variables			Observations			
	nr.	var.	cor./uncor.	nr.	type	pos [x]	cor/uncor
4.1	2	F, EI	uncor.	2	Defl., Mom.	L, θ	uncor.

Table 5.14: Cantilever Beam Problem settings used for testing the method parameter influences on the aBUS-SuS analysis results.

Method parameters true parameter values

The used true parameter values are based on the prior parameter values mentioned in (subsection 4.2.2 CBP prior parameters). For EI the true parameter value is 25% larger than its prior parameter value. The prior standard deviation of EI is set equal to five per cent of its prior mean value. The true value of F is taken to be 20% smaller than its prior parameter value. If a parameter is considered a constant it means that its value is equal to the prior parameter value (table 4.1).

Method parameters problem parameters					
Parameter	Unit	Prior mean	Prior stdev.	True mean	Distribution
F	[kN]	10.0000	0.5000	8.0000	normal
L	[m]	5.0000	-	-	-
EI	[kNm ²]	$2.0250 \cdot 10^4$	$1.0125 \cdot 10^3$	$2.5313 \cdot 10^4$	normal

Table 5.15: The problem parameter values used in the Cantilever Beam Problem Method parameters analysis step.

5.5.1 Method parameters results

The results of changing both the method parameters are presented in (figure 5.17, figure 5.18). In this figure the lines represent the average cantilever beam deflections at the tip of the beam (subsection 5.1 Data point positioning) for the different N, p_0 combinations. Additional to the lines are error bars at every p_0 value which represent a single standard deviation of the updated cantilever beam deflection results for the method parameter sets. Both the prior and observed cantilever beam deflections are not plotted as this would stretch the vertical axis significantly, resulting in a large loss of detail of the average results.

Observing the results in (figure 5.17, figure 5.18) shows that the average updated deflections and moments of force for every N/p_0 combination are roughly the same, Only the line of $N = 100$ deviates from this trend. Other differences between the results are in the standard deviations of the updated behaviour. The standard deviations for the larger N values do not vary significantly and for the moment of force the standard deviations for $N = 100$ increase again for $p_0 > 0.1$. It is noteworthy that for $N = 100$ the value of $p_0 = 0.1$ is the best performing value on average over the beam deflection and moment of force results.

Another aspect that the values of N and p_0 have an influence on is the computation time which is therefore analysed in (subsection 5.5.1 Computation time).

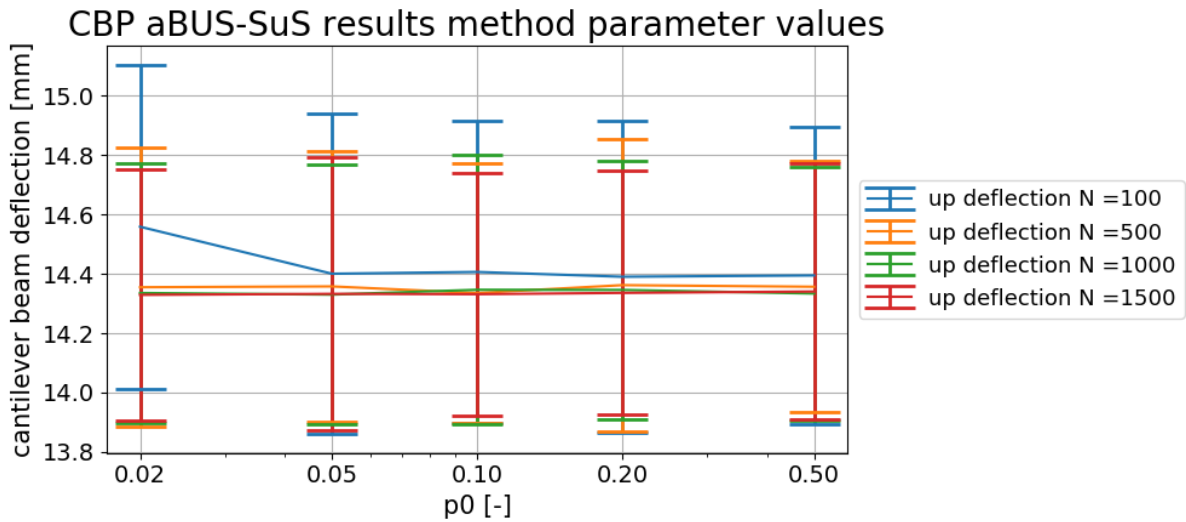


Figure 5.17: Average method parameter influence on posterior beam tip deflection of 50 iterations per N/p_0 combination

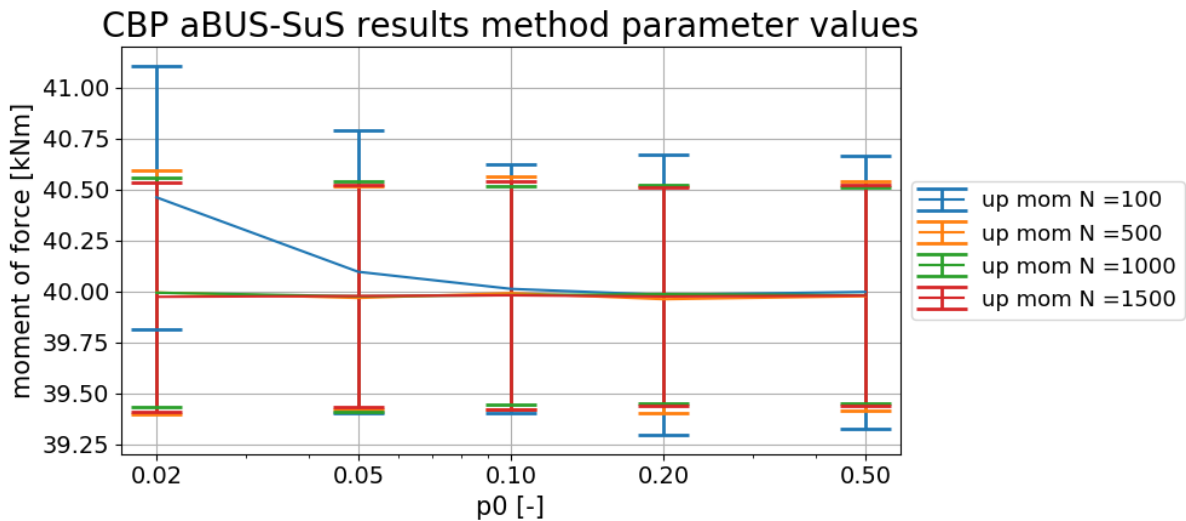


Figure 5.18: Average method parameter influence on posterior maximum moment of force of 50 iterations per N/p_0 combination

Computation time

The computation time of an aBUS-SuS analysis is problem-specific and depends on the individual calculation time. Therefore the number of individual calculations is a much better reference for the analysis' computation time. Below in (figure 5.19), the number of LF calls of the method parameter analyses are plotted for the different N/p_0 combinations. Every LF call represents a single CBP calculation.

Two evident conclusions can be made based on (figure 5.19). One, a larger N value strongly increases the computation time of an aBUS-SuS analysis and two, a larger p_0 value increases the computation time of an aBUS-SuS analysis.

The reason for the increase of LF calls with a larger N value is straight forward as the value of N represents the number of parameter sets per subsets (subsection 3.2.4 Detailed method description). Method parameter p_0 causes an increase in the LF calls in a different way, as p_0 defines the minimum number of seed parameter sets to be taken for the next subset (subsection 3.2.4 Detailed method description). By increasing this number of seed parameter sets the next subset progresses less from the previous subset compared to when a lower p_0 value is used. This way the aBUS-SuS analysis requires more subsets before convergence and therefore leads to increased computation times.

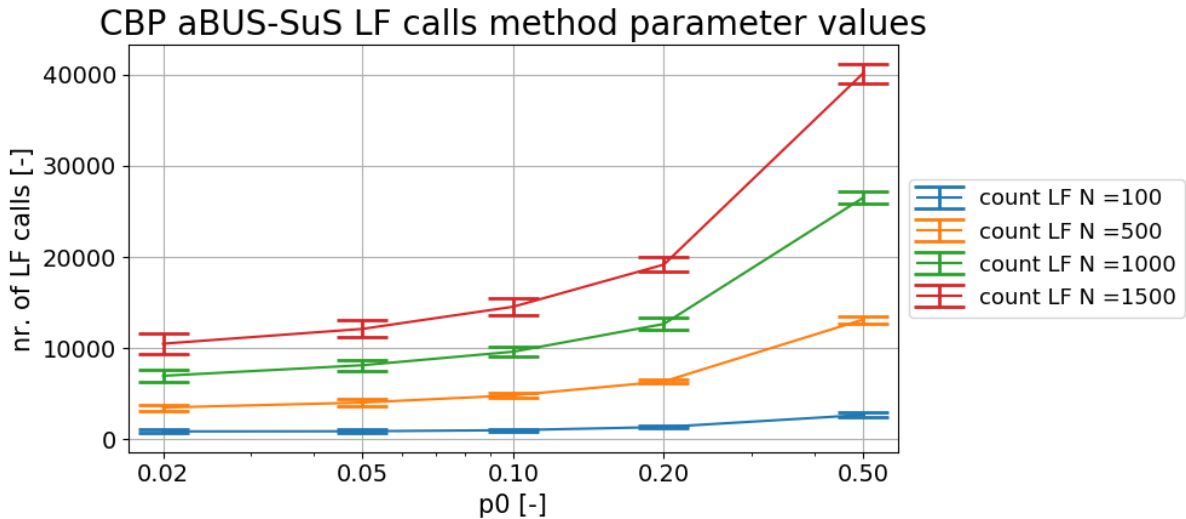


Figure 5.19: Method parameter influence on the number of likelihood function calls of the CBP

5.6 Conclusions

Throughout this chapter, a series of analyses are performed. Based on the results of these analyses a number of conclusions can be drawn on the influences of different settings in the aBUS-SuS method.

The first conclusion is that if not enough observations are used to enforce a unique solution to the problem, the aBUS-SuS method will converge to the most likely solution, which is very likely to be the closest solution. In the analysis (subsection 5.2.2 Two variables one observation) the most likely solution is the closest point along the line of possible solutions to the prior variable values. The method attempts to converge to this solution but it is very unlikely that the method actually reaches it. Due to the inherent randomness of the method, the analysis will not produce the same results every time it converges towards the same solution. In the case of the two variables one observation analysis a so-called FORM analysis (subsection 3.2.1 Reliability updating) will return this closest point as its result.

The second conclusion is on the use of correlated observations. As mentioned before in (section 6.1 Observation correlations) the observation correlations represent the correlations of the observation errors. The results of the synthetic analyses in (subsection 5.3 Multiple observations and observation correlations) show that the aBUS-SuS method is able of approaching the used observations a lot closer and update the CBP variables with higher accuracy and reliability if strong observation correlations are used. But there is a big remark to be made on these results.

The analyses with multiple correlated observations are performed as synthetic inverse analyses. The observations used in these analyses are synthetically generated with known variable values (section 3.3 Synthetic analysis) and with the analytical solutions of the CBP (equation 4.1, equation 4.2). Therefore the used deflection observations all correspond with the analytical solution deflections as indicated in (figure 5.20). This allows the aBUS-SuS method to converge to a more accurate solution of the CBP if strongly correlated observations are used. In reality, the observations are more likely to look like the realistic measurements in (figure 5.20) where the observations randomly deviate from the theoretical beam profile. Therefore it is expected that if a realistic set of measurements is used in the aBUS-SuS analysis with strong observation correlations the method would have much more difficulty converging and possibly would not be able to. This could be simulated by applying noise to the synthetic measurements, although it was chosen not to do this in (section 3.3.2 Synthetic analysis application).

Another downside of the correlated observations is the smaller LF domain as shown in (figure 5.14). This side effect of increasing the observation correlations reduces the workable distance between the prior predictions and observations for the analysis to be able to converge.

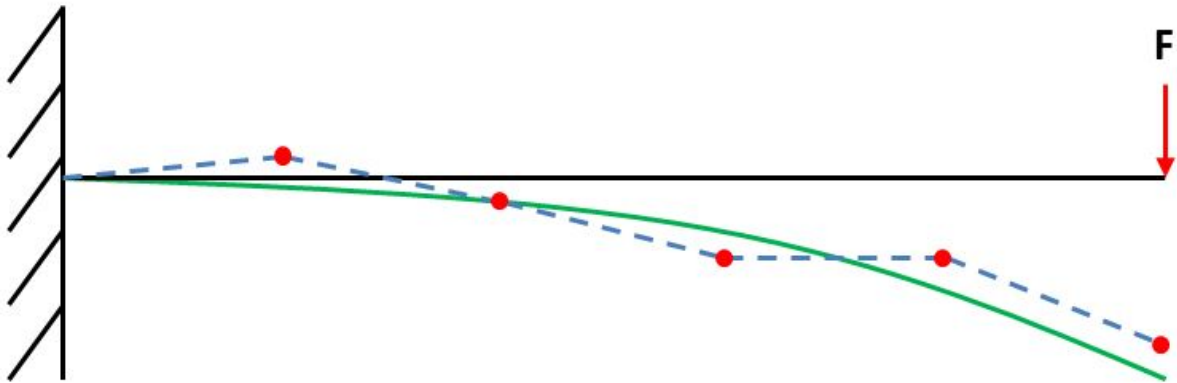


Figure 5.20: CBP correlated observations discussion example of the synthetic generated observations which are used in this chapter against realistic CBP measurements.

Based on the reasoning described above it is concluded that the best settings for the observation correlations are to implement the observations as uncorrelated

The third conclusion is on the use of correlated variables. Using correlated variables can have a significant positive contribution to the analysis results and computation time, but the user is advised to be cautious. With the analyses in (section 5.4 Correlated variables), the true parameter values are known. In reality, the solution isn't known, making it difficult to determine which correlation coefficients are beneficial for the analysis. This is important to realise as correlation coefficients between parameters that are described in research do not take into account potential prior parameter value determination errors. These errors can result in the situation where the theoretical correlation coefficient between two variables is described as positive while one variable's true value is higher than the used prior mean value and the other variable's true value is lower than the used prior mean value. This is what happens in analysis 3.3 (table 5.9).

The fourth conclusion is on the method parameters N and p_0 . The value for N is case-specific, depending on problem complexity. For the value of p_0 , it is advised to select it depending on the value of N . If a large number of samples per subset is used it might be favourable to use a

p_0 value smaller than 0.1. If a small value for N is used the value of 0.1 for p_0 is a reliable and efficient value concerning results consistency and computation time.

Chapter 6 Synthetic Inverse analysis of a Sheet Pile Wall

6.1 Introduction

As described in (chapter 4 Cases Set-Up) the medium complicated problem is used to test the aBUS-SuS method's ability to update the parameter set of a more complicated problem. Which is in this case represented by a FEM model of a sheet pile wall. In this chapter, a series of synthetic inverse aBUS-SuS analyses are performed on the sheet pile wall model. From here on referred to as the synthetic sheet pile wall problem (SSPWP). This series is divided into four main sections (figure 6.1).

Every section has a different objective which is described in detail in the concerning sections. Although there are a couple of constant factors that allow for the comparison of the different analyses results. These factors are discussed below.

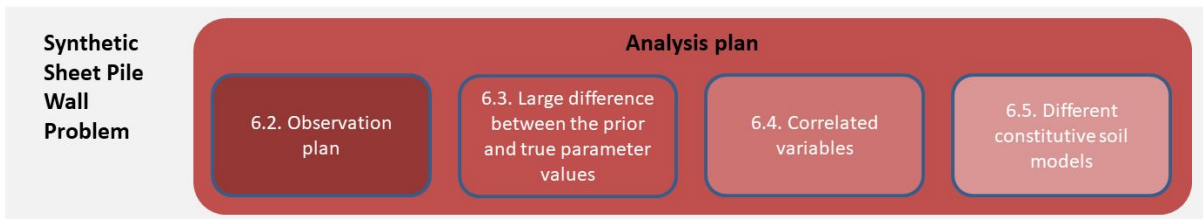


Figure 6.1: Subdivision of the Synthetic Sheet Pile Wall Problem analysis plan into three main sections.

Method parameter values

The used method parameter values are $p0 = 0.1$ and $N = 150$. The value for N is significantly smaller than what was used for the CBP. This is decided on grounds of practicality which has as the biggest influence the computation time. A FEM calculation takes significantly longer to solve than an equation like an analytical solution. The value of $p0$ is selected based on the confirmation of the CBP analyses in the previous chapter (chapter 5 Cantilever Beam Problem Analyses) that the value of 0.1 is efficient in terms of computation time and repetition of the aBUS-SuS analyses results for smaller N values.

Likelihood function

Similar to the CBP for the SSPWP the LF is also based on the multivariate Gaussian distribution.

Observations

Mentioned in (subsection 4.3.2 Hochstetten measurements) there are five available types of measurements performed in the Hochstetten field test. These types of measurements are the horizontal wall displacements, surface settlements, the strut force, bending moments of the sheet pile wall and lateral earth pressures on the sheet pile wall. In the analyses, these same types of observations are used to perform the synthetic inverse analysis. The used data points are indicated in the figure below (figure 6.2).

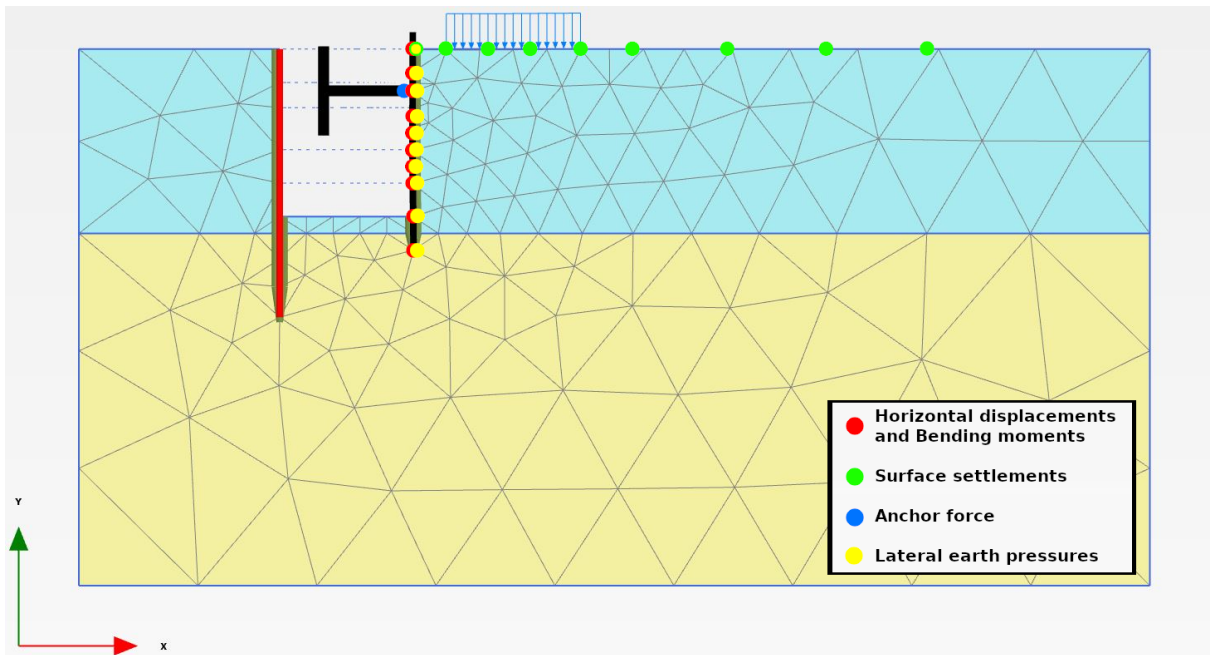


Figure 6.2: Observation locations used in the Synthetic Sheet Pile Wall Problem analysis. The legend shows which types of observations are obtained from the different coloured points.

Observation correlations

The different types of measurements that can be used as observations in the aBUS-SuS analysis can be implemented as correlated or uncorrelated. The effects that possible observation correlations can have on the aBUS-SuS analysis process and results are tested and discussed in the previous chapter (chapter 5 Cantilever Beam Analysis). But the first step is to try and determine through reasoning whether the observations can be considered correlated in the first place.

The different types of observations are obtained using different types of sensors. These different types of sensors are mentioned in (figure 4.8) and it can be assumed that every sensor has its own random measurement error resulting in the assumption that all the observations can be assumed to be uncorrelated.

Constitutive soil models

In the first three sections of this chapter, the HS constitutive model is used for the analyses. The influence of using the MC constitutive model is tested in the final analysis in (section 6.5 Different constitutive soil models analysis).

6.2 SSPWP Observation plan analysis

In this section, it is tested what influences the different types of observations and the number of every type of observation have on the aBUS-SuS parameter updating process. Therefore a series of aBUS-SuS synthetic inverse analyses are performed using different types and quantities of observations. The analysis plan which describes the different observation configurations used in the different analyses is given below (Subsection 6.2 Observation plan analysis plan). Further information is given in the chapter introduction (section 6.1 Introduction) but more information on the used true parameter values and the used observation standard deviations is required. This information is elaborated on below in (subsection 6.2 Observation plan observation standard deviations, subsection 6.2 Observation plan analysis true parameter values).

Observation plan analysis plan

One of the most important conclusions of the CBP (chapter 5 Cantilever Beam Problem Analyses) is that the different types and number of used observations are essential for reliable aBUS-SuS results. Ideally, a set of as little observations as possible is used to create a unique solution. For the CBP, this is easily realised although for the SSPWP with the application of a FEM model it becomes a lot more complicated. With the analytical solutions of the CBP, it is possible to determine upfront how many observations are needed. This isn't as straight forward with a FEM model which is why the different observation configurations are tested for their influences on the aBUS-SuS analysis.

SSPWP Observation plan analysis plan						
Case nr.	Nr. of observations	Types of observations				
		Hor. wall defl.	surf. setl.	anch. force	bend. mom.	soil stress
1.1	1	1	0	0	0	0
1.2	2	1	1	0	0	0
1.3	3	1	1	1	0	0
1.4	4	1	1	1	1	0
1.5	5	1	1	1	1	1
1.10	10	10	0	0	0	0
1.20	20	10	10	0	0	0
1.21	21	10	10	1	0	0
1.31	31	10	10	1	10	0
1.41	41	10	10	1	10	10

Table 6.1: Combinations of numbers and types of observations for the Synthetic Sheet Pile Wall Problem Observation plan analyses. The locations from where the different observations are obtained is visualised in (figure 6.2).

The possible types of observations are given and described in (section 4.3.2 Hochstetten measurements). To test what combination of observations and what number of the different observations is advised to be used, an analysis plan is constructed. This analysis plan is given in (table 6.1). As is indicated in the table a series of ten analyses with different observation configurations are performed on the SSPWP. The first five analyses, numbers 1.1 till 1.5 use only one observation

of the used types of observations. For the analyses 1.10 till 1.41 all the points in (figure 6.2) are used.

Observation plan observation standard deviations

The standard deviations used for the different observations are arbitrary as no consistent information on the different sensor measurement errors is found. But the errors are selected to be of similar orders of magnitude compared to their measurement values. The used standard deviation values are given below in (table 6.2).

SSPWP Observation plan observation standard deviations						
	Hor. wall defl. [mm]	surf. setl. [mm]	anch. force [kN]	bend. mom. [kNm]	soil stress [kPa]	
stdev	0.1	0.1	0.1	0.1	0.1	0.1

Table 6.2: Observation standard deviations used for the first analysis step of the Synthetic Sheet Pile Wall Problem.

Observation plan analysis true parameter values

For these analyses, the differences between the prior and synthetic parameter values are kept small with one main reason, reduction of the computation time. The synthetic parameter values used in this analysis step are given in (table 6.3). The differences between the prior and true parameter values are selected randomly but there is a slight connection to the Hochstetten case (subsection 4.3.2 Hochstetten field test background information). In the field test the updated cohesion showed the largest difference compared to the prior parameter value, this difference comes back in the used true parameter values.

There is the concern that with the small difference between the prior and true parameter values the method could converge to the most likely solution. Especially while the observation combination is not confining enough. Therefore this effect is tested in the next section (section 6.3 Large difference between prior and true parameter values).

SSPWP Observation plan true parameter values						
	$\gamma_{1,dry}$ [kN/m ³]	$E_{1,50}^{ref}$ [kPa]	c'_1 [kPa]	ϕ'_1 [°]	ψ_1 [°]	ϕ'_2 [°]
True values	16.8300	$3.6693 \cdot 10^4$	3.3	39.14	7.84	39.14

Table 6.3: True parameter values used for the first analysis step of the Synthetic Sheet Pile Wall Problem.

Observation plan correlated variables

In the series of tests in this section, the variables are considered uncorrelated. The influences of correlated variables are tested in (section 6.4 Correlated variables analysis).

6.2.1 Observation plan analysis results

Introduction to the observation plan analysis results

The results that are of interest in this section are the updated variable values and the updated predicted behaviour of the model when using the updated variable values. In reviewing these results the analysis numbers 1.1 till 1.5 are referred to with the name '*single observations results*'. The results of the remaining five analysis numbers are referred to as '*multiple observations results*'.

The results of analysis 1.1 are shown in the shape of a bar plot in (figure 6.3). The top bar plot contains the update results of the variable values while the bottom bar plot contains the results of the updated model behaviour. Every bar in the upper plot shows the updated mean normalised variable value combined with error bars which show the standard deviations of the updated values of the variables. The light blue lines represent the normalised true values, in the upper bar plot the true parameter values and in the lower bar plot the observations which are used in the aBUS-SuS analysis. The short red lines indicate the prior parameter values and prior model behaviour.

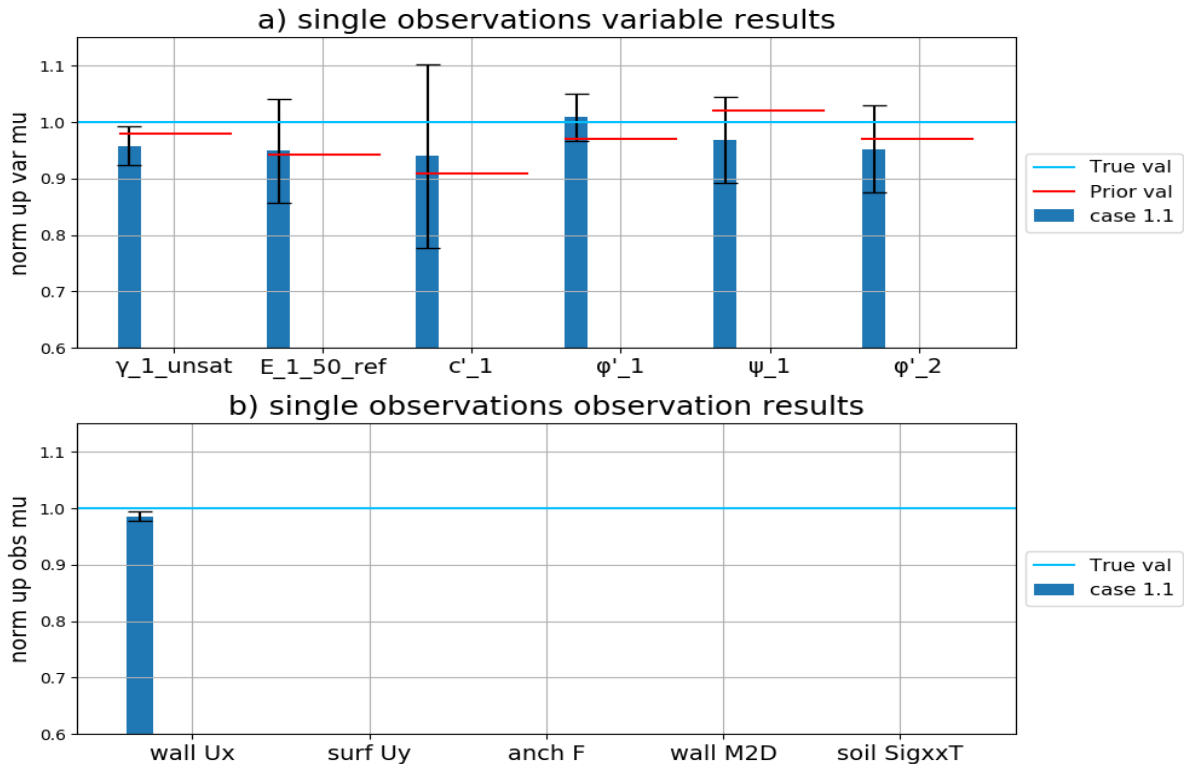


Figure 6.3: The aBUS-SuS synthetic inverse analysis results of the observation combination referred to as analysis number 1.1

The results of analysis 1.10 are shown in (figure 6.4). The formats and functions of the bar plots in this figure are identical to (figure 6.3) but in the case of the multiple observations results, there is one difference. The bars of the observation results represent the average normalised updated model behaviour of the observation types. There is one exception to this adaptation, namely the results of the anchor force of which only one observation is used throughout the entire series of analyses (table 6.1).

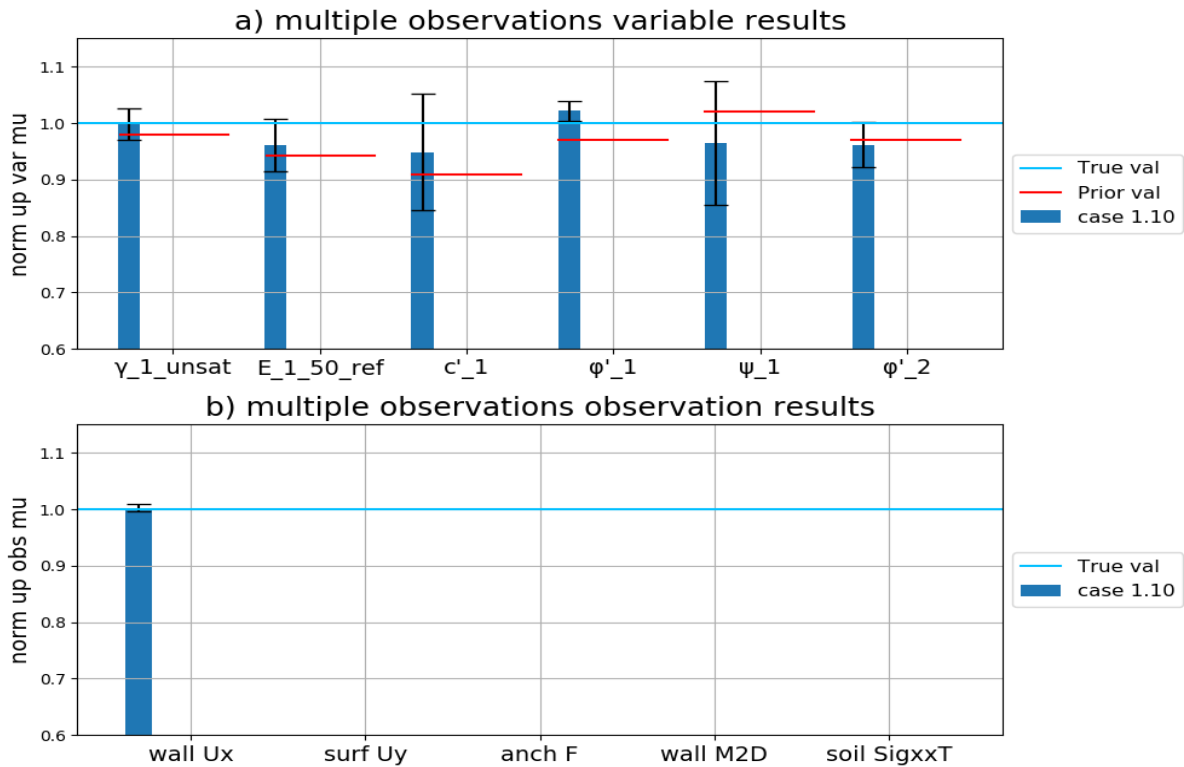


Figure 6.4: The aBUS-SuS synthetic inverse analysis results of the observation combination referred to as analysis number 1.10

Observation plan single observations analyses results

With the understanding of how the plotting of the SSPWP aBUS-SuS results works the results of the analyses can be plotted. The results of the analysis with single observations are plotted below in (figure 6.5). The blue bars represent analysis 1.1, the orange bars represent analysis 1.2, the green bars represent analysis 1.3, the red bars represent analysis 1.4 and finally, the purple bars represent analysis 1.5.

When looking at the bar plots the first observation is that the updating results vary wildly depending on the used observation configuration. Starting with the lower bar plot (figure 6.5 b. single observations observation results) the aBUS-SuS method is capable of approaching the used observations in the analysis. The largest error in approaching the used observations is in analysis 1.5 which shows an underestimation of the horizontal soil stress against the sheet pile wall in *phase 7* (table 4.2) by roughly four per cent. The other four observations are approached by analysis 1.5 within an error range of one and a half per cent over- or underestimation. The analyses 1.1 – 1.4 show updated model behaviour errors of less than one and a half per cent compared to the observations.

Upon observing the upper bar plot (figure 6.5 a. single observations variable results) the spread in the update results is much larger compared to the lower bar plot. The updated variable values vary wildly between the different analyses. Therefore the updated variable values of analysis 1.1 (the blue bars) are reviewed first.

From the six updated variable values only the updated mean value of ϕ'_1 is relatively close to the true parameter value. The other five variables show an underestimation error of three to five

per cent, which is small in geotechnical engineering terms but relatively large in this synthetic inverse analysis setting where there are no soil and model uncertainties. Ideally, the updated mean variable values are between the prior values and true values. But the two variables $\gamma_{1,dry}$ and ϕ'_2 moved away further from their true values. This is a first indication that the aBUS-SuS analysis converges towards a more likely solution than the true solution.

The standard deviations of the updated variable values also show large variations. Where the updated c'_1 values are equal to the updated mean value plus and minus one standard deviation range from a twenty per cent underestimation to a ten per cent overestimation of the true value.

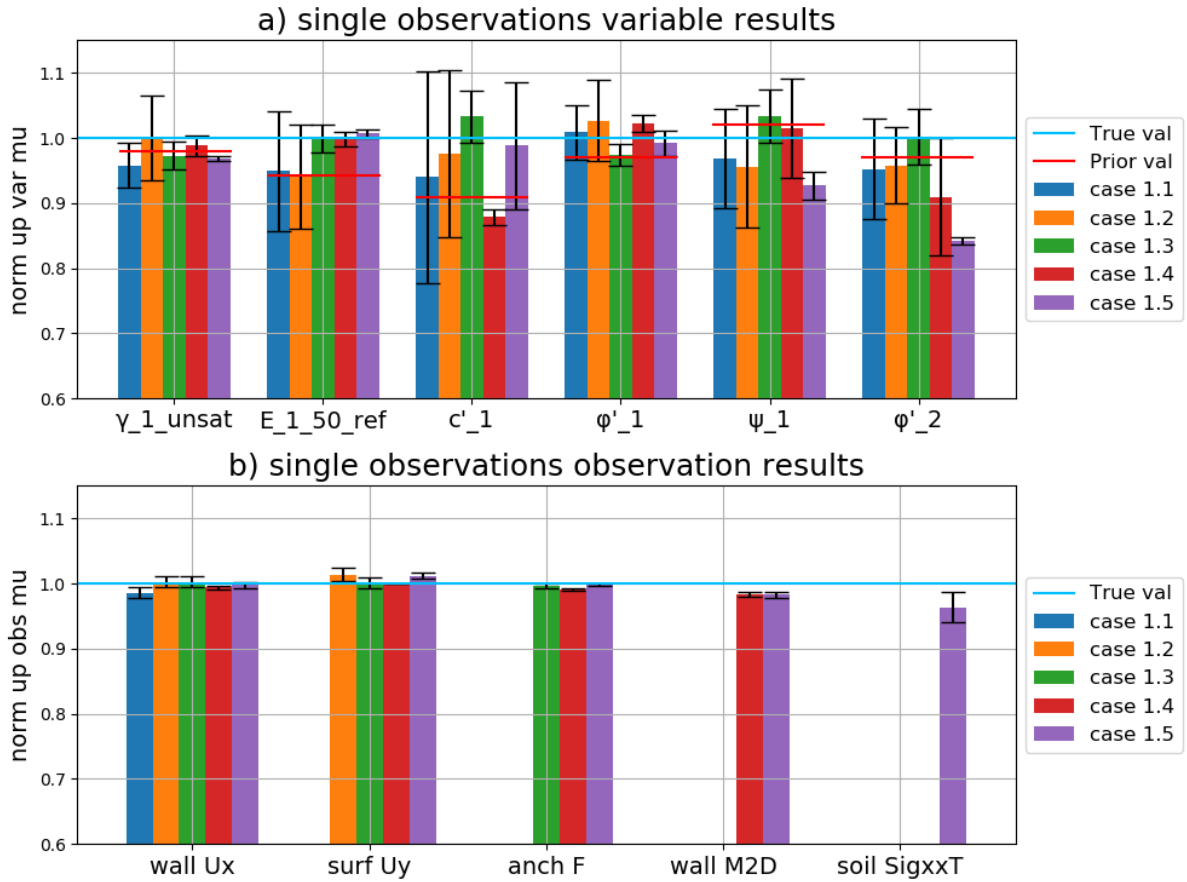


Figure 6.5: The aBUS-SuS synthetic inverse analysis results of the observation combination referred to as analysis numbers 1.1 – 1.5

The results of the other analyses (1.2, 1.3, 1.4 and 1.5) show similar overshooting and undershooting behaviour as analysis 1.1 in the updated values. But in all the analyses the aBUS-SuS method had the least difficulty with updating the variables $\gamma_{1,dry}$, ϕ'_1 and $E_{1,50}^{ref}$. These three variables show the smallest variation in the updated values between the different analyses. For the parameter $E_{1,50}^{ref}$ it depends on the used observation configuration as for the analyses 1.1 and 1.2 the updated values are almost the same as the prior mean values, whether for analyses 1.3, 1.4 and 1.5 the updated mean variable values are almost equal to the true parameter values.

From the analyses with single observations, the following observations are the most important.

Not a single of the five analyses 1.1 – 1.5 is capable of updating all the variables towards their true values. The best performing analysis is 1.3 with three types of observations. But the analyses 1.4 and 1.5 with more types of observations, and thus more available data, converged towards a very different set of updated variable values. This leads to the intermediate conclusion that neither of the observation configurations of analyses 1.1 – 1.5 is sufficient to isolate the unique solution, in this case, the true parameter values of the SSPWP.

Observation plan multiple observations analyses results

Based on the intermediate conclusion of the analyses with single observations, which states *neither of the observation configurations of analyses 1.1 – 1.5 is sufficient to isolate the unique solution, in this case, the true parameter values of the SSPWP.*, the results of the next set of analyses, 1.10 – 1.41, are reviewed. All the results of the multiple observations analyses are given in (figure 6.6).

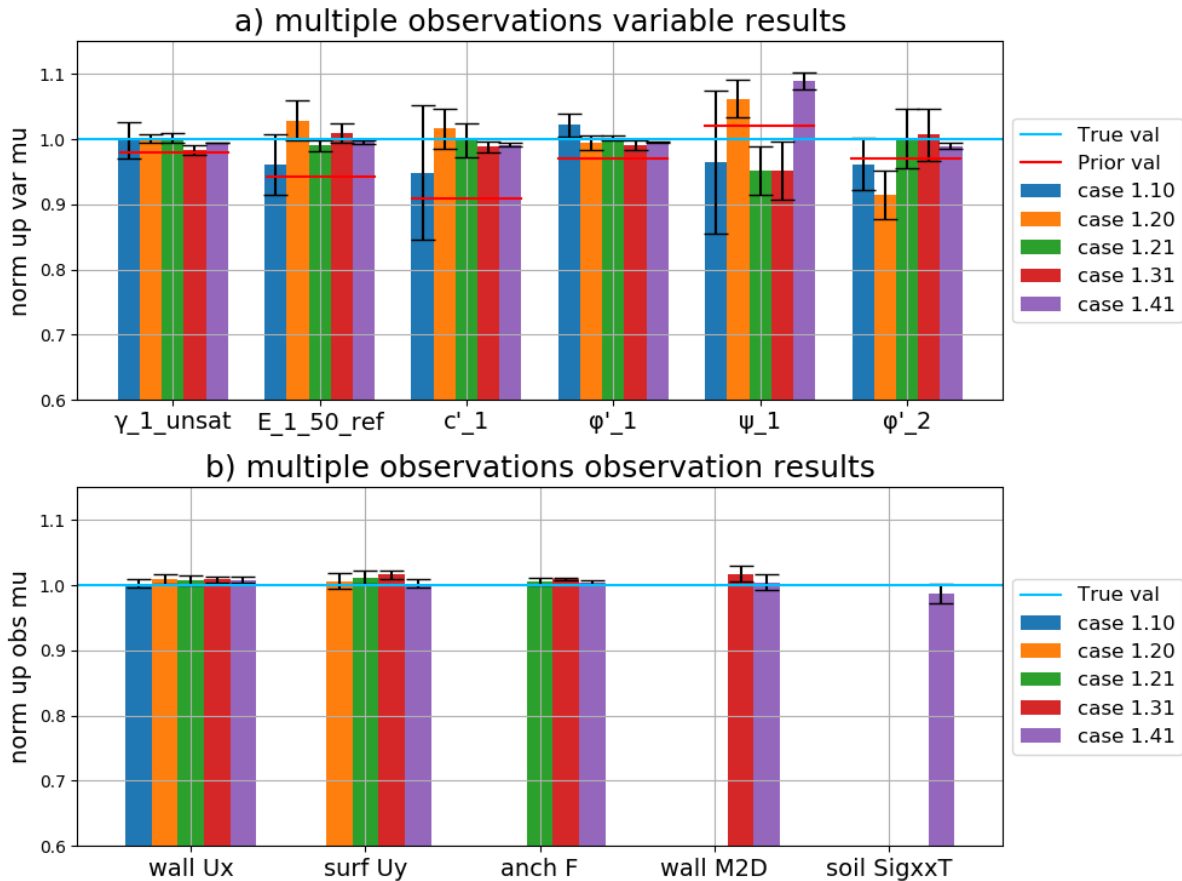


Figure 6.6: The aBUS-SuS synthetic inverse analysis results of the observation combination referred to as analysis numbers 1.10 – 1.41

Starting with the lower bar plot (figure 6.6 b. multiple observations observation results) it is evident that just as for the analyses 1.1 – 1.5 the aBUS-SuS method is capable of approaching the used observations closely for the analyses 1.10 – 1.41. The errors in the updated model behaviour are within the range of one and a half per cent. Compared to the analyses with single observations, where analysis 1.5 showed the largest error in the horizontal soil pressures, analysis 1.41 shows a smaller mean error in the updated horizontal soil pressure prediction. Although the

differences between the analyses with single observations and multiple observations are minimal on the updated model behaviour predictions.

When observing the upper bar plot (figure 6.6 a. multiple observations variable results) and comparing it with the upper bar plot of the single observations results (figure 6.5 a. single observations variable results) it is evident that all the multiple observations results show less variation and are on average closer to the true values. Also, the standard deviations of the updated variable values are smaller for analyses 1.10 – 1.41 compared to 1.1 – 1.5, especially for analysis 1.41 which shows the smallest standard deviations on the updated variable values.

Analyses 1.10 and 1.20 show the largest updated mean variable errors to the true parameter values on $E_{1,50}^{ref}$, c'_1 and ϕ'_2 . These parameters are where the analyses 1.21, 1.31 and 1.41 show updated mean variable values very close to the true parameter values. All the analyses have updated the mean values of $\gamma_{1,dry}$ and ϕ'_1 very consistently and resulted in values close to the true parameter values. All the analyses turned out to have difficulty with the parameter ψ_1 . The analyses 1.10, 1.21 and 1.41 underestimated the updated mean variable value with an error of five per cent, while the analyses 1.20 and 1.41 overestimated the updated mean variable values. Although when taking into account the sensitivity analyses results of the parameter selection procedure (subsection 4.3.3 Parameter sensitivity results) the parameter ψ_1 has the smallest influence on the deformation criteria used in the sensitivity analyses of the unsaturated sand layer. This makes it a difficult variable to update properly as a relatively large difference in its value doesn't have a very large influence on the model behaviour compared to the other variables.

These observations indicate that even with the larger number of observations per observation type the aBUS-SuS method still converges towards another solution. Although it needs to be taken into account that parameter ψ_1 is a difficult parameter to update and that after reconsidering and observing these results it might be a better idea to leave it out of the variable set. Another reason for leaving it out in the future is because it is known to strongly depend on the parameter ψ_1 , allowing for an assumed value for ψ_1 based on ϕ'_1 ([25]).

Conclusions observation plan SSPWP

Taking the results of all the analyses with different observation configurations into account leads to the conclusion that the three analyses 1.21, 1.31 and 1.41 perform the best. With performance is referred to two different aspects of the results. The first aspect is how close the updated model behaviour approaches the used observations. The second aspect is how close the updated values of the variables approach the true values. From the three analyses 1.21, 1.31 and 1.41 it is analysis 1.41 that performs the best. The differences between the three analyses in the first aspect are negligible, especially because of the different combinations of types of observations. In the second aspect, it is the analysis 1.41 which has the smallest standard deviations of the updated values of the variables and has thus converged the closest to a possible solution. This is a reason to conclude that from the observation configurations given in (table 6.1) it is the observation plan with the most observations which results in the best-updated values of the variables.

The next step in the SSPWP analysis plan is testing the aBUS-SuS method's performance on updating the values of the variable when the true parameter values deviate strongly from the prior values. With the research question in mind (section 1.2 Research questions), to perform those analyses the most effective observation configuration is to be selected. As mentioned above the observation configuration of analysis 1.41 performs the best in updating the soil variable values. Although it also requires the most elaborate observation plan which doesn't make it

the most favourable observation configuration. But even with the observation configuration of analysis 1.41 the aBUS-SuS method converges to another solution than the true solution. This is the reason to use as many observations and types of observations as possible to test the aBUS-SuS variable updating performance in the following SSPWP analysis step. Therefore the observation configuration of analysis 1.41 is selected to be used for the following SSPWP analysis step in the following section (section 6.3 Large difference between prior and true parameter values analysis) to test the aBUS-SuS variable updating performance.

6.3 Large difference between prior and true parameter values analysis

Following up on the results of the previous section (section 6.2 SSPWP Observation plan analysis) in this section aBUS-SuS method is tested using large differences between the prior parameter values and the true parameter values. This way it is imposed that the true solution is an unlikely one, depending on if the used observation configuration (subsection 6.2.1 Conclusions observation plan SSPWP) is constrictive enough the aBUS-SuS will be able to converge towards this true solution.

Compared to the problem set up used in the previous series of analyses (section 6.2 SSPWP Observation plan analysis) a couple of things have changed besides the true parameter values. These changes are to the used observation standard deviation and prior variable standard deviations

Observation and prior variable value standard deviations

The standard deviations used for the different observations and prior values of the variables are larger for this analysis than in the preceded analyses. The reason for this increase is the same as encountered in the CBP analyses (subsection 5.2.3 Two variables two observations). This is where a large portion of the first subset's samples fall outside of the measurable domain of the LF, resulting in a value of zero for those samples during the conditional sampling process of the aBUS-SuS method (subsection 3.2.4 Detailed method description). In this case with the large difference between the prior and true parameter values, this LF limit resulted in all the samples of the first MCS subset having assigned a value of zero in the conditional sampling process. Therefore the method is not capable of selecting the given per cent of best-performing samples, which results in the analysis stalling.

To overcome this stalling of the aBUS-SuS analysis, both the prior variable standard deviations and the observation standard deviations are increased to make sure that the analysis doesn't stall after the first MCS step. The in this section used standard deviations for both the prior variables and the observations are given in (table 6.4, table 6.5). These values are arbitrary as they are based on trial and error to determine whether the applied standard deviation combination is successful in preventing the analysis from stalling. Therefore the prior standard deviation values of the variable are no longer justifiable.

SSPWP Increased prior variable standard deviations						
	$\gamma_{1,dry}$	$E_{1,50}^{ref}$	c'_1	ϕ'_1	ψ_1	ϕ'_2
COV [%]	20	20	70	30	30	30

Table 6.4: Prior variable standard deviations used for the second analysis step of the Synthetic Sheet Pile Wall Problem with a large difference between the prior and true parameter values. The standard prior variable coefficients of variation are given in (table 4.4, table 4.5).

SSPWP Increased observation standard deviations						
	Hor. wall defl. [mm]	surf. settl. [mm]	anch. force [kN]	bend. mom. [kNm]	soil stress [kPa]	
stdev	0.3	0.3	0.5	0.3	0.4	

Table 6.5: Observation standard deviations used for the second analysis step of the Synthetic Sheet Pile Wall Problem with a large difference between the prior and true parameter values.

Increased true parameter values

The used true parameter values for this section are given in (table 6.6).

SSPWP Increased true parameter values						
	$\gamma_{1,dry}$ [kN/m ³]	$E_{1,50}^{ref}$ [kPa]	c'_1 [kPa]	ϕ'_1 [°]	ψ_1 [°]	ϕ'_2 [°]
True values	17.3250	$5.1924 \cdot 10^4$	9	41.8	6.4	43.7

Table 6.6: Increased true parameter values used for the second analysis step of the Synthetic Sheet Pile Wall Problem.

Large parameter difference uncorrelated variables analyses results

The results of the aBUS-SuS analysis with uncorrelated variables and a large difference between the prior and true parameter values are given below in (figure 6.7). The format and the way that the results are presented is identical to the results in the previous section (subsection 6.2.1 Introduction to the observation plan analysis results). The only difference is that the range of the vertical axes is larger than in the previous section. This is to allow for additional results with larger updated deviations from the true values to be plotted in the same figure in later sections (section 6.4 Correlated variables analysis, section 6.5 Different constitutive soil models analysis).

Starting with the lower bar plot (figure 6.7 b. large parameter difference observation results) it shows that the aBUS-SuS method is relatively successful in approaching the used observations. For the horizontal wall displacements, anchor force and soil pressures the updated model predictions are within a one per cent error range of the used observations. With the other two types of observations, the surface settlements and bending moments in the wall, the aBUS-SuS method has more difficulty approaching the observations with the updated model behaviour. The updated surface settlement predictions overshoot the observations on average by two per cent while the bending moments in the wall are on average underestimated by three per cent.

These differences in the updated model behaviour predictions also return in their updated standard deviations. The results of the horizontal wall displacements, anchor force and soil pressures show the smallest normalised standard deviations while the results of the surface settlements and the wall's bending moment show the largest uncertainty in their updated mean values.

How the aBUS-SuS method was able to converge with these errors in the average updated model behaviour predictions lays in the larger observation standard deviations. The larger observation standard deviations allow for a larger error in the updated model behaviour predictions during the aBUS-SuS method convergence.

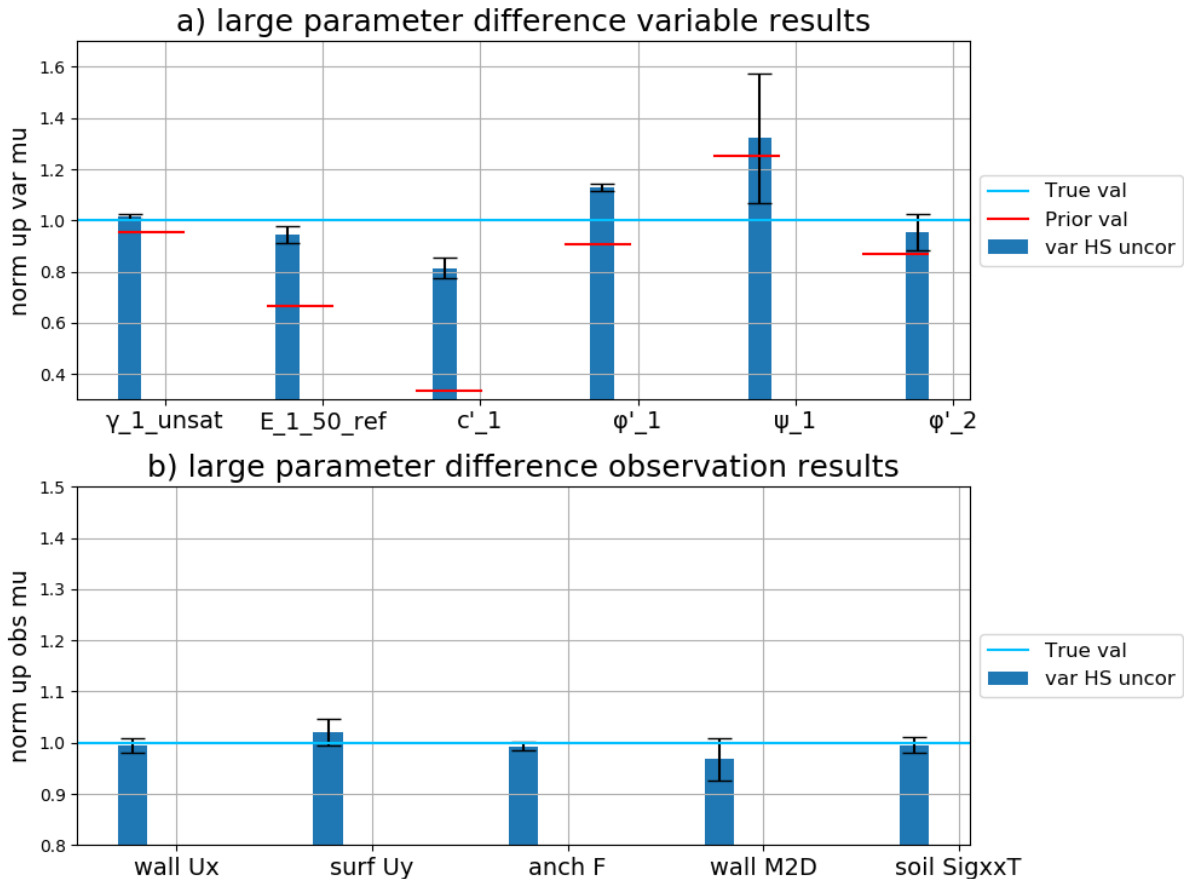


Figure 6.7: The aBUS-SuS synthetic inverse analysis results of the SSPWP with a large difference between the prior and true parameter values with uncorrelated variables

Observing the upper bar plot (figure 6.7 a. large parameter difference variable results) shows large errors in the updated mean variable values. The variable $\gamma_{1,dry}$ is the variable in this analysis of which the updated mean value is the closest to the true value. The updated mean values of $E_{1,50}^{ref}$, c'_1 and ϕ'_2 underestimate the true value with the largest underestimation of almost twenty percent for the effective cohesion. Although these three variable's true values are underestimated, they are updated towards their true values. This is an indication that even though the true values aren't reached, the aBUS-SuS method does attempt approaching their true values. The updated mean values of the final two variables, ϕ'_1 and ψ_1 , overestimate their true values. Although there is a difference between the update paths of these variables. The updated mean value of ϕ'_1 overshoots its true value during the analysis while the updated mean value of ψ_1 moved further away from its true value compared to its prior mean value.

As earlier mentioned in (section 6.2.1 Observation plan analysis results) the process of moving further away from the true value is proof that the aBUS-SuS method converges towards another solution.

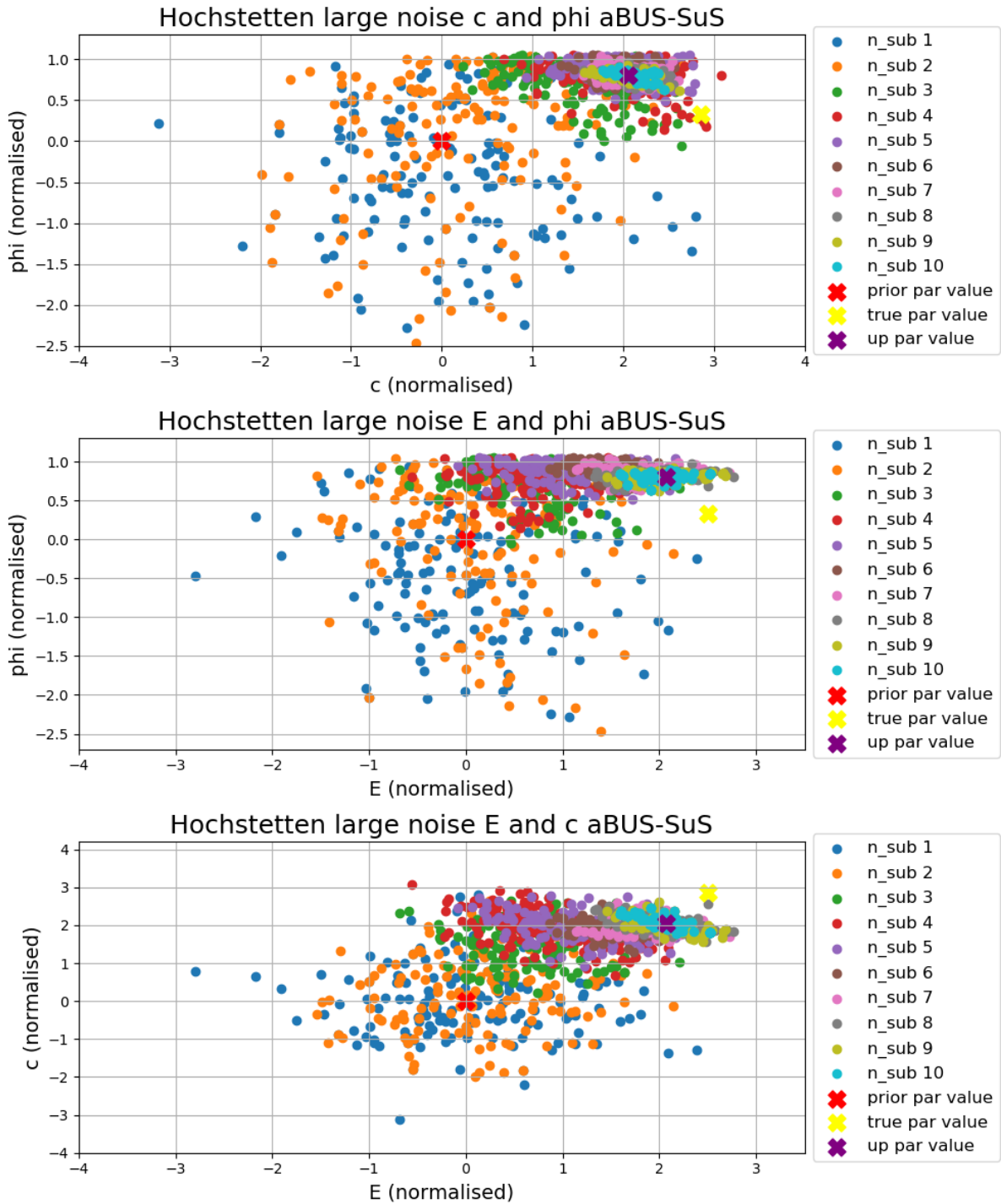


Figure 6.8: The aBUS-SuS synthetic inverse analysis variable results of the SSPWP with a large difference between the prior and true parameter values with uncorrelated variables

Conclusions large parameter difference uncorrelated variables analyses

It is concluded that the analysis with the larger difference between the prior and true parameter values converges towards another solution than the true parameter values. Even though the use of larger observation standard deviations allows for larger errors in the analysis results. Some observations indicate the method has converged towards another solution. The variable ϕ'_1 significantly overshoots its true value during the analysis and the variable ψ_1 moved further away from its true value. These are clear indications that the aBUS-SuS method converged towards another solution than the true solution. Therefore it is concluded that the most elaborate observation configuration of analysis 1.41 (table 6.1) is not confining enough to result in a unique solution of the SSPWP.

The next possibility is to attempt to increase the likelihood of the true solution. Prior variable standard deviations and observation standard deviations are already increased and the observations are assumed to be uncorrelated. Therefore in the next section, the use of correlated variables is tested on the SSPWP.

6.4 Correlated variables analysis

In this section, it is tested whether the use of correlated variables has a significant influence on the aBUS-SuS method when it is applied to a more complex problem. Added to that is the objective of testing if the use of correlated variables increases the likeliness of the true solution. This has the purpose of the aBUS-SuS method converging towards the true solution instead of to the solution it converged to in the previous section (section 6.3 Large difference between prior and true parameter values analysis).

For this reason the exact same settings are used as in the previous section (table 6.4, table 6.5 and table 6.6). The only difference is the use of correlated variables of which the correlation matrix is given in (table 6.7). From literature, it is derived that the variable ϕ'_1 and ψ_1 are generally positively correlated ([25]). Although, based on the results in the previous chapter (section 5.4 Correlated variables) and the arbitrary selected true parameter values it is known that it is not favourable for the analysis to have the variables ϕ'_1 and ψ_1 positively correlated. Therefore the correlation coefficient between these two variables is selected to be equal to zero.

SSPWP correlation matrix correlated variables								
R=	[$\gamma_{1,unsat}$	$E_{1,50}^{ref}$	c'_1	ϕ'_1	ψ_1	ϕ'_2]
		1.0	0.5	0	0.5	0.5	0	
		0.5	1.0	0	0.25	0.25	0	
		0	0	1.0	0	0	0	
		0.5	0.25	0	1.0	0	0	
		0.5	0.25	0	0	1.0	0	
		0	0	0	0	0	1.0	

Table 6.7: Synthetic Sheet Pile Wall Problem correlation matrix of the variables for an analysis with a large difference between the prior and the true parameter values. The matrix is based on information from [3], [35] and [27]

Large parameter difference correlated variables analyses results

The results of the analysis with correlated variables are visualized in (figure 6.9) where they have been added next to the results of (figure 6.7).

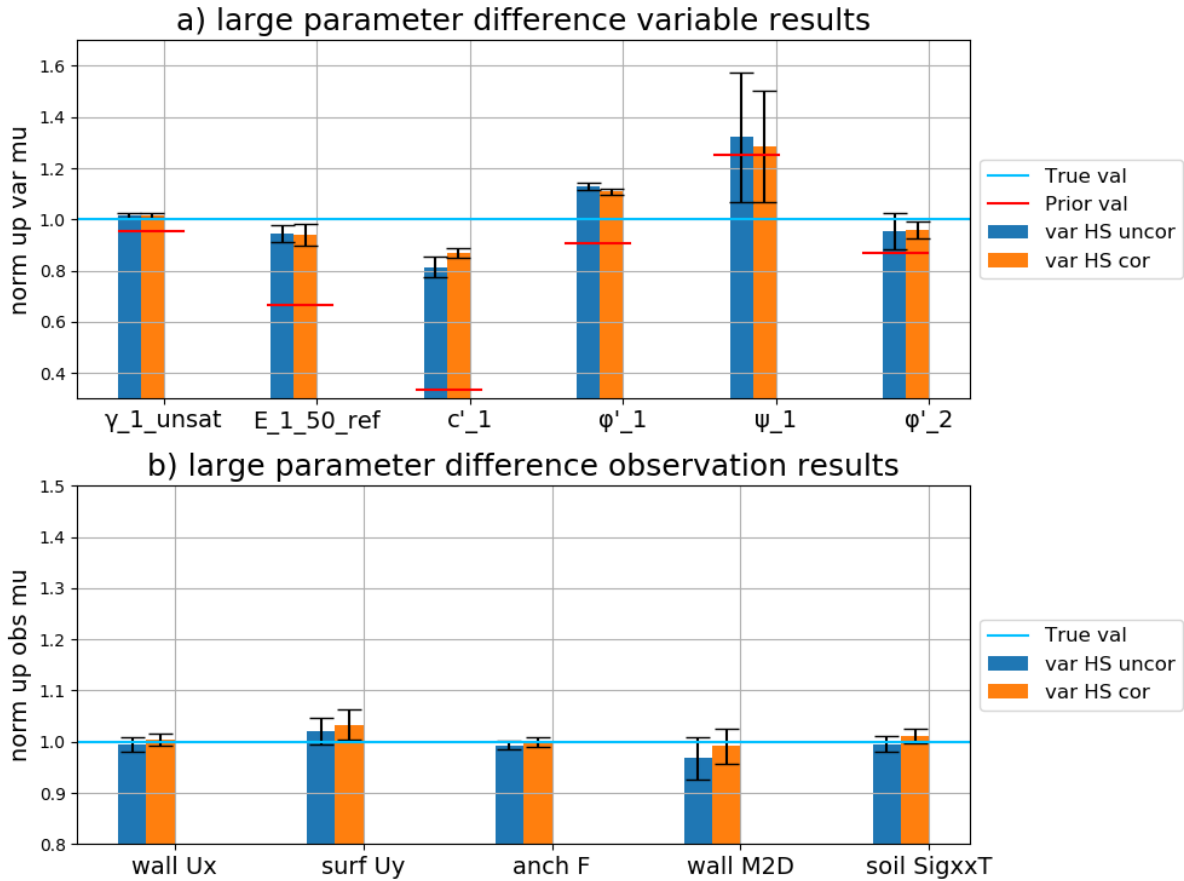


Figure 6.9: The aBUS-SuS synthetic inverse analysis results of the SSPWP with a large difference between the prior and true parameter values with correlated variables

Looking at the lower bar plot (figure 6.9 b. large parameter difference observation results) there aren't many significant differences between the two analyses on how close their results approach the used observations. The analysis with correlated variables approached the bending moment observation very close compared to the analysis with uncorrelated variables. Although the opposite applies to the surface settlements where the analysis with correlated variables overshoots the observation further.

The upper bar plot (figure 6.9 a. large parameter difference variable results) also shows little differences between the results of the two analyses. Where it is concluded that the analysis with uncorrelated variables converged to another solution (subsection 6.3 Conclusions large parameter difference uncorrelated variables analyses) the same observations are made in the results of the analysis with the correlated variables. The overshooting of the variable ϕ'_1 and the moving away from its true value by variable ψ_1 are slightly reduced. Also does the variable c'_1 approach its true value a little bit closer. The differences between the other three variables are neglectable.

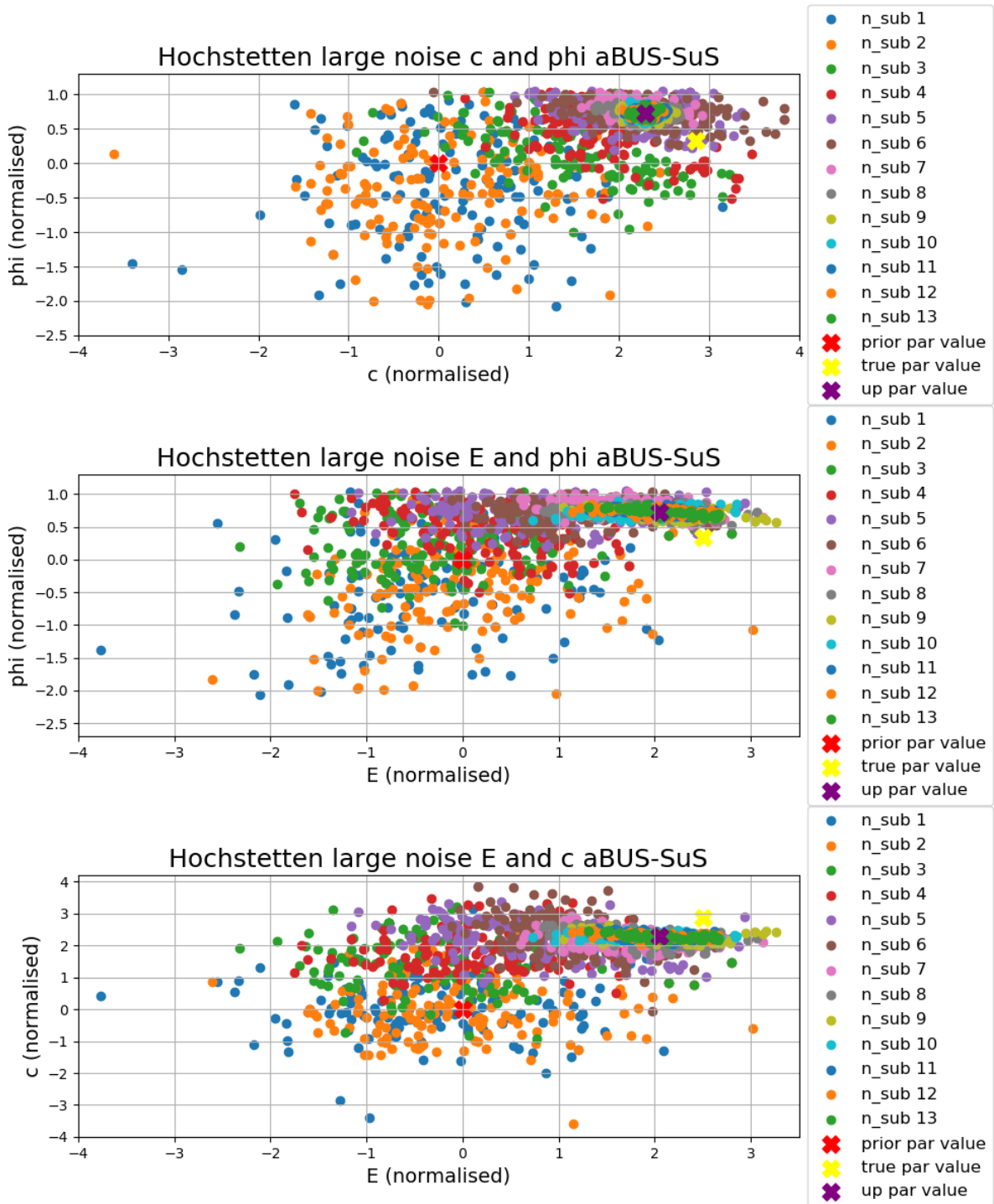


Figure 6.10: The aBUS-SuS synthetic inverse analysis variable results of the SSPWP with a large difference between the prior and true parameter values with correlated variables

With the use of correlated variables the aBUS-SuS method still converges to the same solution the analysis with uncorrelated variables. Together with the inherent randomness of the aBUS-SuS method results, it is not possible to assign the differences in the results to only the use of correlated variables. To see if the correlated variables influenced the aBUS-SuS convergence process the subsets with the variable values are plotted for three different variable combinations

in (figure 6.10).

Comparing the figures (figure 6.8) and (figure 6.10), a couple of observations can be made. The first observation is that the analysis with the correlated variables required more subsets to converge. The second observation is that the values of $E_{1,50}^{ref}$ in the second subset have more weight on the lower values in the analysis with correlated variables compared to the values for $E_{1,50}^{ref}$ in (figure 6.8). The third observation is that the subsets in the top plot with the variables ϕ'_1 and c'_1 show a wider spread in the analysis with correlated variables compared to the analysis with uncorrelated variables. With this larger spread of the variables ϕ'_1 and c'_1 they overlap significantly with their true values, confirming that the solution which the method converged to in these analyses is a more likely solution than the true solution.

Overall the use of correlated variables does have a significant influence on the convergence process of the SSPWP but it doesn't have a significant influence on the updated results.

Conclusions large parameter difference correlated variables analyses

The use of correlated variables has a limited positive influence on the update results. The updated model behaviour of the correlated variables shows small average increases on all the used types of observations. Although these differences are on average not necessarily positive. Concerning the updated values of the variables, the analysis results with correlated variables do show an improvement compared to the results of the analysis with uncorrelated variables. For the variables c'_1 , ϕ'_1 , ψ_1 and ϕ'_2 the updated average values are closer to their true values and the standard deviations are smaller. This doesn't apply to the variable $E_{1,5-}^{ref}$ which has a slightly larger standard deviation in the results of the correlated variables. Although the improved update values of the variables of the analysis with correlated show the same pattern as the updated values of the variables of the analysis with uncorrelated variables. Therefore it is concluded that the use of correlated variables is not effective enough to enforce a unique solution or increase the likeliness of the true solution over the other possible solution.

6.5 Different constitutive soil models analysis

With the conclusions that the previous analyses did not converge to the true solution, there is one more setting that can be varied. In all the previous SSPWP analyses the used constitutive soil model is the HS model. In this analysis, the MC constitutive soil model is used. The used prior variable values are given in (table 4.4) and the selected variables in the sensitivity analysis are the same for the HS and MC (subsection 4.3.3. As can be seen from the prior variable values for the HS and MC models the prior parameter values are the same for both the models except for the use of the Shear Modulus $G_{1,50}^{ref}$ instead of $E_{1,50}^{ref}$. This is the case because of the remote scripting service used to control Plaxis2D (section 2.3) that required $G_{1,50}^{ref}$ as a variable. Although $G_{1,50}^{ref}$ and $E_{1,50}^{ref}$ are directly correlated [25]. The true values for the MC analysis are shown below in (table 6.8). Because of the use of $G_{1,50}^{ref}$ the prior variable standard deviations are also adapted (table 6.9).

With the slightly better results of the analysis with correlated variables compared to the analysis with uncorrelated variables, the MC analysis was chosen to be performed using correlated variables as well. The used correlation matrix is again identical to the one in (section 6.4) but the variable $G_{1,50}^{ref}$ is used instead (table 6.10)

SSPWP Increased true parameter values MC model						
	$\gamma_{1,dry}$ [kN/m ³]	$G_{1,50}^{ref}$ [kPa]	c'_1 [kPa]	ϕ'_1 [°]	ψ_1 [°]	ϕ'_2 [°]
True values	17.3250	$1.0613 \cdot 10^4$	9	41.8	6.4	43.7

Table 6.8: Increased true parameter values used for the MC analysis step of the Synthetic Sheet Pile Wall Problem.

SSPWP Increased prior variable standard deviations MC model						
	$\gamma_{1,dry}$	$G_{1,50}^{ref}$	c'_1	ϕ'_1	ψ_1	ϕ'_2
COV [%]	20	20	70	30	30	30

Table 6.9: Prior variable standard deviations used for the MC analysis step of the Synthetic Sheet Pile Wall Problem with a large difference between the prior and true parameter values. The standard prior variable coefficients of variation are given in (table 4.4, table 4.5).

SSPWP correlation matrix correlated variables MC model							
R=		$\gamma_{1,unsat}$	$G_{1,50}^{ref}$	c'_1	ϕ'_1	ψ_1	ϕ'_2
	$\gamma_{1,unsat}$	1.0	0.5	0	0.5	0.5	0
	$G_{1,50}^{ref}$	0.5	1.0	0	0.25	0.25	0
	c'_1	0	0	1.0	0	0	0
	ϕ'_1	0.5	0.25	0	1.0	0	0
	ψ_1	0.5	0.25	0	0	1.0	0
	ϕ'_2	0	0	0	0	0	1.0

Table 6.10: Synthetic Sheet Pile Wall Problem correlation matrix of the variables for an analysis with a large difference between the prior and the true parameter values and the Mohr-Coulomb constitutive soil model. The matrix is based on information from [3], [35] and [27]

Large parameter difference MC model analyses results

The results of the analysis with the MC model are visualized in (figure 6.11) where they have been added next to the results of (figure 6.9).

Looking at the lower bar plot (figure 6.11 b. large parameter difference observation results) there are significant differences between the HS analyses results and the MC analysis results. The HS analyses performed relatively well on approaching the used observations but the analysis with the MC model generated completely different observations. Average overshooting errors of ten per cent on the bending moments in the wall and close to fifteen per cent on the surface settlements. It is known that the HS model is in general more suitable for predicting the behaviour of sheet pile walls but that should not apply to these results as the aBUS-SuS converges based on the observations using the LF (Subsection 3.2.4 Detailed method description). This raises the question of how the aBUS-SuS method can converge with these observations.

The question of how the aBUS-SuS method can converge with the generated observations becomes more interesting when the upper bar plot is observed (figure 6.11 a. large parameter difference variable results). The upper bar plot shows the updated variable values which show that the updated values of the variables of the analysis with the MC model show similarities with the updated values of the variables of the analyses with the HS model. There are three significant differences between the HS model analyses updated values and the MC model analysis values. These differences are in $E/G_{1,50}^{ref}$, c'_1 and ϕ'_1 . The updated value of the analysis with the MC model for $G_{1,50}^{ref}$ underestimates its true value by almost thirty per cent compared to the close to five per cent of the analyses with the HS model. Although the MC model analysis does approach the true values of c'_1 and ϕ'_1 much closer than the HS model analysis.

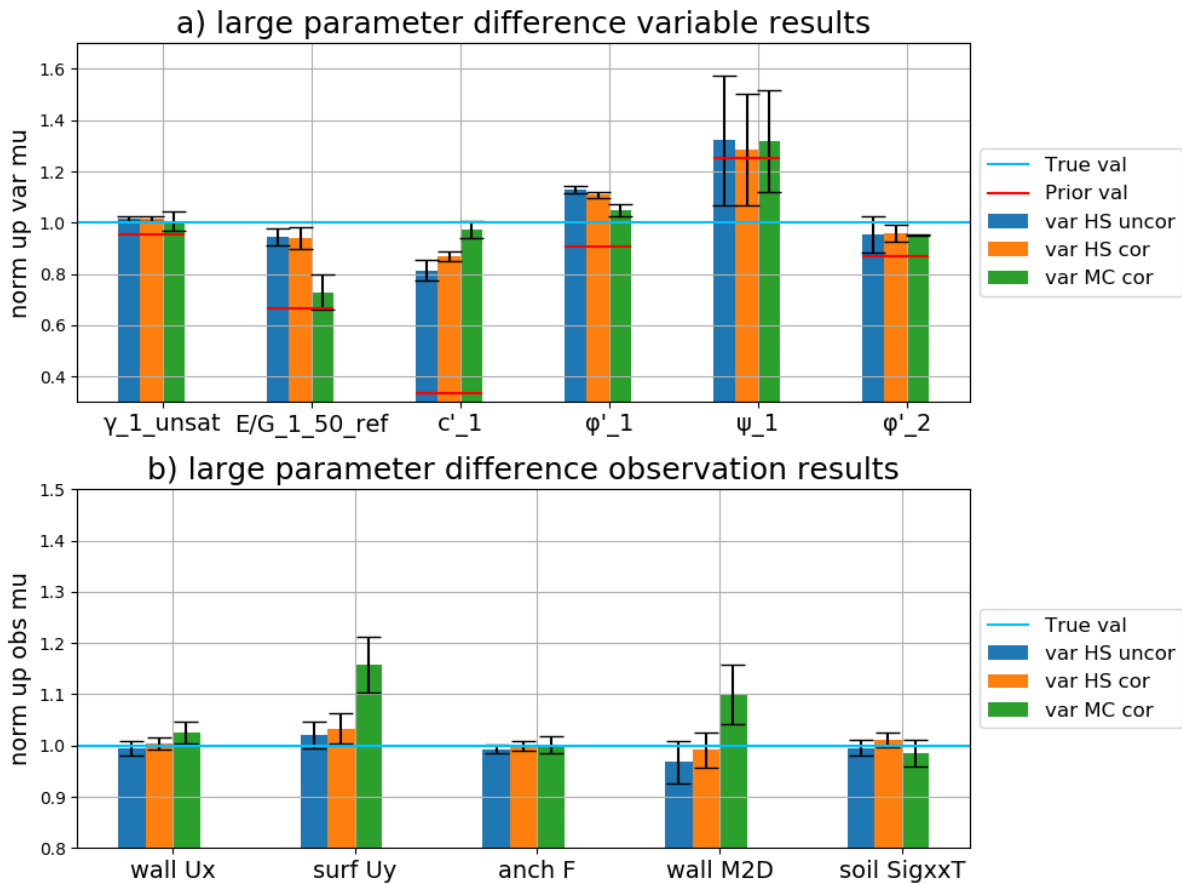


Figure 6.11: The aBUS-SuS synthetic inverse analysis results of the SSPWP with a large difference between the prior and true parameter values with correlated variables and the use of the Mohr-Coulomb soil model

To visualise the convergence path of the MC analysis the same variables as in the HS analyses results are plotted in (figure 6.12). From the top plot (figure 6.12 Hochstetten large noise c and phi aBUS-SuS) it looks like the variables c'_1 and ϕ'_1 are converging towards their true values. But upon looking closer to the convergence path of the different subsets the path they follow is horizontal. If the true values of c'_1 and ϕ'_1 would be the most likely solution the path of the subsets would deflect slightly downwards towards the true values. Although this is not the case and this is an indication that the MC analysis also converges towards another solution than the true solution. The two lower figures (figure 6.12 Hochstetten large noise G and phi aBUS-SuS,

figure 6.12 Hochstetten large noise G and c aBUS-SuS) confirm that the MC model analysis converges towards a different solution than the true solution. The final subset shows a narrow ellipse shape in both plots proofing that the variable $G_{1,50}^{ref}$ is converged close to its most likely value for the analysis.

Conclusions large parameter difference correlated variables analyses MC model

The explanation for the deviating updated model behaviours of the MC model is that the plotted values are the average model behaviour values of the final subset. Comparing the figures (figure 6.8), figure 6.10) and figure 6.12) shows that the spread on the final subsets is larger for the MC analysis compared to the spread of the final subset in both HS analyses. This shows that the MC model is more sensitive to small value changes of the variables. Together with the weight of the final subset not being exactly in the centre of the final subset due to the sample rejection process (subsection 3.2.4 Detailed method description) there is the possibility that the average observation values of the final subset don't completely match with the used observations measurements.

This sensitivity of the MC model to small changes in the values of the variables is explained by the fact that the MC model is a linear elastic perfectly plastic model on element level (subsection 4.3.3 Hochstetten Plaxis 2D model soil parameters and soil models). In *phase7* the Plaxis2D model experiences significant amounts of plastic behaviour (figure 4.12). Therefore small differences in values of the variables result in larger model prediction differences compared to the more modulated non-linear HS model response.

The conclusion that is possible to draw from these results concerning the use of the MC model instead of the HS model is the following. Using the MC model in inverse aBUS-SuS analysis results in larger uncertainty of the updated values of the variables. This is because of the MC model is more sensitive to small changes in the values of its variables. This results in larger spreads of the final subsets compared to when the HS model is used in the analysis and therefore more uncertainty in the update results. But in this specific case, the use of the MC model in the analysis did perform better in updating the soil strength parameters c'_1 and ϕ'_1 than the analyses with the HS model, which is in terms of updating the ULS's a favourable property. The updated value of the soil stiffness parameter $G_{1,50}^{ref}$ of the analysis with the MC model has a larger error compared to the true solution than the updated $E_{1,50}^{ref}$ values of the analyses using the HS model. This difference is explained with the linear elastic perfectly plastic nature of the MC model which is very sensitive to the soil strength parameters once significant amounts of plastic behaviour occur in the FEM model.

6.6 Conclusions

Based on the performed analyses it is concluded that using the HS constitutive soil model in the inverse analysis returns more reliable updated values in terms of approaching the used observations. Although even with the use of the synthetic analysis (section 3.3 Synthetic analysis) and a very elaborate observation configuration (section 6.2 SSPWP Observation plan analysis) the aBUS-SuS method is not able to find the true values of all the variables. The analysis with the MC model did approach the true values of the soil strength parameters c'_1 and ϕ'_1 very close compared to the analyses with the HS model.

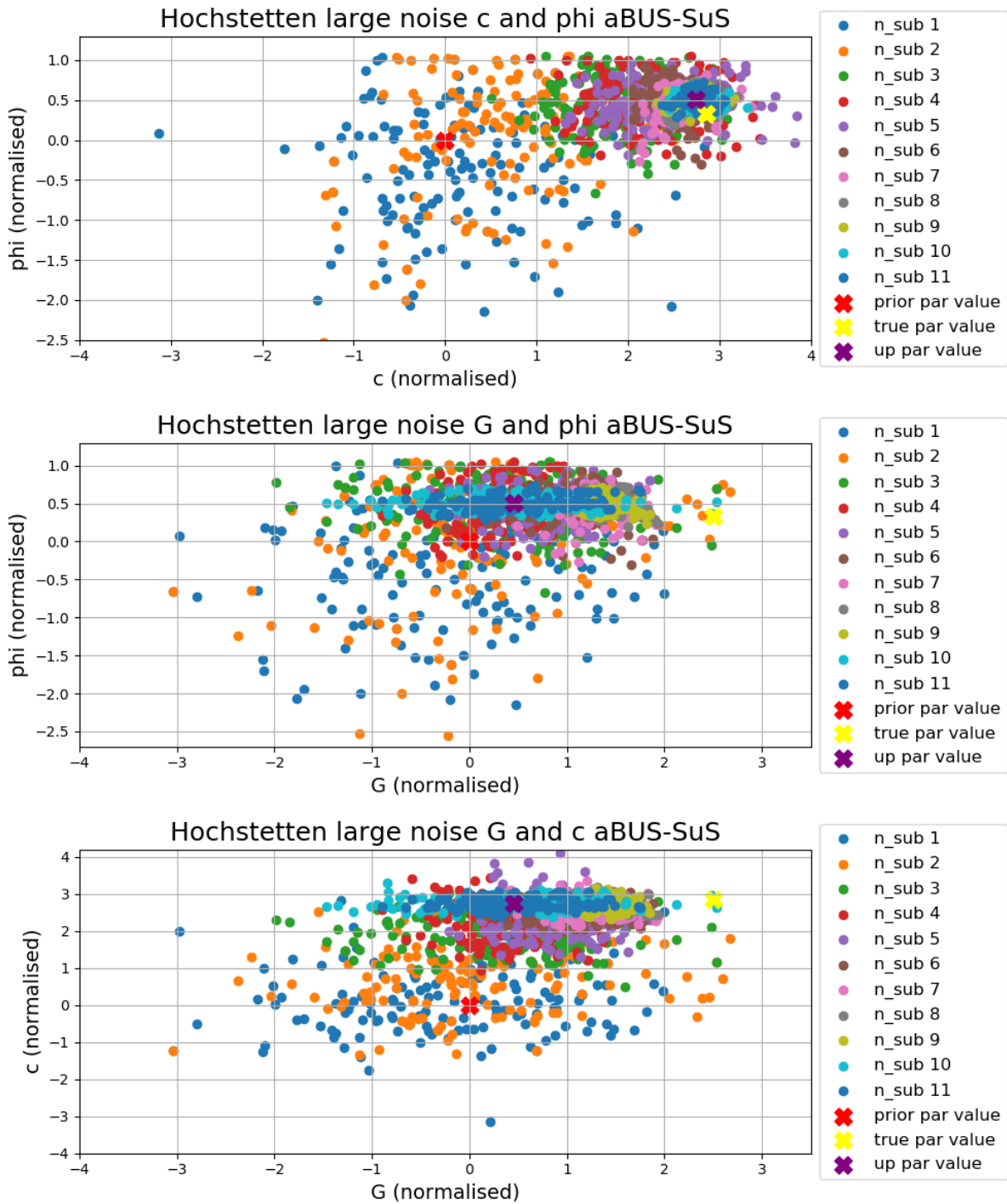


Figure 6.12: The aBUS-SuS synthetic inverse analysis variable results of the SSPWP with a large difference between the prior and true parameter values with correlated variables and the use of the Mohr-Coulomb soil model

In terms of updating the ULS's of a structure, with these being significantly controlled by plastic behaviour, (section 1.1 Problem definition) correctly updating the soil strength parameters is considered a favourable property. Still, did neither of the analyses properly update the value of the variable ψ_1 which is also considered a soil strength parameter.

A remark to be made is that the updated values of the variables depend on the used observation standard deviations. For these analyses, the observation standard deviations are the result of a trial and error process on preventing the aBUS-SuS method from stalling after the first Monte Carlo Simulation step. This is a topic that requires more research. With the observation standard deviation errors, it is not possible to know exactly to which solution the aBUS-SuS method is converging in the performed analyses. Therefore the inverse analysis might result in significantly different results when other observation correlation values are used.

Other possible contributions to the aBUS-SuS method not being able to find the true values of the parameters in the in this chapter performed inverse analyses are the increased prior standard deviations of the variables (that significantly increases the spread of the variable ϕ'_1 in the first MCS step of the uncorrelated results) and the fact that only the observations of *phase 7* (table 4.2) are used for the aBUS-SuS analysis.

Because of the larger prior variable standard deviations the true solution might become more unlikely compared to the solution that the analyses converged to in this chapter. But in reality one doesn't know what the true parameter values are and one relies on the selected inverse analysis method to return the true updated variable values even if the prior variable standard deviations are artificially changed to prevent stalling of the analysis.

Secondly, only using the observations of *phase 7* of the sheet pile wall allows for a large variety in how these observations are approached. This results in the possible situation simulated in sections (section 6.3 Large difference between prior and true parameter values analysis, section 6.4 Correlated variables analysis, section 6.5, Different constitutive soil models analysis) that there is a large difference between the prior variable values and their true values and only one set of observations to refer to while updating these variables. If the variables are updated throughout the construction process of the sheet pile wall, the first update analysis also has a large difference between the prior and true values of the variables. But the second analysis has a much smaller parameter value difference as the updated values of the variables of the first analysis are the prior values of the second analysis.

Although measurement data of the construction phases of a structure is by far not always available. Even having access to five different types of observations of a structure can be considered a luxury. If the required sensors are not installed during construction the installation needs to be taken into account and certain load tests still need to be performed to obtain measurement data [1].

Chapter 7 Conclusions and Discussion

The conclusions of this research are presented in the order of the research questions in (section 1.2 Research questions). First, it is attempted to answer the sub-questions and finally, an answer is given on the main research question itself.

Sub question 1: *Which reliability updating method is the most suitable for updating the calculated reliability of sheet pile walls?*

Criteria that the inverse analysis method is required to meet are the following. The method is capable of approaching non-linear target functions and generates stochastic results, the method does not require a large timespan of measurements and the method script is readily available in the python programming language. Thereafter the method is applied to the problem of updating parameter values in a sheet pile wall FEM model. The two methods that meet these requirements are the MCMC-MH and aBUS-SuS methods. Although the aBUS-SuS method has advantages over the MCMC-MH method. The aBUS-SuS method is better suited for calculating small failure probabilities and it doesn't suffer from dependency on the starting value. Therefore the inverse analysis method that is considered the most suitable for this research is the aBUS-SuS method.

Sub question 2: *Do advanced constitutive soil models have a parameter updating advantage over the linear elastic perfectly plastic Mohr-Coulomb soil model when applied in an inverse analysis method*

The Hardening Soil model is used as an advanced constitutive soil model in the sheet pile wall FEM model. When using service domain measurements as observations in the inverse analysis, the Hardening Soil model does prove to have an advantage over the Mohr-Coulomb model. Using the Hardening Soil model in the aBUS-SuS analysis results in the updated model behaviour approaching the used observations closer and more reliably than with the Mohr-Coulomb model.

This outcome of the comparison between the two soil models is not a coincidence. The Hardening Soil model is used because of its property of reliably predicting service domain structure behaviour. Therefore this outcome is to be expected. Although differences between the use of the Hardening Soil model and Mohr-Coulomb model in updating the soil parameters are discussed in sub-question three.

Sub question 3: *Given the available service domain measurement data, can the soil strength parameters be updated effectively in order to update a sheet pile wall's ULS's?*

It is concluded that in terms of the updated values of the variables neither of the analyses returned the true values of the entire used set of variables. The set of six soil variables are used in the FEM model of a sheet pile wall and exists out of both soil stiffness and strength

parameters. Although the focus lays on the soil strength parameters to update the sheet pile wall's ultimate limit state.

Using the Mohr-Coulomb model resulted in updated values for soil strength variables c'_1 and ϕ'_1 with errors smaller than five per cent, compared to errors larger than ten per cent from the analyses using the Hardening Soil model. Even though the updated value of ψ_1 in the analysis with the Mohr-Coulomb model is in the same order of magnitude as the updated values in the analyses with the Hardening Soil model, namely thirteen per cent. This is explained by the significant smaller influence of ψ_1 on the sensitivity analysis criteria compared to c'_1 and ϕ'_1 . Therefore it is concluded that for updating a sheet pile wall model's soil strength parameters the Mohr-Coulomb model is the most effective.

Research question: *Which types and what amounts of service domain measurement data are most effective in updating the calculated reliability (ULS's) of sheet pile walls?*

The five types of observations; horizontal wall displacements, surface settlements, bending moments in the wall, horizontal earth pressures and the anchor force are not confining enough to enforce a unique solution in the inverse analysis of a sheet pile wall FEM model. Using multiple observations per type of observations increases the accuracy of the updated values of the variables but is not enough to enforce a unique solution. In general, it is the most elaborate observation configuration that returns the most accurate answer in a synthetic inverse analysis. Requiring the use of more observations is considered to be reducing the effectiveness of the aBUS-SuS method. This reduction is counteracted by the increase in accuracy of the updated values of the variables. Therefore it is concluded that larger numbers of observations of different types of observations result in increased effectiveness in updating the soil parameter values. Therefore larger numbers of observations of different types of observations increase the effectiveness of the aBUS-SuS method in updating the ultimate limit states of sheet pile wall structures.

Overall the aBUS-SuS method proved itself to be an effective method as it generally approaches the used observations very closely. Although for practical applications a lot of measurements of different types are required for the aBUS-SuS method to effectively perform an update. Also, the stratigraphy of the soil is of large importance. More soil layers equals more variables in an analysis which increases the computation complexity and requires more measurements.

Discussion

There are some uncertainties in the used results of the analyses. These uncertainties are based on the used observation standard deviations and the number of used observations.

The used observation standard deviations have been increased significantly throughout the series of analyses. This is done to allow the method to converge. The second uncertainty is in the fact that the analysis with the Mohr-Coulomb model converges towards another solution than the true values for the variables results. It is not known where the aBUS-SuS method will converge to if other observation standard deviations are used. Therefore there are doubts about the reliability of these results.

After the results of the analyses in (chapter 6 Synthetic Inverse analysis of a Sheet Pile Wall) it is concluded that the most elaborate observation configuration used to obtain service domain measurement data is not confining enough to enforce a unique solution in the inverse analysis. This means that more measurements are required to be able to enforce a unique solution in

the inverse analysis. This can be interpreted as more different types of measurements, more measurements per measurement type or more measurements over time and different loading conditions.

The analysis results in (section 6.2 SSPWP Observation plan analysis) prove that more different types of measurements are useful in the process updating the values of the set of soil variables. Although requiring more different types of measurements is also considered a reduction in effectiveness (section 1.2 Research questions) of the updating process.

The analyses results in (section 6.2 SSPWP Observation plan analysis) also show that more measurements per measurement type is an effective measure. Although there are expected to be limitations to this approach. Once, for example, the curvature of the sheet pile wall deformations is measured along ten points it is questionable if fifteen measurement points provide a significant extra amount of information. Also, more observation points are considered to reduce the effectiveness of the updating process.

Finally, the possibility of using more measurements over time and different loading conditions are not tested in this research. In the aspect of the method being able to update the values of the soil variables based on a single set of measurements to their most likely values, the aBUS-SuS method can be considered effective. The method generally does approach the used observations very closely. Although there are still multiple possibilities on improving the inverse analysis approach for updating the variables of the soil.

Chapter 8 Recommendations

During the analyses, there are a couple of aspects that could use more research before conclusive answers can be given to the research questions of this thesis.

The results of the analyses show that the aBUS-SuS method has limitations on the distance it can cover between the prior model predictions and the used observations. In (chapter 6 Synthetic Inverse analysis of a Sheet Pile Wall) the prior standard deviations of the variables had to be increased in combination with the observation standard deviations to prevent the aBUS-SuS method from stalling. More research could be performed on the influences on the results of increasing the standard deviations of the prior variables.

Another possible research topic is to test how the aBUS-SuS method performs when a series of inverse analyses are performed to update the values of the variables instead of one analysis as in this research. When using the Hochstetten field test or a similar test which is extensively monitored as a reference case one could perform parameter updates throughout the construction process of the field test. This way it can be tested if the aBUS-SuS method does filter out the true solution as the most likely solution.

During this research it is assumed that the variables of all problems are normally distributed. In reality, the soil variables are not always normally distributed and are more likely to be distributed more like a log-normal distribution. The aBUS-SuS analysis does perform a Nataf transformation at the beginning of the analysis to make sure that an independent set of normally distributed normalised variables is used during the analysis. It could be interesting to test the influence of using other types of distributions for the variables in the aBUS-SuS method.

Similar research can be performed on the type of likelihood function that is used. The in this research used likelihood functions are all based on the mono-variate normal or multi-variate normal distribution, partly for simplicity reasons but also for its symmetry. The symmetry argument applies to the domain of the likelihood function in the sense that it doesn't matter from which side the aBUS-SuS method approaches the likelihood function because it is normally distributed. When using a likelihood function based on a log-normal distribution it does matter from which side it is approached because of its non-symmetry.

Finally, a remark can be made on the applicability of the aBUS-SuS method. For this research, it required a significant amount of time to get the aBUS-SuS analysis working. This is mostly caused by the complexity of the Plaxis2D software and not being familiar with the remote scripting server. But it requires a significant amount of time to understand how the aBUS-SuS method works precisely.

Bibliography

- [1] N. den Adel. “Load testing of a Quay Wall”. MA thesis. Delft University of Technology, 2018.
- [2] S.N. Jonkman et al. “Probabilistic Design; Risk and Reliability Analysis in Civil Engineering”. In: *Delft University of Technology* (2017). Lecture notes.
- [3] D.S.Y.A Massih et al. “Reliability-Based Analysis and Design of Strip Footings against Bearing Capacity Failure”. In: *Journal of Geotechnical and Geoenvironmental Engineering* (2009).
- [4] P. Arnold, G.A. Fenton, and M.A. Hicks. *Modern Geotechnical Design Codes of Practice*. Amsterdam, the Netherlands. IOS Press, 2012.
- [5] S.K. Au and J.L. Beck. “Estimation of small failure probabilities in high dimension subset simulation”. In: *Elsevier: Probabilistic Engineering Mechanics* 16 (2001), pp. 263–277.
- [6] K.J. Bakker. “Backanalysis of Sheetpile Wall Test Karlsruhe”. In: (1993). URL: <https://www.researchgate.net/publication/264949477>.
- [7] K.J. Bakker. “Soil Retaining Structure; development of models for structural analysis”. PhD thesis. Delft University of Technology, 2000.
- [8] G. Bishop and G. Welch. “An introduction to the Kalman filter”. In: (2001). Proc of SIGGRAPH Course 8.
- [9] R.B.J. Brinkgreve and W. Broere. *Manual Plaxis2D-Version 9.0*. Delft University of Technology and Plaxis bv. 2008.
- [10] S. Chib and E. Greenberg. “Understanding the metropolis-hastings algorithm”. In: *The American Statistician* 49.4 (), pp. 327–335.
- [11] D.A. Coley. *An introduction to genetic algorithms for scientists and engineers*. Singapore. World Scientific Publishing Co., 1999.
- [12] F. Elmi et al. *Elastoplastic joint element for the finite element analysis of the Hochstetten sheet pile wall*. London. Taylor & Francis Group, 2006.
- [13] G. Evensen. “The Ensemble Kalman Filter; theoretical formulation and practical implementation”. In: *Ocean Dynamics* 53.4 (), pp. 343–367.
- [14] *Geotechnical design of structures part 1*. NEN 9997-1. Supplied under license by NEN to: Witteveen+Bos gb witteveen on 15 march 2019. NEN. 2017.
- [15] E.R. Gilks, S. Richardson, and D.J. Spiegelhalter. *Markov Chain Monte Carlo in practice*. London. Chapman and Hall, 1996.
- [16] Engineering Risk Analysis Group. *aBUS-SuS Software packages*. Technical University of Munich. URL: <https://www.bgu.tum.de/era/software/>.
- [17] D.A. Kort. “Steel Sheet Pile Walls In Soft Soil”. PhD thesis. Delft University of Technology, 2002.

- [18] D.A. Kort and N.P.A.W. Kelleners. “Sheet Pile Wall Field Test Rotterdam”. In: (2000). Delft University of Technology and Stichting CUR.
- [19] S. Levasseur et al. “Soil parameter identification using a genetic algorithm”. In: *International Journal for Numerical and Analytical Methods in Geomechanics* 32 (2008), pp. 189–213.
- [20] S. Levasseur et al. “Statistical inverse analysis based on genetic algorithm and principal component analysis; Applications to excavation problems and pressuremeter tests”. In: *International Journal for Numerical and Analytical Methods in Geomechanics* 34 (2009), pp. 471–491.
- [21] A. Mavritsakis. “Evaluation of inverse analysis methods with numerical simulation for slope excavation”. MA thesis. Delft University of Technology, 2017.
- [22] P. Mestat and N. Arafati. “Modélisation par éléments finis du comportement du rideau de palplanches expérimental de Hochstetten”. In: *Bulletin des Laboratoires des Ponts et Chaussée* 216 (1998), pp. 19–39.
- [23] M. Mitchell. *An introduction to genetic algorithm*. Cambridge, Mass. MIT Press, 1996.
- [24] E. Orhan. “Particle filtering”. In: 8.11 (2012). University of Rochester, NY.
- [25] *Plaxis Material Models Manual*. Plaxis bv. 2019.
- [26] T. Schanz, P.A. Vermeer, and P.G. Bonnier. *The hardening soil model: Formulation and verification*. Beyond 2000 in Computational Geotechnics - 10 years of Plaxis. Rotterdam. Balkema, 1998.
- [27] I.J.M Schrijver. “Reliability of Flexible Dolphins”. MA thesis. Delft University of Technology, 2016.
- [28] D. Straub. “Efficient Algorithms and Models for Bayesian Updating in Structural Reliability”. In: (2012). URL: <https://www.researchgate.net/publication/268588245>.
- [29] D. Straub, W. Betz, and I. Papaioannou. “Adaptive variant of the BUS approach to Bayesian updating”. In: *Eurodyn* (2014). Porto, Portugal.
- [30] D. Straub and I. Papaioannou. “Bayesian Updating with Structural Reliability Methods”. In: *Journal of Engineering Mechanics* 141 (2014).
- [31] G.A. Terejanu. *Extended kalman filter tutorial*. Department of Computer Science and Engineering. University at Buffalo, 2008.
- [32] T.J. van der Wel. “Reliability based Assessment of Quay Walls”. MA thesis. Delft University of Technology, 2018.
- [33] C.K. Wikle and L.M. Berliner. “A Bayesian tutorial for data assimilation”. In: *Physica D: Nonlinear Phenomena* 260.1 (2007), pp. 1–16.
- [34] P.A. von Wolfersdorff. *Vervormungsprognosen für Stützkonstruktionen*. des Institutes für Bodenmechanik und Felsmechanik der Universität Fridericiana in Karlsruhe. 1997.
- [35] H.J. Wolters. “Reliability of Quay Walls”. MA thesis. Delft University of Technology, 2012.